Spring 1-1-2013

Release of Intracellular Metabolites from Cyanobacteria During Oxidation Processes in Drinking Water

Eric Craig Wert
University of Colorado at Boulder, eric.wert@colorado.edu

RELEASE OF INTRACELLULAR METABOLITES FROM CYANOBACTERIA DURING OXIDATION PROCESSES IN DRINKING WATER

by

ERIC CRAIG WERT

B.S., West Virginia University, 1999

M.E., Pennsylvania State University, 2000

A thesis submitted to the

Faculty of the Graduate School of the

University of Colorado in partial fulfillment

of the requirement for the degree of

Doctor of Philosophy

Department of Civil, Environmental, and Architectural Engineering

2013

This thesis entitled:

Release of Intracellular Metabolites from Cyanobacteria

during Oxidation Processes in Drinking Water

written by Eric Craig Wert

has been approved for the

Department of Civil, Environmental, and Architectural Engineering

Fernando L. Rosario-Ortiz, (chair)

Diane McKnight

JoAnn Silverstein

R. Scott Summers

Djanette Khiari

Date _____

The final copy of this thesis has been examined by the signatories, and we find that both the content and the form meet acceptable presentation standards of scholarly work in the above mentioned discipline.

ABSTRACT

Wert, Eric Craig (Ph.D., Environmental Engineering)

Release of Intracellular Metabolites from Cyanobacteria during Oxidation Processes in Drinking Water

Thesis directed by Fernando Rosario-Ortiz, Assistant Professor, Department of Civil, Environmental and Architectural Engineering, University of Colorado at Boulder

Drinking water utilities often begin the treatment process by using an oxidation process to meet different water quality objectives (e.g. disinfection, control of invasive species, oxidation of organic or inorganic contaminants). If cyanobacteria cells are not removed prior to oxidation, cell damage or lysis may result in the release of intracellular organic matter (IOM) into the water supply. The objective of this research was to determine the effect of common preoxidants used during drinking water treatment on the integrity of cyanobacteria cells, and to evaluate the subsequent release of toxic metabolites, odorous metabolites, and/or disinfection byproduct (DBP) precursors.

Three cyanobacteria (i.e. *Microcystis aeruginosa* (MA), *Oscillatoria sp*. (OSC), and *Lyngbya sp*. (LYN)) were selected based upon (1) occurrence in source water supplies, (2) availability of an axenic culture, (3) ability to produce odorous or toxic metabolites, and (4) morphology. In order to evaluate cell degradation, digital flow cytometry in combination with chlorophyll-a measurements provided an assessment of cyanobacteria cell damage and lysis after oxidation using ozone, chlorine, chlorine dioxide, and chloramine. The release of toxic (i.e. microcystin-LR (MC-LR)) or odorous metabolites

(i.e. 2-methylisoborneol (MIB), geosmin) was evaluated after oxidation of cyanobacteria cells added to Colorado River water. The formation of DBPs was evaluated during the chlorination and chloramination of IOM extracted from the different cyanobacteria.

Results showed that cyanobacteria cell damage occurred without complete lysis or fragmentation of the cell membrane under the conditions tested. The unicellular morphology of MA was more susceptible to oxidation than the filamentous morphology of OSC and LYN. Cell damage resulted in the release of IOM, which contained MC-LR, MIB, geosmin, and DBP precursor material. Subsequent oxidation of released (or extracellular) metabolites (i.e. MC-LR, MIB, and geosmin) coincided with kinetic information found in the literature. The yield of DBPs from IOM was identified for carbonaceous DBPs (i.e. trihalomethanes, haloacetic acids) and nitrogenous DBPs (haloacetonitriles, trichloronitromethane, and nitrosamines). Utilities can use this research to better manage their pretreatment conditions in order to minimize the risk of releasing toxic metabolites, odorous metabolites, or DBP precursors.

DEDICATION

I dedicate this work to my wife Becky, son Quentin, daughter Addison, and daughter Brooke for their full and unwavering support, especially during the weekly travel between Las Vegas and Denver during the Fall semester of 2011. I also dedicate this work to my family (Craig and Kathryn Wert, Robert and Susan Blasius, Harriet Fasick, Paul and Kathryn Kister, and Blake and Florine Wert), who provided me with inspiration and encouragement to pursue higher education.

ACKNOWLEDGEMENTS

There are many people and agencies who contributed to the completion of this project. Dr. Fernando Rosario-Ortiz (advisor) provided me with exceptional insight and encouragement from proposal development and experimental design to data interpretation and publishing. Dr. Rosario-Ortiz and his family also provided me with great friendship and hospitality throughout the entire process. I thank my PhD committee members (Dr. R. Scott Summers, Dr. JoAnn Silverstein, Dr. Diane McKnight, and Dr. Djanette Khiari) for their advice and productive discussions regarding the project. Julie Korak and Dorothy Noble also provided assistance and analytical support.

The Water Research Foundation (WaterRF) provided financial support of this project (#4406). The WaterRF project advisory committee members (Dr. Aaron Dotson, Dr. Lenore Tedesco, Jeff Neemann, and Karie Holtermann) also provided advice and constructive comments regarding the project approach. Fluid Imaging Technologies (Jonathan Dawson) provided training and input regarding the use of the FlowCAM.

Many members of the Southern Nevada Water Authority were responsible for the completion of this project. Ron Zegers and Dave Rexing supported the Tailored Collaboration project with the WaterRF and application of the work toward obtaining a doctoral degree. Mei Mei (Vivy) Dong, Julia Lew, and Holly McNaught provided assistance during cell culturing and oxidant testing. Beck Trenholm, Janie Zeigler-Holady, and Brett Vanderford provided assistance with analytical methods for microcystin, MIB, geosmin and nitrosamines. The Laboratory division provided assistance with sample analysis, bottle preparation, and sample shipping. Chuck Meyer provided assistance with cyanobacteria cell culturing.

CONTENTS

TABLES

FIGURES

ABBREVIATIONS

AIM – Auto Image mode operation using the FlowCAM

AOC – Assimilable organic carbon

AOM – Algal organic matter

BAA – Bromoacetic acid

BCAA – Bromochloroacetic acid

BCAN - Bromochloroacetonitrile

BDCAA – Bromodichloroacetic acid

C-DBPs – Carbonaceous disinfection byproducts

CAA – monochloroacetic acid

CCL3 – USEPA Contaminant Candidate List 3

CDBAA – Chlorodibromoacetic acid

ClO2 – Chlorine dioxide

CRW – Colorado River water

CT – Oxidant exposure measured by the integration of oxidant residual over time

DBAA – Dibromoacetic acid

DBAN – Dibromoacetonitrile

DBP – Disinfection byproduct

DCAA – Dichloroacetic acid

DCAN – Dichloroacetonitrile

DOC – Dissolved organic carbon

DON – Dissolved organic nitrogen

ELISA – Enzyme-Linked ImmunoSorbent Assay

EOM – Extracellular organic matter

FCl2 – Free chlorine

FP – Formation potential

HAA – Haloacetic acid

HAA5 – Sum of five regulated HAA species (i.e. CAA, DCAA, TCAA, BAA, DBAA)

HAA9 – Sum of nine HAA species (i.e. HAA5, BCAA, DBAA, BDCAA, CDBAA, TBAA)

HAN – Haloacetonitrile

IOM – Intracellular organic matter

LYN – Lyngbya sp.

MA – Microcystis aeruginosa

MC-LR – Microcystin-LR

MIB – 2-methylisoborneol

MQ – MilliQ water or ultrapure water

MRL – Minimum reporting limit

MW – Molecular weight

MWDSC – Metropolitan Water District of Southern California

N-DBPs – Nitrogenous disinfection byproducts

NDBA – N-nitrosodibutylamine

NDEA – N-nitrosodiethylamine

NDMA – N-nitrosodimethylamine

NDPA – N-nitrosodipropylamine

NDPhA – N-nitrosophenylamine

NH2Cl – Chloramine

NMEA – N-nitrosomethylethylamine

NMOR – N-nitrosomorpholine

NOM – Natural organic matter

NPIP – N-nitrosopiperidine

NPYR – N-nitrosopyrrolidine

O3 – Ozone

O3/FCl2 – Sequential oxidation process of ozone followed by chlorination

O3/NH2Cl – Sequential oxidation process of ozone followed by chloramination

OSC – Oscillatoria sp.

RSD – Relative standard deviation

SEM – Scanning electron microscopy

SM – Standard Method

SUVA – Specific UV absorbance at 254 nm

TBAA – Tribromoacetic acid

TCAA – Trichloroacetic acid

TCAN - Trichloroacetonitrile

TCNM – Trichloronitromethane

THM – Trihalomethane

THM4 - Sum of four regulated THM species (i.e. CHCl3, CHBrCl2, CHBr2Cl, CHBr3)

TM – Trigger mode operation using the FlowCAM

TN – Total nitrogen

TOX – Total organic halogen

USEPA – United States Environmental Protection Agency

UTOX – Unknown total organic halogen

WHO – World Health Organization

CHAPTER 1. Introduction

1.1. Statement of Problem

Freshwater blooms of cyanobacteria (blue-green algae) have emerged as an area of concern to drinking water utilities. The occurrence of freshwater blooms is largely dependent upon the presence of nutrients (nitrogen and phosphorus). However, other factors have also been linked to expanding populations of harmful cyanobacteria, including climate change (i.e. hydrology, temperature, carbon dioxide)[1] and invasive species (e.g. quagga mussels)[2, 3]. These blooms can become problematic for drinking water utilities for several reasons including filter clogging and the production of metabolites (i.e. taste and odor compounds, cyanotoxins). As a result, drinking water utilities must begin developing strategies to better manage water quality and treatment issues caused by cyanobacteria in surface water supplies (e.g. lakes, reservoirs, and rivers).

Cyanobacteria-derived organic matter released into the water can have multiple effects on regulatory compliance for utilities. For example, algal-derived organic matter (AOM) has been shown to be a precursor for trihalomethane (THM) and haloacetic acid (HAA) formation that could have different reactivity when compared to dissolved organic matter (DOM) found in water supplies[4-8]. The recently promulgated Stage 2 Disinfectants/Disinfection Byproducts (D/DBP) Rule has already made compliance more stringent for utilities and additional AOM may increase the DBP precursor pool. Another group of DBPs that may be formed from algal precursor material includes nitrogenous

DBPs (N-DBPs). Algae are known sources of dissolved nitrogen, which could lead to the formation of various nitrogenous DBPs (i.e. dichloroactonitrile (DCAN), cyanogens chloride (CNCl), and trichloronitromethane (TCNM)) [9]. These DBPs are considered to be more toxic than the regulated THMs and HAAs [10, 11]. However, limited work has been performed regarding natural sources of N-DBP precursor material.

The physical, chemical, and biological treatment of extracellular cyanotoxins and taste and odor compounds (2-methylisoborneol (MIB) and geosmin) has been well documented in the literature [14-17]. The World Health Organization has established provisional guideline value of 1 µg/L for microcystin-LR [18]. In 2009, three cyanotoxins (i.e. anatoxin-a, microcystin-LR, and cylindrospermopsin) were added to United States Environmental Protection Agency's Contaminant Candidate List 3 (CCL3) [19]. MIB and geosmin are the two most frequently detected in drinking water sources with threshold odor values reported from 1.3-4.0 ng/L and 6.3-15 ng/L, respectively [20, 21]. Although these compounds do not pose any human health risk, the aesthetics of the drinking water with respect to taste and odor directly impact consumer confidence [21]. In summary, extracellular cyanobacterial metabolites can pose both regulated and unregulated water quality challenges to drinking water treatment facilities.

Most research has focused on the treatment of extracellular metabolites found in the source water supplies of utilities. Few studies have investigated the risk of releasing cell-bound, intracellular organic matter (IOM) during preoxidation processes including ozone, chlorine dioxide, chloramines, and free chlorine [22-24]. Additional research is needed

regarding the effect of preoxidants on cyanobacteria and the potential to release intracellular metabolites within the treatment plant via cell damage. Preoxidation can provide multiple benefits for utilities including disinfection, mussel control, iron and manganese oxidation, and routine system maintenance. However, cell damage or lysis may occur when the cyanobacteria cells are not physically removed prior to an oxidation process. This project will investigate the ability of different preoxidants to release algal metabolites within the treatment process and subsequent production of DBPs. The proposed research builds upon other work conducted in the area and will expand a few critical areas, including total organic halide analysis, characterization of N-DBPs, and physical transformation of cyanobacteria cells.

1.2. Background

The specific treatment technology for the removal of algal metabolites depends on their physical state. Intracellular toxins and odorous metabolites are removed with their parent algae through conventional treatment processes (i.e. clarification, filtration) and other process such as dissolved air flotation and microstrainers. Extracellular toxins and odorous metabolites on the other hand can be removed through oxidation or adsorption processes [12]. However, if chemical pretreatments are needed for mussel control or other treatment objectives, then algae cells may become lysed resulting in the release of intracellular algal metabolites. Ozonation is a common preoxidant for drinking water utilities for several reasons including disinfection, taste and odor removal, iron/manganese oxidation, coagulation/flocculation benefits, and oxidation of

disinfection byproduct precursors. As a strong oxidant, ozone also has the potential to release these algal metabolites via cell lysis [13].

Cyanobacteria (blue-green algae) typically produce the toxic and odorous metabolites of concern. Several studies have summarized which algal species were found to produce taste and odor (T&O) compounds [14-16]. The two most well documented compounds known to create taste and odor episodes in drinking water are MIB and geosmin [17]. Taste and odor threshold values for these compounds are commonly in the 1.3-22 ng/L range [18, 19]. Algal toxins are other metabolic byproducts of algae [20, 21]. As mentioned previously, anatoxin-a, microcystin-LR, and cylindrospermopsin were listed on the CCL3. Most research in these areas has focused on the oxidation of these contaminants present as extracellular metabolites found in the source waters of drinking water plants.

The ability of ozone and hydroxyl radicals to oxidize many taste and odor compounds has also been well established [22-24]. The removal of MIB and geosmin during the ozone process is primarily due to oxidation by hydroxyl radicals. However, most studies have used MIB and geosmin standards to evaluate oxidation efficiency, and have not investigated the oxidation of samples containing algal cells or filaments. In the case of preoxidation with ozone, the rate of release of these compounds via cell lysis may exceed the rate of oxidation by hydroxyl radicals due to the slow reaction rate with molecular ozone. This could result in greater concentrations of MIB and geosmin after oxidation. Since these substances can cause taste and odor complaints at ng/L concentrations, a

minor release of intracellular organic matter (IOM) could result in additional customer complaints for utilities.

The ability of ozone and hydroxyl radicals to oxidize many algal toxins has also been well established [25-28]. According to kinetic information, microcystin-LR and cylindrospermopsin are rapidly oxidized by molecular ozone. If these toxins are released via cell lysis, the rate constant indicates that a significant portion would be rapidly oxidized. Although in one study, ozonation appeared to release intracellular microcystins and increase the amount of extracellular microcystins using an ozone dose of 0.3 mg/L [29]. However, there are few other studies that have investigated the release of algal toxins by ozonation via cell lysis [13]. Anatoxin-a has a slightly slower rate constant and may present a case where the toxin concentration could increase during preoxidation with ozone. Furthermore, the saxitoxin class (i.e. GTX2, GTX3, C1, and C2) of algal toxins has been shown to be even more resistant to ozone treatment [25]. Therefore, saxitoxins present a case where preoxidation could release a cyanotoxin at a rate greater than rate of oxidation.

Another concern with algae is the release of AOM. AOM consists of extracellular organic matter (EOM) and IOM. EOM contains algal metabolites that are excreted from the algal cells into the surrounding water. IOM refers to the cytoplasm and biopolymers contained inside the algal cells [30]. When a preoxidant is added, IOM may be released from inside the cell walls. Few studies have been performed investigating the effect of oxidation on cell lysis and structural damage [13, 31, 32]. Some research has been performed

regarding the effects of chlorination on algae and potential to release IOM via algal cell lysis [33-35]. In one study, chlorine, copper sulfate, and potassium permanganate were shown to cause physical damage to algal cells resulting in the release of DOC and geosmin from one algae (*Aphanizomenon flos-aquae*) [32].

Several studies have investigated the characteristics of AOM [7, 9, 36]. One study characterized the AOM contained in a sample of both IOM and EOM of four algal species (i.e. *Chlorella vulgaris* (green), *Microcystis aeruginosa* (cyanobacteria), *Asterionella formosa* (diatom) and *Melosira* sp. (diatom)) [36]. The study concluded that the AOM was dominated by hydrophilic polysaccharides, and hydrophobic proteins. For the algae samples, 55-62% of the AOM had a molecular weight greater than 30 kDa, while 30-38% was less than 1 kDa. For the diatom samples, only 9-30% of the AOM had a MW greater than 30 kDa, while 53-81% was less than 1 kDa. Another study focused on the green algae, *Scenedesmus quadricauda*, and found that 25% of the EOM was present as hydrophobic acids [7]. Both of these studies indicated that AOM had a different character than conventional DOM One recent study showed that EOM and IOM had similar fluorescence properties, with peaks indicating the presence of protein-like organic matter or organic nitrogen rich compounds [9]. There have been few studies performed regarding the effect of algal matter (either particulate or dissolved) on ozone demand and decay rate along with hydroxyl radical scavenging.

AOM has also been shown to increase the formation of chlorinated byproducts as shown [6, 7, 37]. Most of the literature has investigated the formation of THMs and HAAs from

AOM isolates. Chlorinated disinfection byproducts have been mentioned as a potential contaminant grouping class for regulation by USEPA. However, there is minimal research investigating the formation total organic halides (TOX) from algae sources. TOX analysis would determine whether other unknown chlorinated byproducts are formed from AOM aside from chloroform.

Algae laden waters can also be a source of dissolved organic nitrogen (DON) [38]. DON can result in the formation of N-DBPs upon chlorination or chloramination. Nitrosamines have also been given consideration as a potential grouping class for regulation by USEPA. However, there is minimal research investigating the formation of nitrogenous DBPs using DON from algal sources [9]. Ozone has been demonstrated to rapidly oxidize NDMA precursors [39, 40]. Therefore, precursor material may be immediately transformed by ozone even if DON is released from the algal cells. In one study, algae was not considered to be a source of NDMA precursor material [41]. In another study, algae was found to be a precursor for dihaloactonitriles (DHAN) [42].

Minimal research has been performed regarding the effects of preozonation on the physical destruction of algae and corresponding cell lysis [43]. Several studies have documented the physical destruction of algal cells and filaments using ozonation using scanning electron microscopy (SEM) pictures [37, 43-45]. However, the SEM photos provide more qualitative data regarding cell lysis and destruction. More quantitative information is needed regarding the potential to release dissolved algal metabolites (i.e. algal toxins, taste and odor compounds) during oxidation processes, which may place greater

emphasis on physical removal processes during drinking water treatment. Alternatively, guidelines could be established for ozone in order to minimize the degree of cell lysing.

These topics focus on water quality and treatment issues that could have a direct impact on regulatory compliance for utilities. Since most oxidation studies investigating algal metabolites have been performed using isolates or standards, utilities may be underestimating the risk to release these compounds during preoxidation with ozone. Under certain conditions, a utility may release algal metabolites at a greater rate than they are destroyed resulting in a net increase of these compounds.

1.3. Research Objectives

To determine the effect of common preoxidants used during drinking water treatment on the integrity of cyanobacteria cells, and to evaluate the subsequent release of toxic metabolites, odorous metabolites, and/or disinfection byproduct precursors. The research will benefit utilities susceptible to harmful cyanobacteria blooms by offering guidance related to different preoxidation conditions.

Three hypotheses were developed in order to better understand the risk of intracellular release of cyanobacteria metabolites during drinking water treatment:

(1) Release of intracellular cyanobacterial metabolites will be dependent upon the morphology and oxidant exposure (CT).

(2) Intracellular organic matter (IOM) will generate more DBPs than Colorado River Water on a per carbon basis.

(3) Oxidation processes will release and transform the IOM, lowering the reactivity and subsequent yield of DBPs on a per carbon basis.

1.4. Thesis Organization

The present thesis is organized into five chapters. Chapter 1 presents background information regarding the project, and explains research objectives. Chapter 2 investigates the degradation of cyanobacteria cells during oxidation process common during drinking water treatment. Chapter 3 investigates the release of intracellular toxic or odorous metabolites from cyanobacteria during oxidation processes. Chapter 4 investigates the formation of carbonaceous and nitrogenous disinfection byproducts during the chlorination and chloramination of extracted intracellular organic matter. Chapter 5 presents an outlook regarding the potential for future research.

1.5. Application Potential

As a result of this research, oxidant exposure guidelines will benefit utilities seeking to minimize the water quality effects associated with blooms of cyanobacteria. Utilities can use these guidelines to better manage their pretreatment conditions in order to minimize cell lysis and reduce the risk of releasing toxic metabolites, odorous metabolites, or DBP precursors. Furthermore, additional guidance will be developed regarding the reactivity of IOM with both free chlorine and chloramines. Utilities can use this information when developing strategies to comply with USEPA regulations such as the Stage 2 D/DBP Rule. Overall, the research will expand the fundamental knowledge regarding the risk of cell lysis from preoxidation, and provide guidance to drinking water utilities impacted by harmful cyanobacteria blooms.

1.6. References

1. Paerl, H. W.; Huisman, J., Climate change: a catalyst for global expansion of harmful cyanobacterial blooms. *Environmental Microbiology Reports* **2009,** *1*, (1), 27-37.

2. Knoll, L. B.; Sarnelle, O.; Hamilton, S. K.; Kissman, C. E. H.; Wilson, A. E.; Rose, J. B.; Morgan, M. R., Invasive zebra mussels (Dreissena polymorpha) increase cyanobacterial toxin concentrations in low-nutrient lakes. *Canadian Journal of Fisheries and Aquatic Sciences* **2008,** *65*, (3), 448-455.

3. Vanderploeg, H. A.; Liebig, J. R.; Carmichael, W. W.; Agy, M. A.; Johengen, T. H.; Fahnenstiel, G. L.; Nalepa, T. F., Zebra mussel (Dreissena polymorpha) selective filtration promoted toxic Microcystis blooms in Saginaw Bay (Lake Huron) and Lake Erie. *Can. J. Fish Aquat. Sci.* **2001,** *58*, (2001), 1208-1221.

4. Huang, J.; Graham, N.; Templeton, M. R.; Zhang, Y.; Collins, C.; Nieuwenhuijsen, M., A comparison of the role of two blue-green algae in THM and HAA formation. *Water Res.* **2009,** *43*, (12), 3009-3018.

5. Graham, N. J. D.; Wardlaw, V. E.; Perry, R.; Jiang, J.-Q., The Significance of Algae as Trihalomethane Precursors. *Water Science & Technology* **1998,** *37*, (2), 83-89.

6. Hoehn, R. C.; Barnes, D. B.; Thompson, B. C.; Randall, C. W.; Grizzard, T. J.; Shaffer, P. T. B., Algae as Sources of Trihalomethane Precursors. *J.-Am. Water Works Assoc.* **1980,** *72*, (6), 344-350.

7. Nguyen, M.-L.; Westerhoff, P.; Baker, L.; Hu, Q.; Esparza-Soto, M.; Sommerfield, M., Characteristics and Reactivity of Algae-Produced Dissolved Organic Carbon. *Journal of Environmental Engineering* **2005,** *131*, (11), 1574-1582.

8. Hong, H. C.; Mazumder, A.; Wong, M. H.; Liang, Y., Yield of trihalomethanes and haloacetic acids upon chlorinating algal cells, and its prediction via algal cellular biochemical composition. *Water Res.* **2008,** *42*, (20), 4941-4948.

9. Fang, J.; Yang, X.; Ma, J.; Shang, C.; Zhao, Q., Characterization of algal organic matter and formation of DBPs from chlor(am)ination. *Water Res.* **2010,** *44*, (20), 5897-5906.

10. Plewa, M. J.; Wagner, E. D.; Jazwierska, P.; Richardson, S. D.; Chen, P. H.; McKague, A. B., Halonitromethane drinking water disinfection byproducts: Chemical characterization and mammalian cell cytotoxicity and genotoxicity. *Environmental Science & Technology* **2004,** *38*, (1), 62-68.

11. Muellner, M. G.; Wagner, E. D.; McCalla, K.; Richardson, S. D.; Woo, Y. T.; Plewa, M. J., Haloacetonitriles vs. regulated haloacetic acids: Are nitrogen-containing DBPs more toxic? *Environmental Science & Technology* **2007,** *41*, (2), 645-651.

12. Newcombe, G. *Removal of Algal Toxins from Drinking Water Using Ozone and GAC*; 90904; Water Research Foundation: 2002.

13. Ding, J.; Shi, H.; Timmons, T.; Adams, C., Release and Removal of Microcystins from Microcystis during Oxidative-, Physical-, and UV-Based Disinfection. *Journal of Environmental Engineering* **2010,** *136*, (1), 2-11.

14. Smith, J. L.; Boyer, G. L.; Zimba, P. V., A review of cyanobacterial odorous and bioactive metabolites: Impacts and management alternatives in aquaculture. *Aquaculture* **2008,** *280*, (1-4), 5-20.

15. Watson, S. B., Cyanobacterial and eukaryotic algal odour compounds: signals or by-products? A review of their biological activity. *Phycologia* **2003,** *42*, (4), 332-350.

16. Juttner, F.; Watson, S. B., Biochemical and Ecological Control of Geosmin and 2-Methylisoborneol in Source Waters. *Applied and Environmental Microbiology* **2007,** *73*, (14), 4395-4406.

17. Izaguirre, G.; Hwang, C. J.; Krasner, S. W.; McGuire, M. J., Geosmin and 2-Methylisoborneol from Cyanobacteria in Three Water Supply Systems. *Applied and Environmental Microbiology* **1982,** *43*, (3), 708-714.

18. Young, W. F.; Horth, H.; Crane, R.; Ogden, T.; Arnott, M., Taste and Odour Threshold Concentrations of Potential Potable Water Contaminants. *Water Res.* **1996,** *30*, (2), 331-340.

19. Nerenberg, R.; Rittman, B. E.; Soucie, W. J., Ozone/Biofiltration for Removing MIB and Geosmin. *J.-Am. Water Works Assoc.* **2000,** *92*, (12), 85-95.

20. Van Dolah, F. M., Marine algal toxins: origins, health effects, and their increased occurrence. *Environ. Health Perspect.* **2000,** *108*, (1), 133-141.

21. Haddix, P. L.; Hughley, C. J.; Lechevallier, M. W., Occurence of microcystins in 33 US water supplies. *American Water Works Association* **2007,** *99*, (9), 118-125.

22. Peter, A.; von Gunten, U., Oxidation Kinetics of Selected Taste and Odor Compounds During Ozonation of Drinking Water. *Environmental Science & Technology* **2007,** *41*, (2), 626-631.

23. Glaze, W. H.; Schep, R.; Chauncey, W.; Ruth, E. C.; Zarnoch, J. J.; Aieta, E. M.; Tate, C. H.; McGuire, M. J., Evaluating Oxidants for the Removal of Model Taste and

Odor Compounds From a Municipal Water Supply. *J.-Am. Water Works Assoc.* **1990,** *82*, (5), 79-84.

24. Westerhoff, P.; Nalinakumari, B.; Pei, P., Kinetics of MIB and Geosmin Oxidation during Ozonation. *Ozone Sci. Eng.* **2006,** *28*, (5), 277-286.

25. Rositano, J.; Newcombe, G.; Nicholson, B.; Sztajnbok, P., Ozonation of NOM and Algal Toxins in Four Treated Waters. *Water Res.* **2001,** *35*, (1), 23-32.

26. Bruchet, A.; Bernazeau, F.; Baudin, I.; Pieronne, P., Algal toxins in surface waters: analysis and treatment. *Water Supply* **1998,** *16*, (1-2), 611-623.

27. Onstad, G. D.; Strauch, S.; Meriluoto, J.; Codd, G. A.; von Gunten, U., Selective Oxidation of Key Functional Groups in Cyanotoxins during Drinking Water Ozonation. *Environ. Sci. Technol.* **2007,** *41*, (12), 4397-4404.

28. Rodriguez, E.; Onstad, G. D.; Kull, T. P. J.; Metcalf, J. S.; Acero, J. L.; von Gunten, U., Oxidative elimination of cyanotoxins: Comparison of ozone, chlorine, chlorine dioxide and permanganate. *Water Res.* **2007,** *41*, (2007), 3381-3393.

29. Schmidt, W.; Willmitzer, H.; Bornmann, K.; Pietsch, J., Production of drinking water from raw water containing cyanobacteria - pilot plant studies for assessing the risk of microcystin breakthrough. *Environmental Toxicology* **2002,** *17*, (4), 375-385.

30. Chandrakanth, M. S.; Krishnan, S.; Amy, G. L., Interactions between Ozone, AOM, and Particle in Water Treatment. *Journal of Environmental Engineering* **1996,** *122*, (6), 459-468.

31. Bouteleux, C.; Saby, S.; Tozza, D.; Cavard, J.; Lahoussine, V.; Hartemann, P.; Mathieu, L., Escherichia coli Behavior in the Presence of Organic Matter Released by Algae Exposed to Water Treatment Chemicals. *Applied and Environmental Microbiology* **2005,** *71*, (2), 734-740.

32. Peterson, H. G.; Hrudey, S. E.; Cantin, I. A.; Perley, T. R.; Kenefick, S. L., Physiological toxicity, cell membrane damage and the release of dissolved organic carbon and geosmin by aphanizomenon flos-aquae after exposure to water treatment chemicals. *Water Res.* **1995,** *29*, (6), 1515-1523.

33. Lin, T.-F.; Chang, D.-W.; Lien, S.-K.; Tseng, Y.-S.; Chiu, Y.-T.; Wang, Y.-S., Effect of chlorination on the cell integrity of two noxious cyanobacteria and their releases of odorants. *Journal of Water Supply: Research and Technology-AQUA* **2009,** *58*, (8), 539-551.

34. Daly, R.; Ho, L.; Brookes, J. D., Effect of Chlorination on Microcystis aeruginosa Cell Integrity and Subsequent Microcystin Release and Degradation. *Environ. Sci. Technol.* **2007,** *41*, (12), 4447-4453.

35. Zamyadi, A.; Ho, L.; Newcombe, G.; Daly, R. I.; Burch, M.; Baker, P.; Prevost, M., Release and Oxidation of Cell-Bound Saxitoxins during Chlorination of Anabaena circinalis Cells. *Environ. Sci. Technol.* **2010,** *44*, (23), 9055-9061.

36. Henderson, R. K.; Baker, A.; Parsons, S. A.; Jefferson, B., Characterisation of algogenic organic matter extracted from cyanobacteria, green algae and diatoms. *Water Res.* **2008,** *42*, (13), 3435-3445.

37. Plummer, J. D.; Edzwald, J. K., Effect of Ozone on Algae as Precursors for Trihalomethane and Haloacetic Acid Production. *Environmental Science & Technology* **2001,** *35*, (18), 3661-3668.

38. Mitch, W. A.; Krasner, S. W.; Westerhoff, P.; Dotson, A. *Occurrence and Formation of Nitrogenous Disinfection By-Products*; Water Research Foundation: 2009.

39. Lee, C.; Schmidt, C.; Yoon, J.; von Gunten, U., Oxidation of N-Nitrosodimethylamine (NDMA) Precursors with Ozone and Chlorine Dioxide: Kinetics and Effect on NDMA Formation Potential. *Environmental Science & Technology* **2007,** *41*, (6), 2056-2063.

40. Chen, Z.; Valentine, R. L., The Influence of the Pre-Oxidation of Natural Organic Matter on the Formation of N-Nitrosodimethylamine (NDMA). *Environ. Sci. Technol.* **2008,** *42*, (14), 5062-5067.

41. Gerecke, A. C.; Sedlak, D. L., Precursors of N-Nitrosodimethylamine in Natural Waters. *Environ. Sci. Technol.* **2003,** *37*, (7), 1331-1336.

42. Oliver, B. G., Dihaloacetonitriles in drinking water: algae and fulvic acid as precursors. *Environ. Sci. Technol.* **1983,** *17*, (2), 80-83.

43. Plummer, J. D.; Edzwald, J. K., Effects of chlorine and ozone on algal cell properties and removal of algae by coagulation. *Journal of Water Supply: Research and Technology-AQUA* **2002,** *51*, (6), 307-318.

44. Huang, W.-J.; Cheng, B.-L.; Hu, S.-K.; Chu, C., Ozonation of Algae and Odor Causing Substances in Eutrophic Waters. *Journal of Environmental Science and Health Part A* **2006,** *41*, (8), 1587-1605.

45. Miao, H.; Tao, W., The mechanisms of ozonation on cyanobacteria and its toxins removal. *Separation Science and Technology* **2009,** *66*, (1), 187-193.

CHAPTER 2. Using Digital Flow Cytometry to Assess the Degradation of Three Cyanobacteria Species after Oxidation Processes

(This chapter has been submitted to *Water Research*)

2.1. Abstract

Depending on drinking water treatment conditions, oxidation processes may result in the degradation of cyanobacteria cells causing the release of toxic metabolites (microcystin), odorous metabolites (MIB, geosmin), or disinfection byproduct precursors. In this study, a digital flow cytometer (FlowCAM®) in combination with chlorophyll-a analysis was used to evaluate the ability of ozone, chlorine, chlorine dioxide, and chloramine to damage or lyse cyanobacteria cells added to Colorado River water. *Microcystis aeruginosa* (MA), *Oscillatoria sp.* (OSC) and *Lyngbya sp.* (LYN) were selected for the study due to their occurrence in surface water supplies, metabolite production, and morphology. Results showed that cell damage was observed without complete lysis or fragmentation of the cell membrane under many of the conditions tested. During ozone and chlorine experiments, the unicellular MA was more susceptible to oxidation than the filamentous OSC and LYN. Rate constants were developed based on the loss of chlorophyll-a and oxidant exposure, which showed the oxidants degraded MA, OSC, and LYN according to the order of ozone > chlorine ~ chlorine dioxide > chloramine. Digital and binary images taken by the digital flow cytometer provided qualitative insight regarding cell damage. When applying this information, drinking water utilities can better understand the risk of cell damage or lysis during oxidation processes.

2.2. Introduction

Freshwater algal blooms have emerged as an area of concern to drinking water utilities. The occurrence of freshwater algal blooms is largely dependent upon the presence of nutrients (nitrogen and phosphorus). However, effects from climate change (i.e. temperature, carbon dioxide, hydrology) have also been linked to expanding populations of harmful cyanobacteria [1]. These cyanobacteria blooms can become problematic for drinking water utilities for several reasons, including filter clogging and the production of toxic metabolites (e.g. microcystin, anatoxin, cylindrospermopsin) and/or odorous metabolites (e.g. MIB, geosmin).

The production and release of toxic and odorous metabolites is common during cell activity and cell death. Multiple studies have investigated toxin occurrence from different genus and species of cyanobacteria [2-6]. Furthermore, numerous cyanobacteria are known to produce a variety of taste and odor compounds [7, 8] with threshold odor values reported for geosmin (1.3-4.0 ng/L) and MIB (6.3-15 ng/L) [9, 10]. Due to public health concern regarding algal toxins and consumer confidence impacted by taste and odor compounds, research has focused on the ability of common chemical, biological, and physical processes to remove these toxic or odorous metabolites from drinking water supplies [11-15]. The efficacy of different chemical oxidation processes to eliminate a specific metabolite can be assessed using kinetic parameters [13, 16]. If incorporating a chemical oxidation process prior to physical removal of cyanobacteria cells, release of intracellular (or cell bound) metabolites may also become a concern due to cell damage or lysis by an oxidant with slow kinetics.

Many drinking water treatment processes begin with chemical oxidation to meet objectives such as mussel/biofilm control on intake pipelines, oxidation of inorganic and organic contaminants, and reduction of disinfection byproduct (DBP) precursors. Different oxidation processes have been shown to release intracellular microcystin-LR from *Microcystis aeruginosa* under drinking water treatment conditions [17-20]. The effect of chlorination on cell lysis, toxin release, and DBP formation has been observed using *Anabaena circinalis*, *Microcystis aeruginosa*, *Cylindrospermopsis raciborskii*, and *Aphanizomenon issatsckenka* [21-23]. In another study of bacterial cells, cell membrane damage occurred in the following order according to the measured second order rate constant: ozone > chlorine > chlorine dioxide > chloramine [24].

The exact mechanism of oxidant transport across the cell membrane is not well understood and may occur via active diffusion, passive diffusion, or reaction with the cell membrane. In case of *E. coli*, ozone was theorized to have reacted with the negatively charged lipid bilayer resulting in cell damage or lysis [25]. If reacting with the lipid bilayer, the cell morphology may also may a role in the ability of oxidants to degrade cyanobacteria. Some cyanobacteria may develop a mucilaginous sheath and/or a protective surface layer on their cell wall, commonly referred to as s-layers [26]. During cell decay, the membrane becomes compromised resulting in the release of intracellular matter [27, 28].

Cell viability and membrane integrity have been assessed after oxidation processes through flow cytometry [17-20], and the release of potassium [29]. When using flow cytometry, a nucleic acid stain such as SYTOX green (green fluorescence) or propidium iodide (red fluorescence) is often added to permeate through compromised cell walls causing the damaged or non-viable cells to fluoresce. Other studies have qualitatively documented the physical destruction of various cyanobacteria after oxidation using scanning electron microscopy (SEM) [20, 30-33]. While effective, SEM captures only a few cells or filaments per image and is subject to a freeze-drying process during sample preparation.

In this study, digital flow cytometry was used along chlorophyll-a measurements to investigate cyanobacterial cell damage and lysis resulting from oxidation by ozone, chlorine, chloramine, or chlorine dioxide. *Microcystis aeruginosa* (MA), *Oscillatoria sp*. (OSC), and *Lyngbya sp.* (LYN) were selected for the study based upon occurrence in source water supplies, availability of an axenic culture, ability to produce odorous or toxic metabolites, and cell morphology. The objectives of this research were (1) to assess cell damage after oxidation using the chlorophyll-a concentration and the fluorescent cell concentration, (2) to assess cell lysis or fragmentation using the total cell concentration, (3) to evaluate the kinetics of the cell damage using the chlorophyll-a concentration, fluorescent cell concentration, and oxidant exposure, and (4) to observe cell damage using digital and binary images generated by the digital flow cytometer. The combination of flow cytometry, fluorescence detection, chlorophyll-a analysis, and digital imaging provided a qualitative and quantitative approach to investigate

cyanobacteria cell damage and lysis during different oxidation processes. The approach offers an alternative to manual cell counting using conventional light microscopy to evaluate cyanobacteria cell degradation during oxidation processes in drinking water treatment.

2.3. Materials and Methods

2.3.1. Culturing of Cyanobacteria

Axenic cultures of MA, OSC, and LYN were procured from different cyanobacteria culture collections. MA (LB 2385, Culture Collection of Algae at the University of Texas, Austin, TX, USA) was a confirmed producer of microcystin-LR and exhibited a unicellular morphology. OSC (LM 603d, Metropolitan Water District of Southern California (MWDSC), La Verne, CA, USA) was a confirmed MIB and geosmin producer and exhibited a filamentous morphology with no mucilaginous sheath. LYN (SDC 202d, MWDSC, La Verne, CA, USA) was a confirmed geosmin producer and exhibited a filamentous morphology with a 0.6-1.0 μm thick mucilaginous sheath.

A batch culture method was selected due to the simplicity of the system and volume of cells required. Culturing of cyanobacteria was performed inside of a temperature and light controlled growth chamber (Geneva Scientific, Fontana, WI, USA). The light settings were programmed to provide 12 hours of light exposure followed by 12 hours of darkness. The light intensity at the growth media surface was measured using a light meter (VCAT# 3151, Fisher Scientific, Pittsburgh, PA, USA). The intensity was measured as 2400 lux, 900 lux, and 1600 lux when culturing strains of MA, OSC, and

LYN, respectively. The growth media surface was approximately 45.7 cm (18 in) away from the light source in the culture chamber. The temperature was maintained at 22°C in the growth chamber.

During culturing, the chamber was loaded with sixty 500 mL capacity Erlenmeyer flasks. Each flask contained 300 mL of either BG-11 growth media (for OSC and LYN) or Bold 3N growth media (for MA). The nutrient content for each of the growth media is provided in the Supplemental Information (Table S1.1 and S1.2). Initially, an aliquot of 10 mL was added from a stock cell culture of the specific cyanobacteria strain to each flask in order begin the growth cycle. Cell populations were allowed to increase until reaching the late exponential growth phase. In order to determine the growth condition, a digital flow cytometer was used to provide a rapid assessment of the cell concentration along with measuring the optical density at 730 nm. All optical density measurements were collected without any screening and measured using a spectrophotometer (DR 5000, Hach Company, Loveland, CO, USA). Cell counts were measured at the same time each day to minimize any variability associated with the light/dark cycle. The growth curves for the three cyanobacteria strains are included in the Supplemental Information (Figures S1.1-S1.3). Cells were harvested when the culture approached the late exponential growth phase (28 days). At this growth stage, the concentration of intracellular metabolites is expected to be the greatest [34-36].

2.3.2. Preparation and Characterization of Cell Suspension

When the culture approached the late exponential growth phase, the cells were separated from the growth media by centrifuging the cells and decanting the supernatant containing extracellular organic matter (EOM). The remaining cell pellet was rinsed with 10 mM phosphate buffered MilliQ water (pH=7.5), resuspended via gentle shaking, and centrifuged to separate the cells. The supernatant containing the rinse water was discarded, and the cells resuspended in buffered MilliQ water (pH=7.5). It was essential to remove as much of the growth media as possible to minimize the quantity of EOM and inorganic nitrogen added to the samples.

Once the rinsing process was completed, the cell concentration was characterized using a digital flow cytometer (FlowCAM®, Fluid Imaging Technologies, Yarmouth, ME, USA), which combines flow cytometry, light microscopy, and fluorescence detection to provide rapid particle enumeration and analysis. Digital flow cytometry has been used during other applications to rapidly quantify phytoplankton concentration and size distribution [37-39]. Magnification levels of 20x, 10x, and 10x were used to measure the cell concentrations and properties of MA, OSC, and LYN, respectively. In the cases of the filamentous OSC and LYN, these samples required screening through a 100 μm mesh screen in order to avoid clogging the 10x flow cell, which has cell depth of 100 μm and width of 2000 μm. As a result, a significant portion of the cultured cell mass for these strains was removed on the screen and not used during the oxidation experiments. MA cells did not require any screening since the cells were typically 4-6 μm in diameter, which would not clog the 20x flow cell. Context settings for 10x magnification were as follows: 2 mL sample volume, 0.3 mL/min fluid rate, 20 frames per second imaging

collection, length filter of 10 to 600 μm, and intensity filter of 0 to 150. Context settings for 20x magnification were similar to 10x magnification with the exceptions of a slower fluid rate of 0.025 mL/min and no length or intensity filter implemented. Light microscopy was used to determine the average cell width for the filamentous cyanobacteria OSC (0.2 μm) and LYN (0.13 μm). These measurements were used to determine the cell concentration based upon the total number of particles (or filaments) and the average filament length determined by the digital flow cytometer. After the cell suspension was screened and analyzed, additional particle agglomeration and clumping was visually observed with the OSC and LYN strains. As a result, the suspensions remained on a stir plate throughout the cell spiking process to minimize clumping. The characterized cell suspension was then ready for use during the oxidation experiments.

2.3.3. Experimental Methods

Oxidation experiments were performed as batch processes at room temperature (20-25°C) using Colorado River water (CRW): total organic carbon (2.65 mg/L), pH (8.0), alkalinity (138 mg/L), and UV_{254} (0.052 cm^{-1}). Aliquots of MA, OSC, and LYN were transferred from the concentrated cell suspension into individual 1L amber glass bottles to achieve cell concentrations of 200,000 cells/mL, 2,800 cells/mL, and 1,600 cells/mL, respectively. Then, either chlorine, ozone, monochloramine, or chlorine dioxide was applied to achieve an oxidant:DOC mass ratio of 0, 0.25, 0.50, 0.75, 1.0, and 2.0 based upon an estimated DOC concentration of 2.5 mg/L in CRW. These ratios correspond to applied dosages of 0, 0.63, 1.25, 1.88, 2.5, and 5.0 mg/L. After a 24 hour reaction period, samples dosed with chlorine, chloramine, and chlorine dioxide were quenched with 80

mg/L of sodium thiosulfate. During the ozone experiments, residual ozone had decayed within 30 minutes and no quenching agent was required. The ozone-treated samples remained loosely capped and stagnant for a 24 hour period prior to filtration in order to maintain continuity with the other oxidants. The combination of the dosage and contact time produced oxidant exposures that may be realized during drinking water treatment, especially if cells or filaments are retained on the surface of a media filter and continuously oxidized until backwashing. The oxidant exposure (CT) was determined by integrating the residual over time according to Equation (1):

$$CT = \int_0^t [Oxidant]dt = \frac{C_o}{k}(e^{kt} - 1) \quad (1)$$

where C_o is the initial residual concentration (mg/L), k is the first order decay rate for the oxidant (min^{-1}), and t is the exposure time (min). The average measured CT value for each oxidant is shown in Figure 2.1. Oxidant residual decay curves are provided in Figures S1.22-S1.33. After 24 hours, a sample was collected to measure the total and fluorescent cell concentration, and the remaining sample was filtered through a 0.70 µm glass fiber filter, which was used to measure the chlorophyll-a concentration.

Dissolved ozone stock solutions were made by dissolving a high concentration of gaseous ozone into deionized water at 2°C. Dissolved ozone stock solutions were typically 80 mg/L as measured using the indigo method (Standard Methods 4500-O3) [40]. All dissolved ozone residuals were measured using the indigo method (Standard Method 4500-O3). Chlorination experiments were performed using 5.6% liquid sodium

hypochlorite (NaOCl, Fisher Scientific, USA). Stock solutions of chlorine were prepared in DI water at 1,200 mg/L, and verified for accuracy on the day of testing. Free chlorine residuals were measured by the DPD Method using a spectrophotometer. A preformed chloramine solution was generated by first adding ammonia followed by sodium hypochlorite using a chlorine:ammonia ratio of 3:1. Stock solutions of each chemical were created from 29% ammonium hydroxide (J.T. Baker, USA) and 5.6% sodium hypochlorite (NaOCl, Fisher Scientific, USA). The pH of the preformed chloramine standard solution was maintained above 10, which favors monochloramine (pH>7.5) at the time of addition. Chlorine dioxide experiments were performed using a 3,000 mg/L solution (CDG Environmental, Bethlehem, PA, USA). Chlorine dioxide residuals were measured using the DPD method, which involved the addition of glycine to eliminate interference from free chlorine.

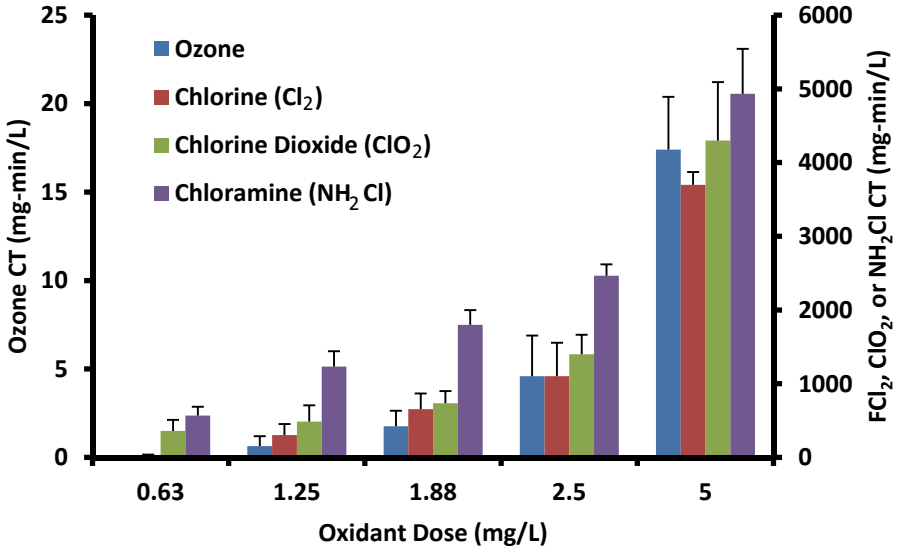

Figure 2.1. Relationship between Oxidant Dose and Oxidant Exposure (CT) among the four oxidants evaluated. (Note: Error bars indicate 1 standard deviation)

2.3.4. Analysis Methods

The digital flow cytometer was used to analyze samples for total particles (Auto-Image Mode (AIM)) and fluorescent particles (Trigger Mode (TM)). In TM, an excitation light source laser with a peak wavelength of 532 nm (green) was used to excite particles which pass in front of the magnification objective. Two photomultiplier tubes (PMTs), one capable of detecting fluorescence emissions of wavelength > 650 nm and the other 575 ± 30 nm, detect fluorescence emissions and in turn trigger the camera to capture images of the fluorescence-emitting particles. During TM analysis of the MA control samples, a 1:10 dilution was required so that 1 particle was imaged per frame by the digital flow cytometer. Chlorophyll-a analysis was performed using the spectrophotometric method described by Standard Method 10200H [40]. Cell damage was defined by a decrease in the TM cell concentration and chlorophyll-a concentration after oxidation. Cell lysis or fragmentation was defined by a decrease in the AIM cell concentration after oxidation.

For morphological analysis by VisualSpreadsheet, the FlowCAM® operating and analysis software, the color digital images are converted to binary images consisting of black and white pixels. The software compares the intensity of each pixel within the particle image to the intensity of the same pixel within the calibration (or background) image. If the pixels within the particle are lighter or darker than the background, and the difference in intensity is greater than the user-defined segmentation threshold (ΔIntensity=20), then the pixel is considered to be part of the particle (white pixel). Black pixels represent the background and are not considered part of the particle.

2.4. Results and Discussion

2.4.1. Assessment of Cyanobacteria Cell Damage

The fluorescent cell concentration and chlorophyll-a concentration are compared for ozone, chlorine, chlorine dioxide, and chloramine in Figures 2.2-2.5, respectively. The relative standard deviation (RSD) was determined from replicate experiments for fluorescent cell concentration (MA: RSD=21%, n=4, OSC: RSD=27%, n=8, LYN: RSD=27%, n=12) and chlorophyll-a concentration (MA: RSD=9%, n=13, OSC: RSD=11%, n=8, LYN: RSD=14%, n=11). The control chlorophyll-a concentration was measured to be 30.4 ± 0.6 μg/L for MA (200,000 cells/mL), 12.0 ± 3.6 μg/L for OSC (2,800 cells/mL), and 19.4 ± 2.1 μg/L of LYN (1,600 cells/mL). In most cases the fluorescent cell concentration correlated well with chlorophyll-a concentration indicating a loss of photosynthetic pigments.

Results from ozone oxidation showed that MA was more susceptible to cell damage than either OSC or LYN (Figure 2.2). Most MA cell damage occurred when using an ozone dose of 0.63 mg/L, which was near the ozone demand (apparent CT=0 mg-min/L). In the case of OSC and LYN, an ozone dose of 5 mg/L was required to reduce the chlorophyll-a concentration below 1 μg/L. Cell damage due to chlorine and chlorine dioxide oxidation showed a similar dose response in Figures 2.3 and 2.4, respectively. Again, MA appeared to be more susceptible to cell damage than either OSC or LYN based upon the chlorine or chlorine dioxide dose. Results from chloramine oxidation showed an initial 50% loss of chlorophyll-a independent of the applied dose for MA (Figure 2.5). These

results indicate that chloramine oxidation of MA involves an initial reaction (Phase 1) followed by a secondary reaction (Phase 2). OSC and LYN were resistant to chloramine oxidation with a minimal decrease in either the fluorescent cell concentration or the chlorophyll-a concentration.

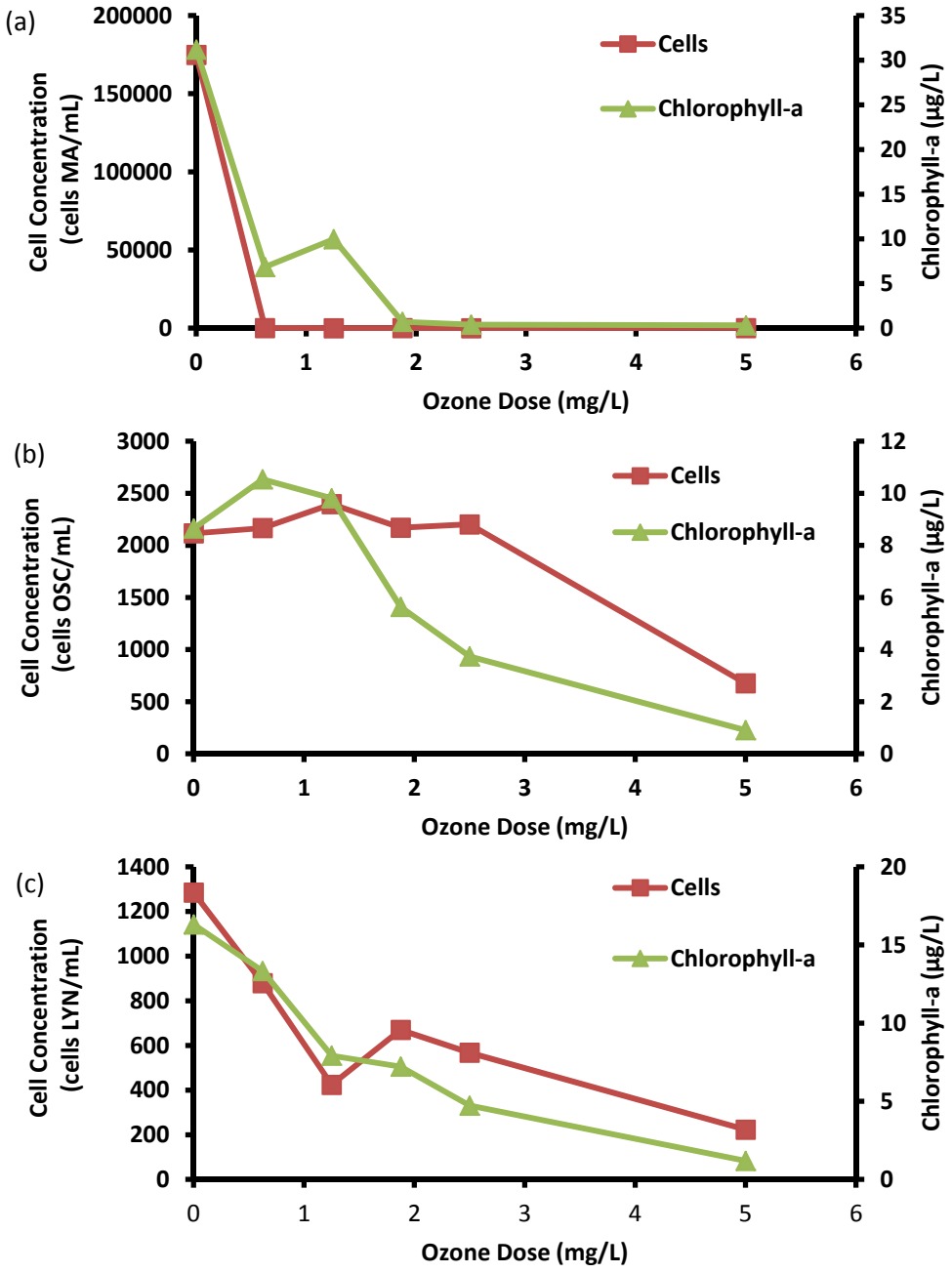

Figure 2.2. Decrease in fluorescent cell concentration and chlorophyll-a after ozone oxidation of cyanobacteria: (a) MA, (b) OSC, and (c) LYN.

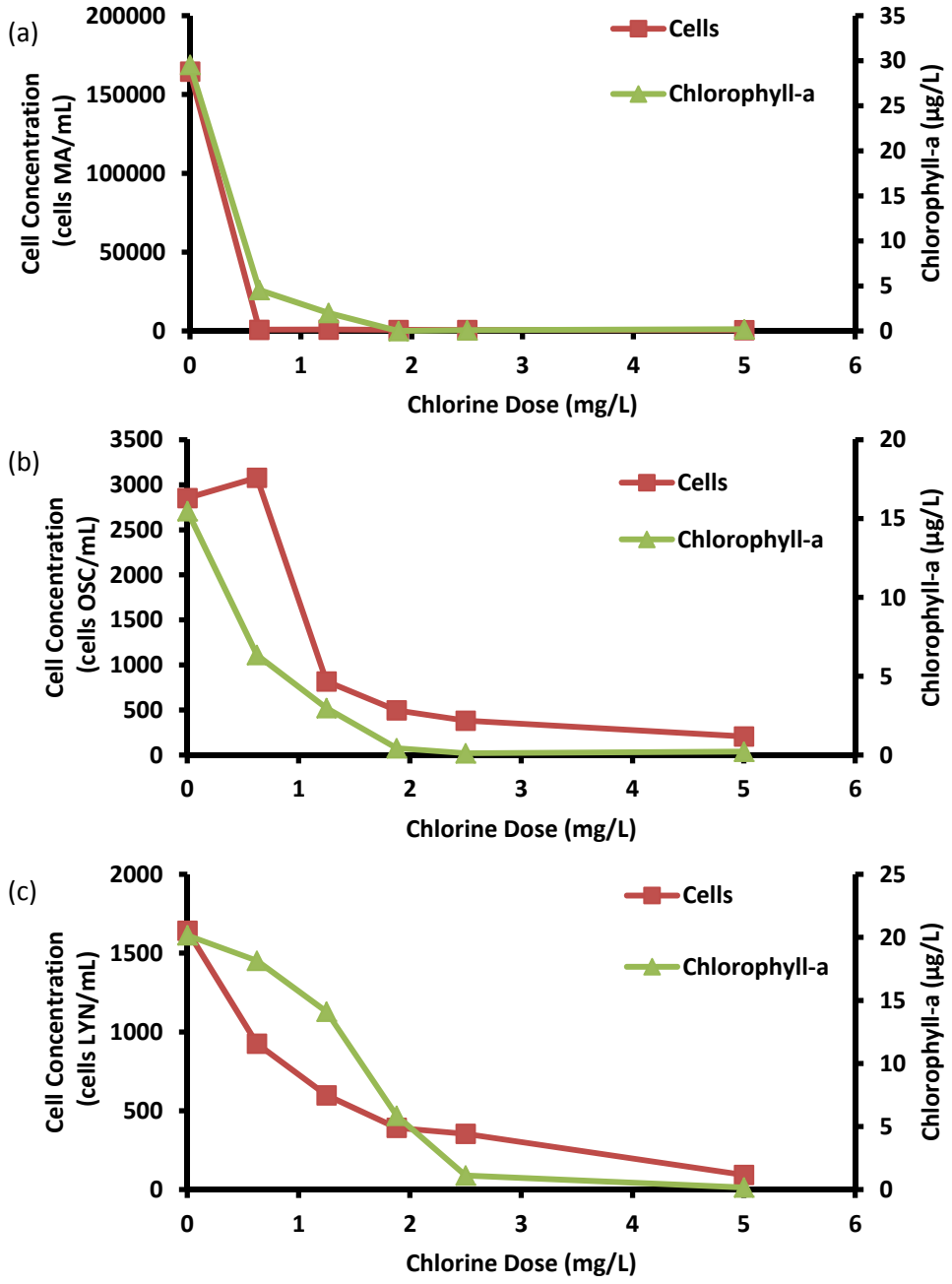

Figure 2.3. Decrease in fluorescent cell concentration and chlorophyll-a after chlorine oxidation of cyanobacteria: (a) MA, (b) OSC, and (c) LYN.

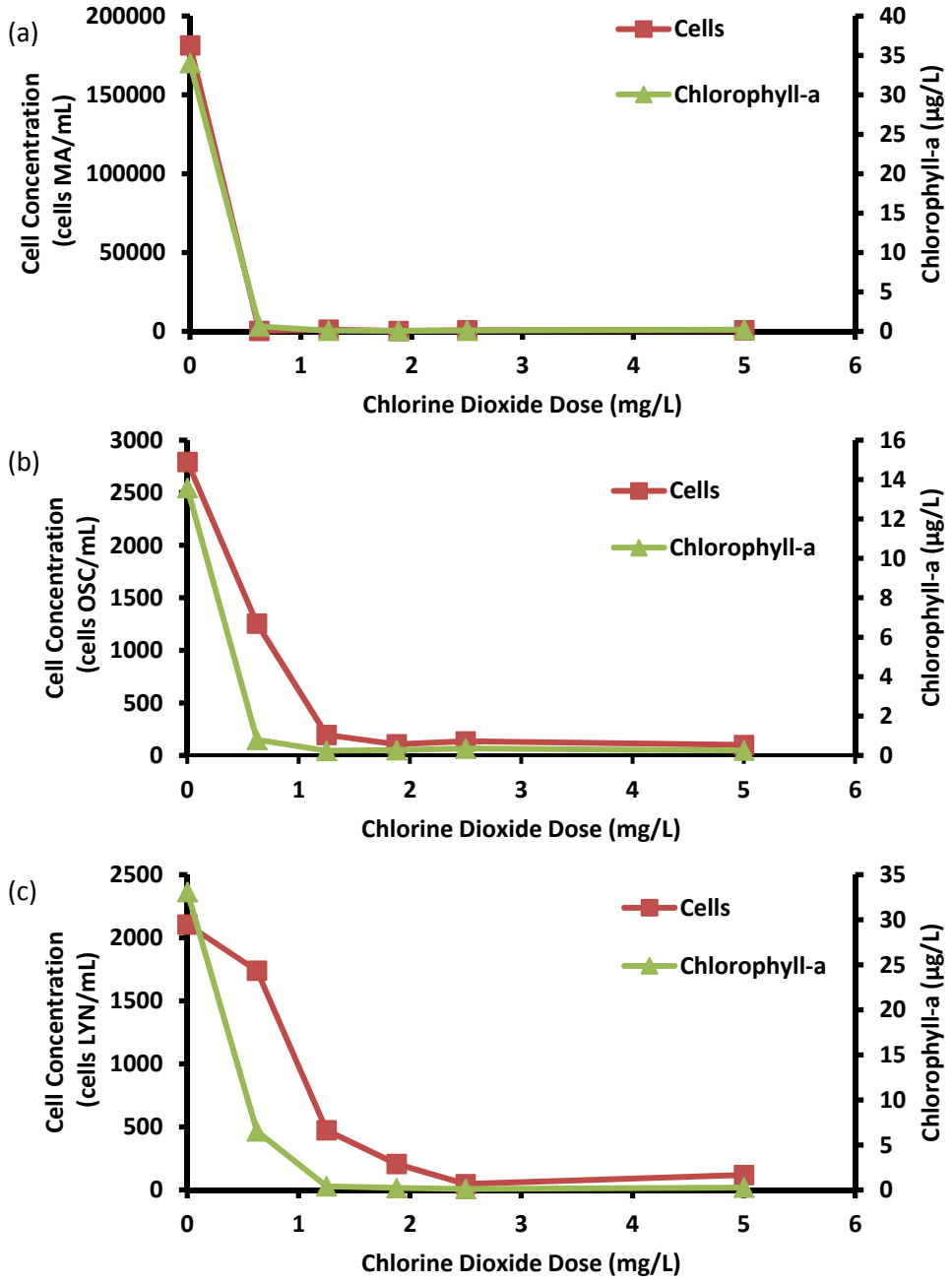

Figure 2.4. Decrease in fluorescent cell concentration and chlorophyll-a after chlorine dioxide oxidation of cyanobacteria: (a) MA, (b) OSC, and (c) LYN.

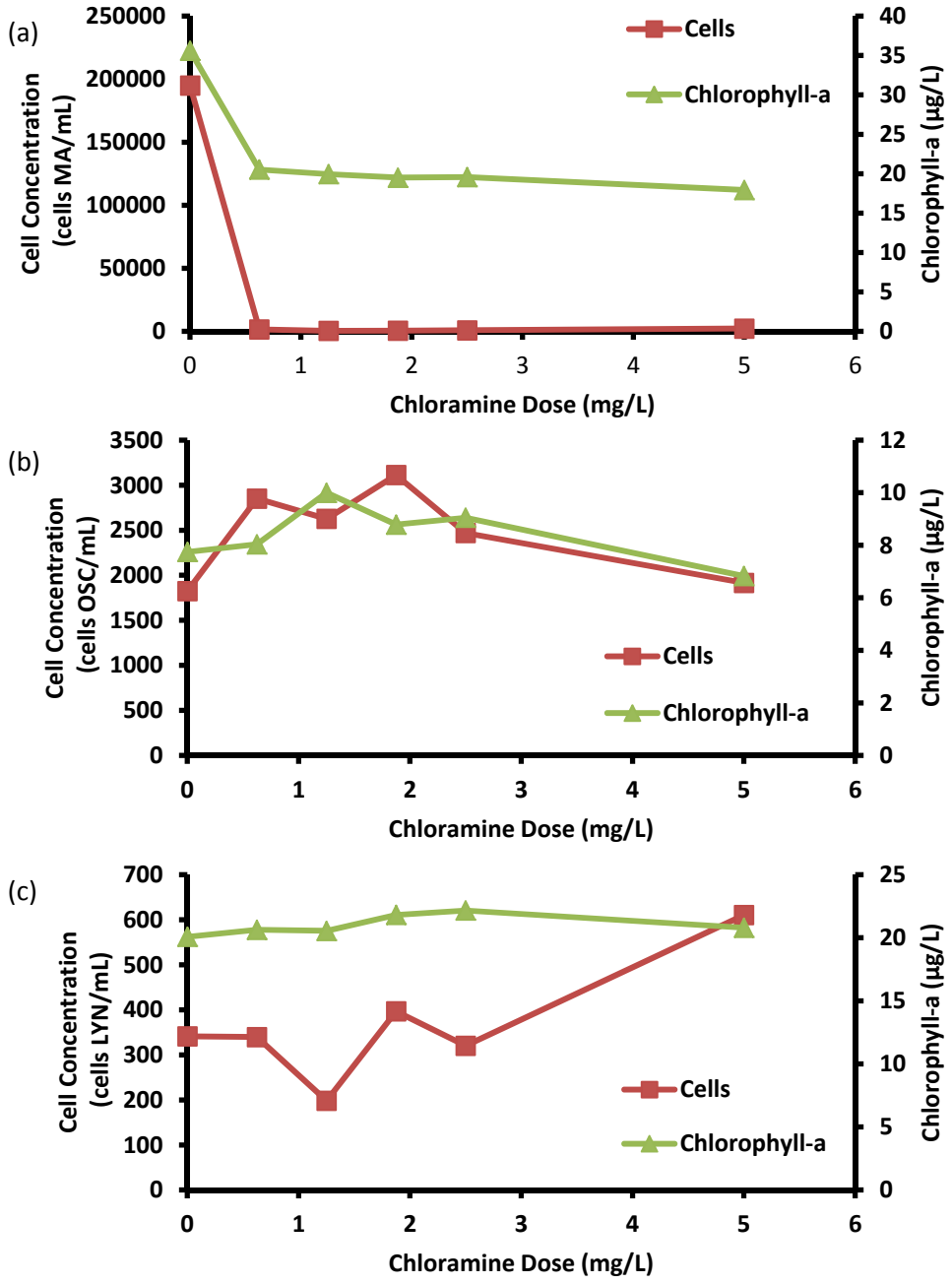

Figure 2.5. Fluorescent cell concentration and chlorophyll-a concentration after chloramine oxidation of cyanobacteria: (a) MA, (b) OSC, and (c) LYN.

2.4.2. Assessment of Cyanobacteria Cell Lysis

Total cell concentrations after oxidation by ozone, chlorine, chlorine dioxide, and chloramine are shown in Figure 2.6. In the case of MA, the lower ozone dosages of 0.63 mg/L and 1.25 mg/L decreased the total number of particles. As the ozone dose increased from 1.88 mg/L to 5 mg/L, there was a decrease in the total number of cells providing evidence of cell lysis. The decrease in the total particle concentration indicates that MA cells were degraded into fragments too small to be imaged, since the 20x objective can only capture particles greater than 3 μm in diameter. There was no significant decrease in total cell concentration after oxidation of OSC or LYN in Figures 2.6b and 2.6c, respectively. Since the total number of cells remained constant while the number of fluorescent particles decreased, the results indicate that the cells are being damaged (Figures 2.2-2.5) without resulting in complete lysis or fragmentation of the cell membrane (Figure 2.6) under the conditions studied.

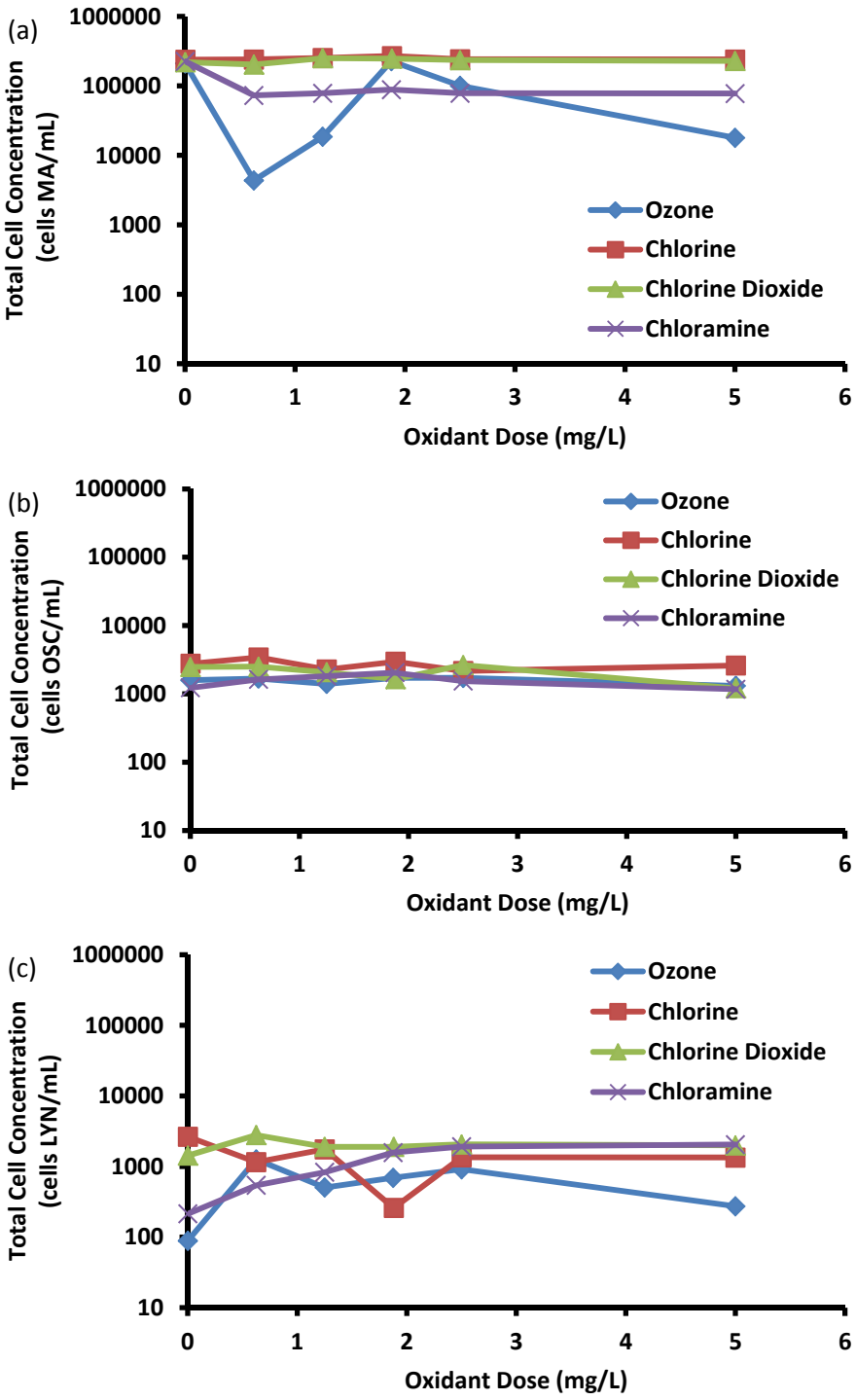

Figure 2.6. Total cell concentration after oxidation of cyanobacteria: (a) MA, (b) OSC, and (c) LYN.

2.4.3. Kinetics of Cyanobacteria Cell Damage

The kinetics of cyanobacteria cell damage were determined using the Chick-Watson equation [41, 42]. Using Equation (2), where N_o is the initial chlorophyll-a or TM cell concentration, N is the chlorophyll-a or TM cell concentration after oxidation, and the oxidant exposure ($\int$[Oxidant]dt), the second order rate constant (k_{damage}) can be determined for MA, OSC, and LYN. Chlorophyll-a data from Figures 2.2-2.5 was used to develop the rate constants using only the data when the chlorophyll-a concentration was greater than 0.5 µg/L. The relationship between chlorophyll-a degradation ($\ln(N/N_0)$) and ozone exposure is illustrated in Figure 2.7. The plots for chlorine, chlorine dioxide and chloramine are shown in Figures S1.4-S1.6 (based on chlorophyll-a) and Figures S1.7-S1.10 (based on TM cell concentration).

$$\ln\left(\frac{N}{N_0}\right) = -k_{damage} \int [\text{Oxidant}]\, dt \qquad (2)$$

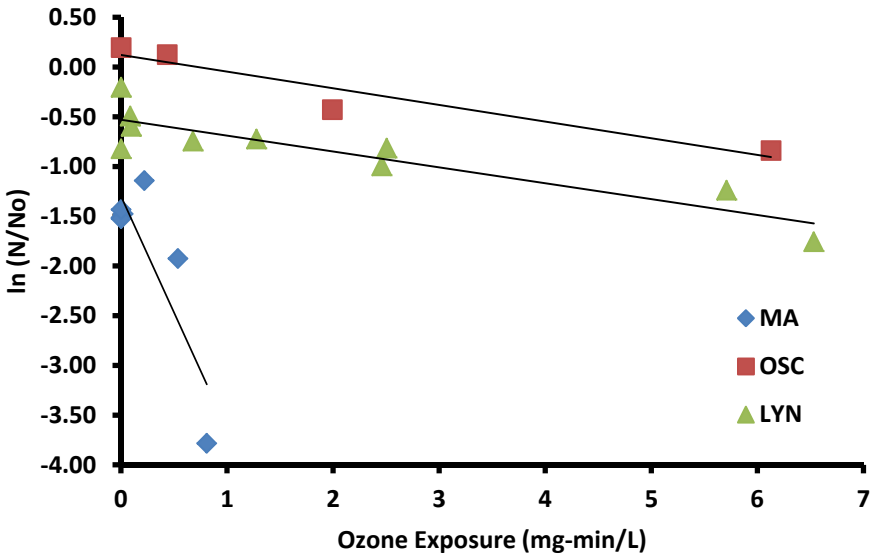

Figure 2.7. Relationship between ln(C/Co) and ozone exposure illustrating the determination of the second order rate constant for MA, OSC, and LYN in CRW at pH=8 and T=22°C.

The reaction rate constants obtained for MA, OSC, and LYN with ozone, chlorine, chlorine dioxide and chloramine are summarized in Table 2.1 using the chlorophyll-a concentration and Table 2.2 using the TM cell concentration. Additional data sets using MA (50,000 cells/mL) and LYN (800 cell/mL) were incorporated into the ozone and chlorine plots to increase the number of data points used in the rate constant determination. Rate constants developed for chlorine dioxide (MA, OSC, and LYN) and chlorine (MA only) were developed using a linear fit through the origin and data collected using a dose of 0.63 mg/L (n=2-3). All other rate constants were determined from the slope of the best fit linear regression line using chlorophyll-a (n=4-12, R^2=0.72-0.98) or TM cell concentration (n=4-10, R^2=0.59-0.91). The calculated rate constants were similar whether based on chlorophyll-a or TM cell concentration.

Results showed ozone and chlorine reacted with MA at a faster rate than OSC and LYN (Tables 2.1 and 2.2). The differences in these reaction rates indicate that the unicellular MA was more susceptible to oxidation than the filamentous OSC and LYN. However, other studies using chlorine have shown the rate constants with filamentous cyanobacteria (i.e. *Anabaena circinalis, Cylindrospermopsis raciborskii, Aphanizomenon issatsckenka*) are faster (k_{appt}=1,607-4,190 $M^{-1}s^{-1}$) than with the unicellular of colonial MA (k_{appt}=756-1,100 $M^{-1}s^{-1}$) [20, 21]. Many factors may contribute to these differences including cyanobacteria strain specificity, filament thickness, cell membrane thickness, growth stage, and the presence or absence of a mucilaginous sheath. Furthermore, other research identified differences in the s-layer lattice patterns of MA (hexagonal), OSC (square), and LYN (square) [26]. Since OSC and LYN were shown to have similar rate

constants, the thick mucilaginous sheath observed with LYN did not appear to decrease the rate of oxidation.

Based upon the rate constants in Tables 2.1 and 2.2, the ability of these oxidants to degrade the three cyanobacteria studied increases according to ozone > chlorine ~ chlorine dioxide > chloramine. These rates were similar in magnitude to those developed for bacterial cell membranes [24]. They also coincide with another study that concluded the degradation effect of chlorine dioxide on algae was similar or better than chlorine [43]. The second order rate constant between chlorine and MA cells (on a chlorophyll-a basis) in this study (2,900 $M^{-1}s^{-1}$) was greater than that reported during other research based upon the loss of cell viability: 670±77 $M^{-1}s^{-1}$ [17], 790-1,100 $M^{-1}s^{-1}$ [20], 756-1,030 $M^{-1}s^{-1}$ [21]. Many factors may contribute to these differences in reaction rate constants including strain specificity of MA, growth phase, and water source.

Table 2.1. Summary of reaction rate constants of cell damage (k_{damage}) obtained from chlorophyll-a degradation in CRW at pH=8 and T=22°C.

Oxidant	Rate Constant[(a)] k, $M^{-1}s^{-1}$		
	MA	OSC	LYN
Ozone	$1.1x10^5$	$6.0x10^3$	$5.5x10^3$
Chlorine	$2.9x10^{3(b)}$	$2.0x10^2$	$1.7x10^2$
Chlorine Dioxide	$4.9x10^{2(b)}$	$9.8x10^{2(b)}$	$3.2x10^{2(b)}$
Chloramine	Phase 1: $70^{(b)}$ Phase 2: 2.1	3.5	<1

(a) Rate constants were determined from the best-fit linear regression line unless otherwise noted (n=4-12, R^2=0.72-0.98).
(b) Rate constants were determined from the slope of the line through the origin and data collected using a dose of 0.63 mg/L (n=2-3).

Table 2.2. Summary of reaction rate constants of cell damage (k_{damage}) obtained from TM cell concentration in CRW at pH=8 and T=22°C.

Oxidant	Rate Constant[(a)] k_{damage}, $M^{-1}s^{-1}$		
	MA	OSC	LYN
Ozone	$5.7x10^5$	$3.1x10^3$	$3.2x10^3$
Chlorine	$8.6x10^{3(b)}$	$9.1x10^1$	$4.2x10^1$
Chlorine Dioxide	$8.4x10^{2(b)}$	$1.5x10^2$	$2.7x10^2$
Chloramine	Phase 1: $5.9x10^{2(b)}$ Phase 2: 7.0	2.8	5.6

(a) Rate constants were determined from the best-fit linear regression line unless otherwise noted (n=4-10, R^2=0.59-0.91).
(b) Rate constants were determined from the slope of the line through the origin and data collected using a dose of 0.63 mg/L (n=2-3).

Results showed ozone and free chlorine reacted with MA at a faster rate than OSC and LYN (Table 2.1). The differences in these reaction rates indicate that the unicellular morphology of MA may be more susceptible to oxidation than the filamentous morphology of OSC and LYN. Since OSC and LYN were shown to have similar rate constants, the thick mucilaginous sheath observed with LYN did not appear to decrease the rate of ozone oxidation. Rate constants developed for chlorine dioxide and chloramine were similar among the three cyanobacteria indicating that cell morphology may have little impact on their degradation. Additional studies would be needed with other genus and species of different morphology to confirm this theory. In addition, the role of hydroxyl radicals on cyanobacteria degradation by ozone was not investigated as part of this study.

Based upon the rate constants in Table 2.1, the ability of these oxidants to degrade the three cyanobacteria studied increases according to ozone > free chlorine ~ chlorine dioxide > chloramine. These rates were similar in magnitude to those developed for bacterial cell membranes [24]. They also coincide with another study that concluded the degradation effect of chlorine dioxide on algae was similar or better than free chlorine [41]. The rate constants can also be used determined the degree of cyanobacteria cell damage during disinfection. Regulatory guidelines often determine the oxidant exposure for disinfection at a given temperature. During the oxidation of MA by chlorine, Daly et. al. reported cell lysis with chlorine exposures between 7-29 mg-min/L [17]. When evaluating these chlorine exposures with the rate constants in Table 2.1, approximately 26% to 72% of chlorophyll-a can be expected to be lost after oxidation. Based upon the rate constant and the oxidant exposure requirement, the corresponding degree of cyanobacteria degradation can be predicted.

2.4.4. Morphological Changes from Cell Oxidation

The digital flow cytometer generates both digital color images and a corresponding binary image as discussed previously. Since images are generated for every particle passing through the flow cell, typical images captured before and after oxidation by ozone, chlorine, chloramine, and chlorine dioxide using a dose of 5 mg/L are presented in Table 2.3. The images are associated with the total cell concentration (AIM mode), which may include both damaged and recalcitrant cyanobacteria cells. Additional digital

and binary images for MA, OSC, and LYN for all dose conditions are included in the Supplemental Information (Figures S1.11-S1.22).

In the case of MA, the binary images before oxidation show an uncompromised intracellular structure, as indicated by the solid white interior shown in the binary image. The image indicates that the light intensity within the cell is greater than the background (exceeds the segmentation threshold), and all pixels are considered to be part of the particle. After ozone and chloramine oxidation, either full or partial interior halos (black pixels) are observed indicating that the intracellular intensity was weaker around the interior perimeter of the cell membrane after oxidation.

In the cases of OSC and LYN, the digital and binary images taken before oxidation show an elongated shape with an uncompromised cell interior (white pixels). After oxidation, the digital color photos provided visual evidence of the loss of chlorophyll-a . Binary images showed that the cell membrane and filament structure remained largely intact after oxidation. In Table 2.3, the binary image taken of OSC after exposure to 5 mg/L of chlorine dioxide illustrates that the interior cell membranes within the filament remain intact. Interestingly, the cells comprising the OSC filament, which are not protected by a mucilaginous sheath, were not separated into individual cells following oxidation. The images also showed that the outer perimeter was damaged by the oxidants to varying degrees, and the ends of some filaments appeared to be compromised first rather than the more uniform oxidation across the entire filament (Figures S1.15-S1.22).

Although providing a qualitative assessment of cell degradation, the color digital images combined with the binary image can be used to assess the relative degree of cell destruction. The images could also lead to a better understanding of how the different oxidants attack these cells or filaments by adjusting the segmentation threshold settings. When used in conjunction with chlorophyll-a and other physical particle properties measured by the digital flow cytometer, a more quantitative approach can be applied to evaluate cyanobacteria cell damage and lysis

Table 2.3. Morphological changes in cyanobacteria cell structure and intensity before and after oxidation according to the digital and binary images collected in AIM by the FlowCAM.

Cyanobacteria	Before Oxidation (Control)	Ozone (5 mg/L)	Chlorine (5 mg/L)	Chlorine Dioxide (5 mg/L)	Chloramine (5 mg/L)
Microcystis aeruginosa	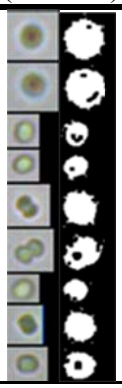		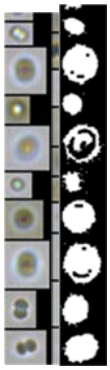	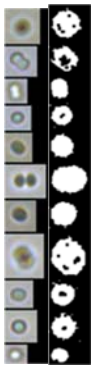	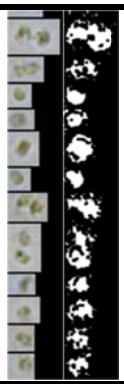
Oscillatoria sp.		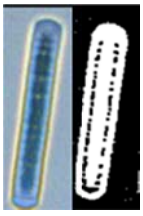	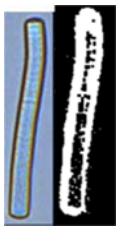	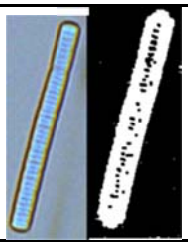	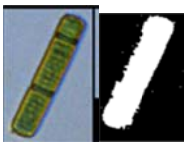
Lyngbya sp.	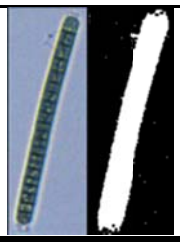		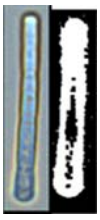	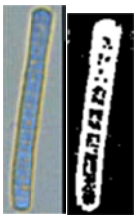	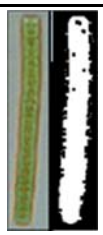

2.5. Conclusions

- The digital flow cytometer provided a rapid method to obtain quantitative and qualitative information regarding cyanobacteria cell damage and lysis. Quantitative results included total particle concentration and fluorescent particle concentration. Qualitative results included digital and binary images collected at 10-20x magnification.
- Cell damage was defined by the loss of chlorophyll-a as quantified using the fluorescent particle concentration and chlorophyll-a analysis. Ozone, chlorine, and chlorine dioxide were able to compromise the cell integrity of each cyanobacteria resulting in a decrease in both fluorescent particles and chlorophyll-a. Chloramines compromised the cell integrity of MA, but were unable to damage OSC or LYN.
- Cell lysis was defined as the fragmentation of the unicellular or filamentous structure, and quantified by a change in the total particle concentration. MA cells were susceptible to cell lysis using ozone and chloramine. OSC and LYN cells were not susceptible to cell lysis by any of the oxidants under the dose conditions tested.
- According to the rate constants developed from the loss of chlorophyll-a, the oxidants degraded the three cyanobacteria studied according to ozone > chlorine ~ chlorine dioxide > chloramine. The mechanism of chlorophyll-a loss was not identified and may result from an intracellular reaction with the oxidant or a release through a damaged cell membrane.

- During ozone and chlorine oxidation experiments, cell morphology appeared to influence the rate constant. During ozonation, the unicellular MA ($k=1.1x10^5$ $M^{-1}s^{-1}$) was more susceptible to oxidation than the filamentous OSC ($k=6.0x10^3$ $M^{-1}s^{-1}$) and LYN ($k=5.5x10^3$ $M^{-1}s^{-1}$).
- Digital and binary images generated by the digital flow cytometer provided some perspective regarding how the oxidants may be damaging the cell structure. In the case of MA, the oxidants appeared to initially damage the cell wall resulting in the oxidation and/or release of chlorophyll-a before causing lysis and fragmentation of the cell membrane.

2.6. References

1. Paerl, H. W.; Huisman, J., Climate change: a catalyst for global expansion of harmful cyanobacterial blooms. *Environmental Microbiology Reports* 2009, *1*, (1), 27-37.

2. Falconer, I. R.; Humpage, A. R., Cyanobacterial (Blue-Green algal) toxins in water supplies: Cylindrospermopsins. *Environmental Toxicology* 2006, *21*, (4), 299-304.

3. Graham, J. L.; Loftin, K. A.; Meyer, M. T.; Ziegler, A. C., Cyanotoxin Mixtures and Taste-and-Odor Compounds in Cyanobacterial Blooms from the Midwestern United States. *Environ. Sci. Technol.* 2010, *44*, (19), 7361-7368.

4. Izaguirre, G.; Jungblut, A.-D.; Neilan, B. A., Benthic cyanobacteria (Oscillatoriaceae) that produce microcystin-LR, isolated from four reservoirs in southern California. *Water Res.* 2007, *41*, (2), 492-498.

5. Kotak, B. G.; Zurawell, R. W., Cyanobacterial toxins in Canadian freshwaters: A review. *Lake and Reservoir Management* 2007, *23*, (2), 109-122.

6. Velzeboer, R. M. A.; Baker, P. D.; Rositano, J.; Heresztyn, T.; Codd, G. A.; Raggett, S. L., Geographical petterns of occurrence and composition of saxitoxins in the cyanobacterial genus Anabaena (Nostocales, Cyanophyta) in Australia. *Phycologia* 2000, *39*, (5), 395-407.

7. Smith, J. L.; Boyer, G. L.; Zimba, P. V., A review of cyanobacterial odorous and bioactive metabolites: Impacts and management alternatives in aquaculture. *Aquaculture* 2008, *280*, (1-4), 5-20.

8. Watson, S. B., Cyanobacterial and eukaryotic algal odour compounds: signals or by-products? A review of their biological activity. *Phycologia* 2003, *42*, (4), 332-350.

9. Young, W. F.; Horth, H.; Crane, R.; Ogden, T.; Arnott, M., Taste and Odour Threshold Concentrations of Potential Potable Water Contaminants. *Water Res.* 1996, *30*, (2), 331-340.

10. Watson, S. B., Aquatic taste and odor: A primary signal of drinking-water integrity. *J. Toxicol. Env. Health Part A* 2004, *67*, (20-22), 1779-1795.

11. Glaze, W. H.; Schep, R.; Chauncey, W.; Ruth, E. C.; Zarnoch, J. J.; Aieta, E. M.; Tate, C. H.; McGuire, M. J., Evaluating Oxidants for the Removal of Model Taste and Odor Compounds From a Municipal Water Supply. *J.-Am. Water Works Assoc.* 1990, *82*, (5), 79-84.

12. Lalezary, S.; Pirbazari, M.; McGuire, M. J., Oxidation of Five Earthy-Musty Taste and Odor Compounds. *J.-Am. Water Works Assoc.* 1986, *78*, (3), 62-69.

13. Rodriguez, E.; Onstad, G. D.; Kull, T. P. J.; Metcalf, J. S.; Acero, J. L.; von Gunten, U., Oxidative elimination of cyanotoxins: Comparison of ozone, chlorine, chlorine dioxide and permanganate. *Water Res.* 2007, *41*, (2007), 3381-3393.

14. Westrick, J. A.; Szlag, D. C.; Southwell, B. J.; Sinclair, J., A review of cyanobacteria and cyanotoxins remova/inactivation in drinking water treatment. *Analytical and Bioanalytical Chemistry* 2010, *397*, (5), 1705-1714.

15. Ho, L.; Sawade, E.; Newcombe, G., Biological treatment options for cyanobacteria metabolite removal - A review. *Water Res.* 2012, *46*, (5), 1536-1548.

16. Peter, A.; von Gunten, U., Oxidation Kinetics of Selected Taste and Odor Compounds During Ozonation of Drinking Water. *Environmental Science & Technology* 2007, *41*, (2), 626-631.

17. Daly, R.; Ho, L.; Brookes, J. D., Effect of Chlorination on Microcystis aeruginosa Cell Integrity and Subsequent Microcystin Release and Degradation. *Environ. Sci. Technol.* 2007, *41*, (12), 4447-4453.

18. Ding, J.; Shi, H.; Timmons, T.; Adams, C., Release and Removal of Microcystins from Microcystis during Oxidative-, Physical-, and UV-Based Disinfection. *Journal of Environmental Engineering* 2010, *136*, (1), 2-11.

19. Ho, L.; Kayal, N.; Trolio, R.; Newcombe, G., Determining the fate of Microcystis aeruginosa cells and microcystin toxins following chloramination. *Water Science and Technology* 2010, *62*, (2), 442-450.

20. Lin, T.-F.; Chang, D.-W.; Lien, S.-K.; Tseng, Y.-S.; Chiu, Y.-T.; Wang, Y.-S., Effect of chlorination on the cell integrity of two noxious cyanobacteria and their releases of odorants. *Journal of Water Supply: Research and Technology-AQUA* 2009, *58*, (8), 539-551.

21. Zamyadi, A.; Ho, L.; Newcombe, G.; Bustamante, H.; Prevost, M., Fate of toxic cyanobacterial cells and disinfection by-products formation after chlorination. *Water Res.* 2012, *46*, (5), 1524-1535.

22. Zamyadi, A.; Ho, L.; Newcombe, G.; Daly, R. I.; Burch, M.; Baker, P.; Prevost, M., Release and Oxidation of Cell-Bound Saxitoxins during Chlorination of Anabaena circinalis Cells. *Environ. Sci. Technol.* 2010, *44*, (23), 9055-9061.

23. Zamyadi, A.; Fan, Y.; Daly, R. I.; Prevost, M., Chlorination of Microcystis aeruginosa: Toxin release and oxidation, cellular chlorine demand and disinfection by-products formation. *Water Res.* 2012.

24. Ramseier, M. K.; von Gunten, U.; Freihofer, P.; Hammes, F., Kinetics of membrane damage to high (HNA) and low (LNA) nucleic acid bacterial clusters in drinking water by ozone, chlorine, chlorine dioxide, monochloramine, ferrate(VI), and permanganate. *Water Res.* 2011, *45*, (3), 1490-1500.

25. Scott, D. B. M.; Lesher, E. C., Effect of Ozone on Survival and Permeability of Escherichia Coli. *Journal of Bacteriology* 1963, *85*, (3), 567-&.

26. Smarda, J.; Smajs, D.; Komrska, J.; Krzyzanek, V., S-layers on cell walls of cyanobacteria. *Micron* 2002, *33*, (3), 257-277.

27. Van Cruchten, S.; Van den Broeck, W., Morphological and biochemical aspects of apoptosis, oncosis and necrosis. *Anat. Histol. Embryol.* 2002, *31*, (4), 214-223.

28. Leist, M.; Jaattela, M., Four deaths and a funeral: From caspases to alternative mechanisms. *Nat. Rev. Mol. Cell Biol.* 2001, *2*, (8), 589-598.

29. Peterson, H. G.; Hrudey, S. E.; Cantin, I. A.; Perley, T. R.; Kenefick, S. L., Physiological toxicity, cell membrane damage and the release of dissolved organic carbon and geosmin by aphanizomenon flos-aquae after exposure to water treatment chemicals. *Water Res.* 1995, *29*, (6), 1515-1523.

30. Huang, W.-J.; Cheng, Y.-L.; Cheng, B.-L., Effect of water quality on destruction of odor causing substances during ozonation processes. *J. Environ. Eng. Manage.* 2007, *17*, (4), 257-265.

31. Ma, M.; Liu, R. P.; Liu, H. J.; Qu, J. H., Chlorination of Microcystis aeruginosa suspension: Cell lysis, toxin release and degradation. *Journal of Hazardous Materials* 2012, *217*, 279-285.

32. Miao, H.; Tao, W., The mechanisms of ozonation on cyanobacteria and its toxins removal. *Separation Science and Technology* 2009, *66*, (1), 187-193.

33. Plummer, J. D.; Edzwald, J. K., Effects of chlorine and ozone on algal cell properties and removal of algae by coagulation. *Journal of Water Supply: Research and Technology-AQUA* 2002, *51*, (6), 307-318.

34. Pietsch, J.; Bornmann, K.; Schmidt, W., Relevance of Intra- and Extracellular Cyanotoxins for Drinking Water Treatment. *Acta Hydrochimica et Hydrobiologica* 2002, *30*, (1), 7-15.

35. Watanabe, M. F.; Harada, K.-I.; Matsuura, K.; Watanabe, M.; Suzuki, M., Heptapeptide toxin production during the batch culture of two microcystis species. *Journal of Applied Phycology* 1989, *1*, 161-165.

36. Watanabe, M. F.; Oishi, S., Effects of environmental factors on toxicity of a cyanobacterium (*Microcystis aeruginosa*) under culture conditions. *Applied and Environmental Microbiology* 1985, *49*, (5), 1342-1344.

37. Jakobsen, H. H.; Carstensen, J., FlowCAM: Sizing cells and understanding the impact of size distributions on biovolume of planktonic community structure. *Aquat. Microb. Ecol.* 2011, *65*, (1), 75-87.

38. Alvarez, E.; Lopez-Urrutia, A.; Nogueira, E.; Fraga, S., How to effectively sample the plankton size spectrum? A case study using FlowCAM. *J. Plankton Res.* 2011, *33*, (7), 1119-1133.

39. Buskey, E. J.; Hyatt, C. J., Use of the FlowCAM for semi-automated recognition and, enumeration of red tide cells (Karenia brevis) in natural plankton samples. *Harmful Algae* 2006, *5*, (6), 685-692.

40. APHA; AWWA; WEF, *Standard Methods for the Examination of Water and Wastewater*. 20th ed.; American Public Health Association, American Water Works Association, Water Environment Federation: Washington D.C., 1998.

41. Watson, H. E., A note on the variation of the rate of disinfection with change in the concentration of the disinfectant. *J. Hyg.* 1908, *8*, (4), 536-542.

42. Chick, H., An investigation of the laws of disinfection. *J. Hyg.* 1908, *8*, (1), 92-158.

43. Junli, H.; Li, W.; Nenqi, R.; Xi, L. X.; Fun, S. R.; Guanle, Y., Disinfection effect of chlorine dioxide on viruses, algae and animal planktons in water. *Water Res.* 1997, *31*, (3), 455-460.

CHAPTER 3. Effect of Oxidant Exposure on the Release of Intracellular Microcystin, MIB, and Geosmin from *Microcystis aeruginosa*, *Oscillatoria sp.*, and *Lyngbya sp.*

3.1. Abstract

The release of intracellular microcystin-LR (MC-LR), 2-methylisoborneol (MIB), and geomsin was investigated after the oxidation of three cyanobacteria (*Microcystis aeruginosa* (MA), *Oscillatoria sp*. (OSC), and *Lyngbya sp*. (LYN). During the oxidation of 200,000 cells/mL of MA, release of intracellular MC-LR exceeded the World Health Organization (WHO) guideline of 1 μg/L during the lowest oxidant exposures (CT) tested: ozone (0 mg-min/L), free chlorine (<40 mg-min/L), chlorine dioxide (<558 mg-min/L), and chloramine (<636 mg-min/L). As the CT increased, ozone, free chlorine, and chlorine dioxide were able to oxidize the released MC-LR, which was expected based upon published kinetic information. During the oxidation of OSC and LYN, release of intracellular MIB and geosmin exceeded reported threshold odor values after exposure to free chlorine, chlorine dioxide, and chloramine, which have low reactivity with these taste and odor compounds. Ozone oxidation of OSC yielded an increase in MIB concentration when insufficient dissolved ozone residual was detected (CT=0 mg-min/L). At greater ozone dosages, there was no net increase in MIB concentration, likely due to sufficient oxidation by hydroxyl radicals. In all cases, the dissolved organic carbon (DOC) release was less than 0.25 mg/L, which lacked the sensitivity to predict the release of MC-LR, MIB, or geosmin. These results expand on available information

regarding the release of toxic or odorous metabolites during oxidation processes in drinking water treatment.

3.2. Introduction

Due to the effects of climate change, the frequency and intensity of harmful cyanobacteria blooms is expected to increase [1]. Harmful cyanobacteria blooms directly impact the quality of drinking water through the production of toxic metabolites, odorous metabolites or both. Several toxins including microcystins, anatoxin-a, saxitoxins, cylindrospermopsin, and nodularins are known to be generated by specific cyanobacteria genera (e.g. *Anabaena*, *Aphanizomenon*, *Lyngbya*, *Microcystis*, *Oscillatoria*, and *Planktothrix*) [2-4]. Of these toxins, microcystin-LR (MC-LR) has received the most attention from regulatory agencies with a provisional guideline values established by the World Health Organization (1 µg/L) [5], a maximum acceptable concentration established by Health Canada (1.5 µg/L) [6], and inclusion on the United States Environmental Protection Agency's Contaminant Candidate List 3 [7]. Studies investigating the occurrence of MC-LR in surface waters have found concentrations ranging from 0.14 to 13,000 µg/L in the United States [8-11] and Canada [12].

The elimination of extracellular MC-LR has been evaluated through physical, chemical, and biological treatment methods [13, 14]. Reaction rate constant values for the oxidation of MC-LR by different oxidants have been reported (pH=8 at 20°C) using ozone (k_{app}=4.1 x 10^5 $M^{-1}s^{-1}$), hydroxyl radicals (HO•, k_{app}=1.1 x 10^{10} $M^{-1}s^{-1}$), chlorine (k_{app}=33 $M^{-1}s^{-1}$), chlorine dioxide (k_{app}=1 $M^{-1}s^{-1}$), and chloramine (k_{app}< 1 $M^{-1}s^{-1}$) [15]. A fast reaction

between ozone and MC-LR resulted in a low ozone dose requirement (0.2-0.7 mg/L) for >95% elimination in waters with dissolved organic carbon (DOC) between 1.6 and 5.7 mg/L [16, 17]. During chlorination, hypochlorous acid (k=475 $M^{-1}s^{-1}$, pH=4.8) was found to be more effective than hypochlorite (k=9.8 $M^{-1}s^{-1}$, pH=8.8) for MC-LR oxidation with a pH less than 8 recommended for degradation during drinking water applications [18]. Due to the low reaction rate constant with chlorine dioxide and competition from background natural organic matter, a chlorine dioxide dose greater than 1 mg/L was recommended for oxidation [19, 20]. Lastly, a slow reaction rate between MC-LR and chloramine implies greater exposure requirements (>30,000 mg-min/L) for significant degradation [21].

Numerous taste and odor compounds have been identified from different cyanobacteria genera including *Anabaena*, *Aphanizomenon*, *Oscillatoria*, *Lyngbya*, *Phormidium*, and *Planktothrix*, which can also produce toxins depending on the specific strain [22-25]. Geosmin and 2-methylisoborneol (MIB) are the two most frequently detected in drinking water sources with threshold odor values reported from 1.3-4.0 ng/L and 6.3-15 ng/L, respectively [25, 26]. Although these compounds do not pose any human health risk, the aesthetics of the drinking water with respect to taste and odor directly impact consumer confidence [25]. Due to this concern, elimination of extracellular MIB and geosmin has been evaluated during oxidation processes [27, 28]. During ozonation, hydroxyl radicals provide the major oxidation pathway for the elimination of MIB (k_{O3}=0.35 $M^{-1}s^{-1}$, k_{HO}=5.1 x 10^9 $M^{-1}s^{-1}$) and geosmin (k_{O3}=0.10 $M^{-1}s^{-1}$, k_{HO}=7.8 x 10^9 $M^{-1}s^{-1}$) [29]. Free chlorine, chloramine, and chlorine dioxide have proven to be ineffective for the oxidation of MIB or geosmin under typical drinking water conditions [27, 28].

While a majority of research has focused on the treatment and occurrence of extracellular metabolites, the release of intracellular (or cell bound) metabolites during drinking water treatment processes can also lead to increased extracellular concentrations. Removing intact cyanobacteria cells is the most effective way to minimize the risk of releasing intracellular organic matter (IOM). Physical treatment techniques such as microstrainers, coagulation/filtration, or dissolved air flotation are capable of removing >98% of problematic cyanobacteria cells (including cell-bound or intracellular metabolites) from the water supply [13]. However, many drinking water treatment plants initially use an oxidation process (referred to as preoxidation) to meet treatment objectives such as disinfection, mussel/biofilm control on intake pipelines, iron/manganese oxidation, oxidation of extracellular taste and odor compounds, oxidation of DBP precursors, etc. As a result, preoxidation may increase the total extracellular concentration of odorous and/or toxic metabolites if cell damage and metabolite release exceed the rate of oxidation during drinking water treatment.

Previous studies have focused on a variety of oxidants (i.e. ozone, chlorine, chlorine dioxide, chloramine, potassium permanganate, ferrate, copper sulfate) and their ability to damage cyanobacteria cells resulting in the release of intracellular metabolites (i.e. geosmin, MC-LR) [30-32]. Oxidants with poor reactivity with the metabolite of concern were more likely to result in accumulation during cell damage. The release and subsequent oxidation of cell-bound metabolites (e.g. MC-LR, cylindrospermopsin, saxitoxin, geosmin) from different cyanobacteria has been studied extensively after

exposure to chlorine [33-37]. Low chlorine exposures (< 4.0 to 29 mg-min/L) have resulted in the loss of cell viability and corresponding toxin release [33, 34, 36]. As a result, the potential to release and accumulate toxic or odorous metabolites warrants further investigation to identify the oxidant exposure conditions resulting in the release of intracellular metabolites.

In this study, the release of intracellular MC-LR, MIB, and geosmin was investigated after the oxidation of three morphologically distinct cyanobacteria (*Microcystis aeruginosa* (MA), *Oscillatoria sp*. (OSC), and *Lyngbya sp*. (LYN)). Cultured cells of MA, OSC, and LYN were used to conduct batch experiments with ozone, free chlorine, chlorine dioxide, and chloramine. The release of intracellular MC-LR, MIB, and geosmin was quantified in extracellular form after oxidation. Oxidant exposures were measured to provide a perspective to utilities regarding the conditions under which these compounds may be released into treated drinking water. The results follow previous research quantifying cell damage and lysis among the same cyanobacteria strains and oxidants using a digital flow cytometer [38].

3.3. Materials and Methods

3.3.1. Selection and Culturing of Cyanobacteria

Three cyanobacteria were selected based upon their occurrence in source water supplies, availability of an axenic culture, ability to produce odorous or toxic metabolites, and morphology. *Microcystis aeruginosa* (LB 2385, Culture Collection of Algae at the University of Texas, Austin, TX, USA) was a confirmed producer of MC-LR and

exhibited unicellular morphology. Axenic cultures of other characterized toxin-producing cyanobacteria were difficult to obtain through available culture collections in the United States. *Oscillatoria sp*. (LM 603d, Metropolitan Water District of Southern California (MWDSC), La Verne, CA, USA) was a confirmed MIB and geosmin producer and exhibited a filamentous morphology with no mucilaginous sheath. *Lyngyba sp*. (SDC 202d, MWDSC, La Verne, CA, USA) was a confirmed geosmin producer and exhibited a filamentous morphology with a mucilaginous sheath.

A batch culture method was selected due to the simplicity of the system and number of cells required. Culturing of cyanobacteria was performed inside a growth chamber (Geneva Scientific, Fontana, WI, USA) with constant light (12 hrs light followed by 12 hrs of darkness) and temperature (22°C) conditions. The cyanobacteria were cultured in either BG-11 growth media (for OSC and LYN) or Bold 3N growth media (for MA). A digital flow cytometer (FlowCAM®, Fluid Imaging Technologies, Yarmouth, ME, USA) was used to quantify the cell concentration in the stock cell suspension. In the case of OSC and LYN, the digital flow cytometer measured filament length and total particles. Light microscopy was used to determine the number of cells per unit length. The information from the digital flow cytometer and light microscopy was combined to give the cell concentration. The OSC and LYN cultures also required screening through a 100 µm mesh screen in order to prevent clogging of the flow cell. Therefore, only filaments <100 µm in length were used to conduct the testing.

Cultures of *Microcystis* have shown that intracellular microcystin content production is greatest at the end of the exponential growth phase, and then begins to decrease gradually decrease during the stationary phase as extracellular toxin release becomes more dominant [39-42]. Therefore, MA, OSC, and LYN cells were harvested at the end of the exponential growth phase (28 days) to maintain consistency among the strains. The cells were separated from the growth media using a centrifuge and the supernatant containing extracellular organic matter (EOM) was discarded. The remaining cell pellet was rinsed with 10 mM phosphate buffered MilliQ water (pH=7.5) prior to quantification using the digital flow cytometer. All cell suspensions were prepared fresh on the day of testing. Additional information regarding the culturing conditions, growth curve development, preparation of the cell suspension, and digital flow cytometer settings can be found elsewhere [38].

A sample of the IOM from each cyanobacteria was extracted by grinding with a mortar and pestle, (3) freeze-thaw sequences, and sonication. The cell debris was separated from the dissolved IOM through filtration (0.7 μm). The IOM standard was diluted in ultrapure water and the concentration of MC-LR, MIB, and geosmin was measured. Additional information regarding the IOM extraction process and IOM properties can be found elsewhere [43].

3.3.2. Experimental Methods

Oxidation experiments were performed as batch processes using Colorado River water (CRW) at ambient pH (7.7-8.0) and temperature (20-25°C). Ozone stock solutions were

made by dissolving a high concentration of gaseous ozone into deionized water at 2°C. Dissolved ozone stock solutions were typically 80 mg/L as measured using the indigo method (Standard Methods 4500-O3) [23]. Chlorination experiments were performed using 5.6% liquid sodium hypochlorite (NaOCl, Fisher Scientific, USA). A preformed chloramine solution was generated by first adding ammonia followed by sodium hypochlorite using a chlorine:ammonia ratio of 3:1. Stock solutions of each chemical were created from 29% ammonium hydroxide (J.T. Baker, USA) and 5.6% sodium hypochlorite (NaOCl, Fisher Scientific, USA). The pH of the preformed chloramine standard solution was maintained above 10, which favors monochloramine (pH>7.5) at the time of addition. Chlorine dioxide experiments were performed using a 3,000 mg/L solution (CDG Environmental, Bethlehem, PA, USA).

Aliquots of the concentrated cell suspension were transferred into individual 1L amber glass bottles to achieve the desired cell concentrations of MA (50,000 and 200,000 cells/mL), OSC (1,400 and 2,800 cells/mL), and LYN (1,600 and 3,200 cells/mL). Cell concentrations for MA were selected with consideration given to published Alert level 1 (2,000 cells/mL, 1 µg/L chlorophyll-a) and Alert level 2 (100,000 cells/mL, 50 µg/L chlorophyll-a), which were derived from the WHO guideline for MC-LR [44]. Then, either free chlorine, ozone, monochloramine, or chlorine dioxide was applied to achieve an oxidant:DOC mass ratio of 0, 0.25, 0.50, 0.75, 1.0, and 2.0 based upon the background DOC concentration of 2.5 mg/L in CRW. These ratios correspond to applied dosages of 0, 0.63, 1.25, 1.88, 2.5, and 5.0 mg/L. Oxidant residuals were measured using the appropriate standard method for ozone (Indigo Colorimetric Method, SM 4500-O3-B),

free chlorine (DPD Colorimetric Method, SM 4500-Cl-G), chlorine dioxide (DPD Method, 4500-ClO2-D), and chloramine (DPD Colorimetric Method, SM 4500-Cl-G) [45]. Oxidant exposure (CT) was determined by integrating the measured residuals over time according to Equation (1):

$$CT = \int_0^t [Oxidant]dt = \frac{C_o}{k}\left(e^{kt} - 1\right) \quad (1)$$

where C_o is the initial residual concentration, k is the first order decay rate for the oxidant, and t is the exposure time. The oxidant exposures were found to be similar during testing with MA, OSC, and LYN. The average CT values for each oxidant condition are shown in Table 3.1 with error bars representing ±1 standard deviation.

During a 24-hour reaction period, the reaction bottles remained loosely capped at room temperature (22°C). Control samples using OSC cells showed that a loosely capped or uncapped bottle resulted in 10% loss of MIB and negligible loss of geosmin due to volatilization compared to a tightly capped sample. After a 24 hour reaction period, samples dosed with free chlorine, chloramine, and chlorine dioxide were quenched with 80 mg/L of sodium thiosulfate. During the ozone experiments, residual ozone had decayed within 30 minutes and no quenching agent was required. The ozone-treated samples remained stagnant for a 24 hour period prior to filtration in order to maintain continuity with the other oxidants. After 24 hours, the samples were filtered (0.70 µm glass fiber filter) and analyzed for the specific metabolite of concern.

Table 3.1. Average oxidant exposures for testing conducted with MA, OSC, and LYN. (Note: Cyanobacteria type and cell concentration listed for each CT).

		CT (mg-min/L)					
	Dose	MA	MA	OSC	OSC	LYN	LYN
Oxidant	(mg/L)	50,000	200,000	2,800	1,400	1,600	800
Ozone	0.63	0	0	0	0.07	0	0.10
	1.25	0.54	0.22	0.82	0.71	1.3	0.68
	1.88	1.6	0.81	2.9	2.2	2.5	2.5
	2.50	3.4	2.0	7.2	7.3	5.7	6.5
	5.00	16	14	22	22	19	23
Free Chlorine	0.63	25	40	186	38	21	30
	1.25	152	413	369	238	134	154
	1.88	935	459	879	938	626	895
	2.50	1648	605	1490	1619	1247	1450
	5.00	4898	3459	3840	4348	3838	4210
Chlorine Dioxide	0.63	313	558	206	209	331	262
	1.25	518	686	299	345	432	330
	1.88	1205	682	739	862	572	669
	2.50	2233	892	1287	1484	1233	1259
	5.00	6051	4061	3746	3788	3967	3611
Chloramine	0.63	605	636	665	700	442	496
	1.25	1294	1434	1302	1346	1027	1021
	1.88	1835	1985	1968	2051	1630	1562
	2.50	2489	2862	2499	2726	2263	2103
	5.00	4514	5614	5641	5978	4384	4581

3.3.3. Analytical Methods

Dissolved organic carbon (DOC) was measured using a TOC analyzer (Shimadzu, Columbia, MD, USA) according to SM 5310B. UV absorbance at 254 nm (UV_{254}) was measured using a spectrophotometer (Lambda 45, Perkin Elmer, Waltham, MA, USA) according to SM 5910B [45]. The UV_{254} data required correction for the aliquot of sodium thiosulfate added to quench any residual oxidant.

Samples for cyanotoxin analysis were collected in 40 mL amber glass vials containing 100 µL of a 5 g/L ascorbic acid solution to quench any residual oxidant and were immediately stored at 4 °C. Just prior to analysis, a small aliquot (approximately 1 - 2 mL) of each sample was transferred to a 2 mL autosampler vial for direct injection analysis. All analyses were performed using liquid chromatography-mass spectrometer (LC-MS/MS) in both positive and negative electrospray ionization (ESI) modes. Each analyte was monitored by both a quantitation transition and at least one additional confirmation product ion. Initial samples were qualitatively screened for target cyanotoxins. Detected analytes were further analyzed and quantified against calibration curves using external calibration with method reporting limits (MRLs) set at 500 ng/L.

Samples for MIB and geosmin analysis were collected in 40 mL amber, glass headspace vials (with no remaining headspace) containing an ascorbic acid solution to quench any residual oxidant, and stored at 4 °C. Samples were extracted and analyzed as soon as possible, typically within 1 to 2 days of collection. All analyses were performed using a 10 mL aliquot of collected samples and solid-phase micro extraction (SPME) gas chromatography-tandem mass spectrometry (GC-MS/MS) operated in positive electron ionization (EI). Quantitation was performed using isotope dilution with isotopically labeled geosmin (geosmin-d3). The MRL was set at 5 ng/L for both MIB and geosmin based on an extracted method detection limit (MDL) study. A series of spiked and unspiked tests were performed on a variety of water matrices in order to assess the robustness of the method.

3.4. Results and Discussion

3.4.1. Release of IOM from Cells

DOC, DON and UV_{254} were monitored before and after the oxidation of MA, OSC, and LYN cells. Replicates were conducted on 21 of 144 tests (15%). Based upon error analysis of these samples, a DOC release < 0.15 mg/L was not considered to be significant. After oxidation, the maximum observed DOC release (ΔDOC) was ≤ 0.25 mg/L from MA, OSC, and LYN, which was ≤ 10% of the DOC in the background CRW. Some of variability in the ΔDOC may be explained by the presence of extracellular organic matter (EOM) in the stock cell suspension. Nonetheless, the ΔDOC observed in this study was consistent with other research, which showed < 0.3 mg/L DOC release after chlorination of similar MA cell concentrations [36, 37].

The DOC/DON varied between 0.18-0.26 according to the IOM properties [43]. As a result, the changes in DON during the oxidation of cyanobacteria cells were expected to be <0.06 mg/L based upon the ΔDOC<0.25 mg/L. The specific UV absorbance at 254 nm ($SUVA_{254}$) of the IOM extracted from MA, OSC, and LYN was determined to be 1.59, 0.66, and 0.26, respectively. During ozone oxidation, the change in UV_{254} (ΔUV_{254}) decreased after the oxidation of MA, OSC, and LYN cells, which was expected due to its ability to rapidly oxidize aromatic rings. During chloramine oxidation, the ΔUV_{254} increased after the oxidation of the MA, OSC, and LYN indicating release of IOM and poor reactivity with aromatic structures. The ΔUV_{254} after free chlorine and chlorine dioxide oxidation were in between ozone and chloramine. In the case of MA, an increase in ΔUV_{254} was observed, which may be explained by the greater aromatic

content of the IOM as determined by $SUVA_{254}$, while minimal ΔUV_{254} was observed after oxidation of OSC and LYN. The ΔUV_{254} for OSC and LYN was lower in magnitude among all cyanobacteria due to its lower aromatic content ($SUVA_{254}$).

3.4.2. Release of MC-LR from MA Cells

MC-LR release after oxidation of MA cells by ozone, free chlorine, chlorine dioxide, and chloramines is shown in Figure 3.1. During the testing with MA, replicates were conducted on 6 of 48 tests (12%). From these samples, the relative standard deviation (RSD) for MC-LR was calculated to be 3.5%. In the case of MA, the cells were easily separated from the growth media and quantified using the digital flow cytometer, which minimized the amount of cell damage and extracellular MC-LR present in the cell suspension. In all cases, the control samples reported MC-LR concentration ≤0.57 µg/L, and many were below the MRL of 0.5 µg/L. The MC-LR content in IOM was found to be 5.4 µg MC-LR/mg_C.

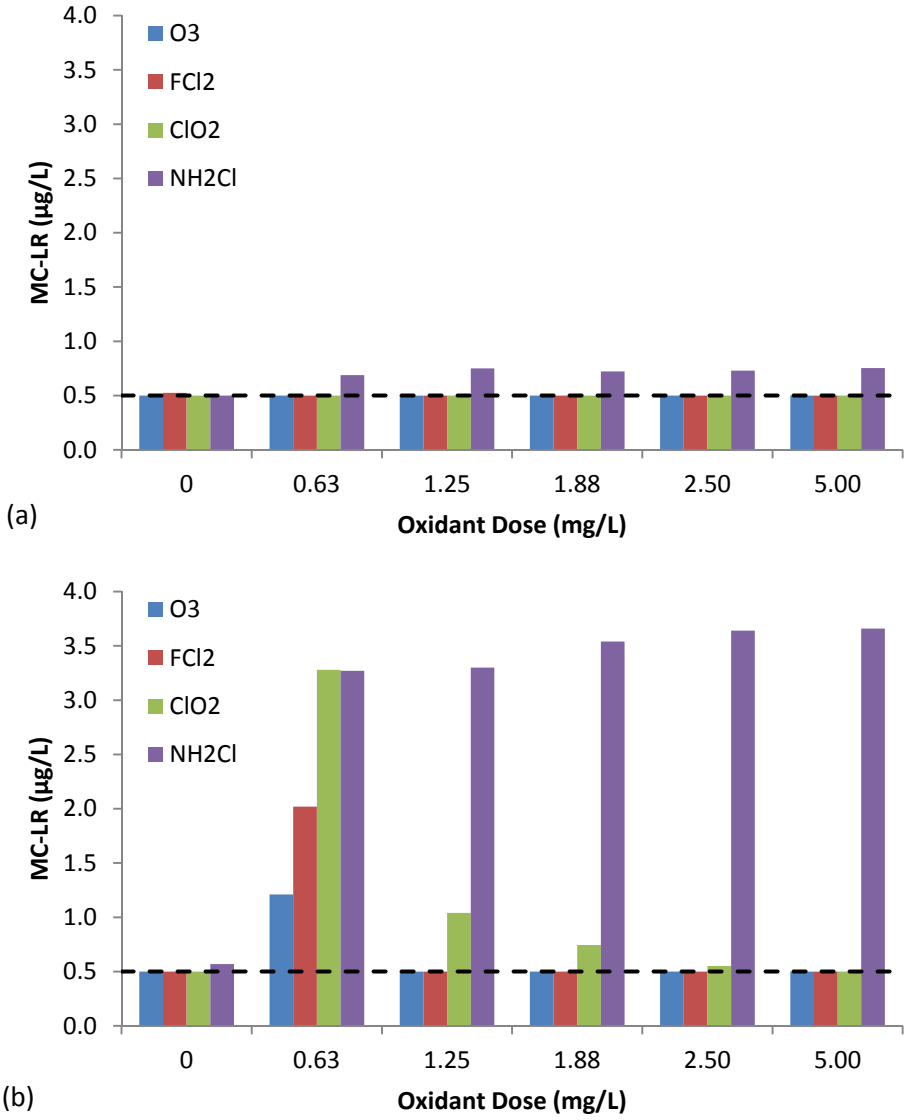

Figure 3.1. Release of MC-LR after oxidation by ozone, free chlorine, chlorine dioxide, and chloramine: (a) 50,000 cells/mL of MA, (b) 200,000 cells/mL of MA. (Note: MRL of 0.5 µg/L indicated by dashed line.).

During the oxidation of 50,000 cells/mL, there was no apparent net increase in the MC-LR concentration after exposure to ozone, free chlorine, and chlorine dioxide. Measurable release of MC-LR was detected after chloramine exposure (0.69-0.75 µg/L). During the ozonation of 200,000 cells/mL, a MC-LR concentration of 1.21 µg/L was

detected after oxidation using a dose of 0.63 mg/L. In this case, the release of MC-LR exceeded the rate of oxidation since there was no measurable dissolved ozone residual (apparent CT=0 mg-min/L). As the ozone dose increased (≥1.25 mg/L, CT≥0.22 mg-min/L), MC-LR concentrations remained below the MRL, which was expected due to the fast reaction rate constant with ozone (k_{app}=4.1 x 10^5 $M^{-1}s^{-1}$) [15].

Similar trends were observed for free chlorine and chlorine dioxide. When applying free chlorine to 200,000 cells/mL of MA, MC-LR increased to 2.02 µg/L when using a dose of 0.63 mg/L (CT=40 mg-min/L), which was similar to the chlorine exposure conditions causing MC-LR release during other studies of MA (7-29 mg-min/L) [33, 34, 36]. At greater chlorine exposures (dose≥1.25 mg/L or CT≥413 mg-min/L), the rate of MC-LR oxidation was sufficient to remove any released toxin resulting in no net increase in concentration. During exposure to chlorine dioxide, the released MC-LR concentration increased to 3.28 µg/L when using a dose of 0.63 mg/L (CT=558 mg-min/L). At dosages greater than 0.63 mg/L (CT≥686 mg-min/L), a dose response was observed illustrating the apparent release and concurrent oxidation of released MC-LR by chlorine dioxide. When using a dose of 5 mg/L (CT=4,061 mg-min/L), there was no evidence of accumulation of MC-LR indicating that any released MC-LR was oxidized.

During exposure to chloramine, an increase in extracellular MC-LR was observed over the entire dose range, and release was not a function of the dose or exposure. The MC-LR concentration increased to 3.27 µg/L when using a dose of 0.63 mg/L (CT=636 mg-min/L). The release of MC-LR was greater than that expected from the measured ΔDOC

and the MC-LR content found in IOM (~1.35 μg/L). An increase in the extracellular MC-LR concentration was expected due to the slow reaction rate with NH2Cl. Under the maximum dose condition (5 mg/L), CT values reached 5,614 mg-min/L, which was significantly less than the 30,000 mg-min/L recommended for oxidation of MC-LR [21]. Therefore, an additional treatment process would be needed to reduce the concentration of MC-LR released during oxidative cell damage.

These results illustrate the potential to release MC-LR during low oxidant exposure (CT) conditions. Under the low dose condition (0.63 mg/L), ozone, free chlorine, chloramine, and chlorine dioxide were each able to release intracellular MC-LR resulting in extracellular concentrations exceeding the WHO guideline of 1 μg/L. Other studies have shown metabolite release occurs at low oxidant exposures and corresponds with the loss of cell viability [30, 36]. In this study, cell viability was not quantified. However, metabolite release occurred at exposures less than those required for chlorophyll-a degradation [38]. At greater CT conditions, ozone, free chlorine, and chlorine dioxide were able to oxidize the released MC-LR resulting in no apparent increase in extracellular MC-LR. The published CT values in Table 3.1 provide some additional guidance to utilities regarding the risk of releasing and accumulating MC-LR in the water supply. However, utilities using chloramines are at the greatest risk for releasing and accumulating MC-LR. Therefore, an additional treatment process may be required to reduce the extracellular MC-LR concentration.

3.4.3. Release of MIB from OSC Cells

MIB release after oxidation of OSC cells by ozone, free chlorine, chlorine dioxide, and chloramines is shown in Figure 3.2. During the testing with OSC, replicates were conducted on 8 of 48 tests (17%). From these samples, the relative standard deviation (RSD) for MIB was calculated to be 4.4%. The OSC filaments had a tendency to form clumps during the culturing process which required shaking and constant mixing of the cell suspension in order to maintain a homogenous cell suspension. As a result, the stock cell suspension became contaminated with extracellular MIB, which was quantified through control samples corresponding to each oxidant series (140-990 ng/L). In Figure 3.2, the change in MIB concentration (ΔMIB) is shown as the difference between the MIB concentration in the oxidized cell sample and MIB concentration in the control sample (no oxidant). The MIB content in IOM was found to be 5,600 ng MIB/mg_C.

There was no apparent increase in MIB concentration during the ozonation of 1,400 cells/mL. During the ozonation of 2,800 cells/mL, the ΔMIB indicated a release of 260 ng/L when using a dose of 0.63 mg/L (apparent CT=0 mg-min/L). The release of MIB appeared to occur when the ozone exposure was near the demand of the CRW and insufficient hydroxyl radicals were produced to eliminate the released MIB. As the ozone dose increased (dose≥1.25 mg/L, CT≥0.82 mg-min/L), the ΔMIB concentration decreased likely due to hydroxyl radical oxidation based on kinetic information discussed previously [29]. When targeting *Cryptosporidium* inactivation, ozone exposures may be able to oxidize any released MIB.

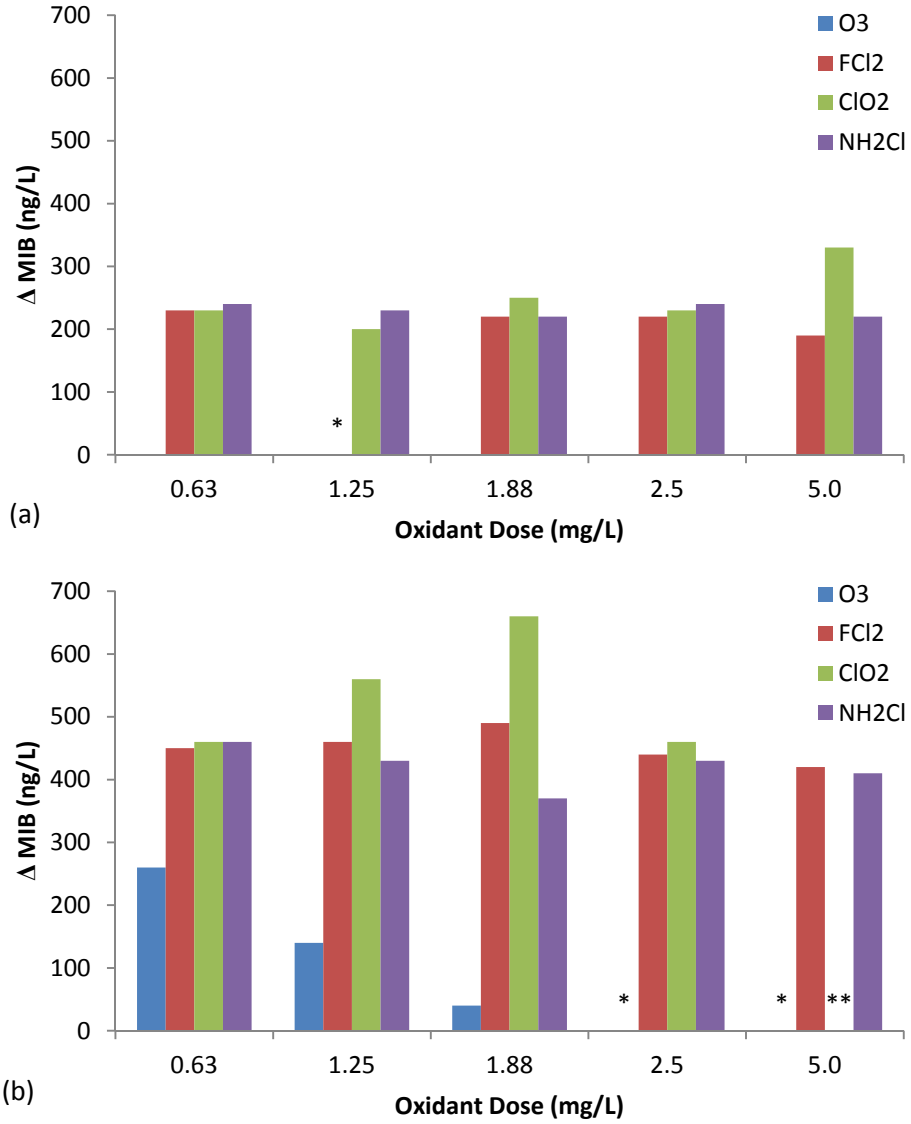

Figure 3.2. ΔMIB after oxidation of OSC cells by ozone, free chlorine, chlorine dioxide, and chloramines: (a) 1,400 cells/mL, and (b) 2,800 cells/mL (Notes: ND=Not detected, *Test failed)

During the oxidation of 2,800 cells/mL by free chlorine, chlorine dioxide, and chloramine, the majority of MIB (ΔMIB~450 ng/L) was released at the lowest oxidant dose evaluated (0.63 mg/L). The corresponding oxidant exposures were as follows:

chlorine (<186 mg-min/L), chlorine dioxide (<206 mg-min/L), and chloramine (<665 mg-min/L). The ΔMIB was within range of the amount of release expected based upon the ΔDOC (0.05-0.10 mg/L) and the expected MIB from IOM analysis (280-560 ng/L). There was no dose response observed with the ΔMIB as the dose increased to 5 mg/L. Since these oxidants are slow reacting with MIB, no subsequent oxidation of released/extracellular MIB was expected. These results indicate that low oxidant exposures can release MIB concentrations that far exceed the threshold odor value of 6.3-15 ng/L. However, several factors may influence the amount of intracellular MIB (e.g. growth phase, light conditions, strain specificity). Therefore, the results should be viewed rather qualitatively. Furthermore, an additional treatment process may be warranted to remove MIB after the oxidation of odor-producing cyanobacteria cells.

3.4.4. Release of Geosmin from LYN Cells

Geosmin release after oxidation of LYN cells by ozone, free chlorine, chlorine dioxide, and chloramines is shown in Figure 3.3. During the testing with LYN, replicates were conducted on 12 of 48 tests (25%). From these samples, the relative standard deviation (RSD) for geosmin was calculated to be 7.5%. Similar to OSC, the LYN filaments had a tendency to form clumps during the culturing process which required shaking and constant mixing of the cell suspension in order to maintain a homogenous cell suspension. Since a fresh cell suspension was prepared on each day of testing, the release of extracellular geosmin was different resulting in the varying concentration in the control samples (17-750 ng/L) when no oxidant was added. In Figure 3.3, the change in geosmin concentration (Δgeosmin) is shown as the difference between the geosmin

concentration in the oxidized cell sample and geosmin concentration in the control sample (no oxidant). The geosmin content in IOM was found to be 3,645 ng/mg_C.

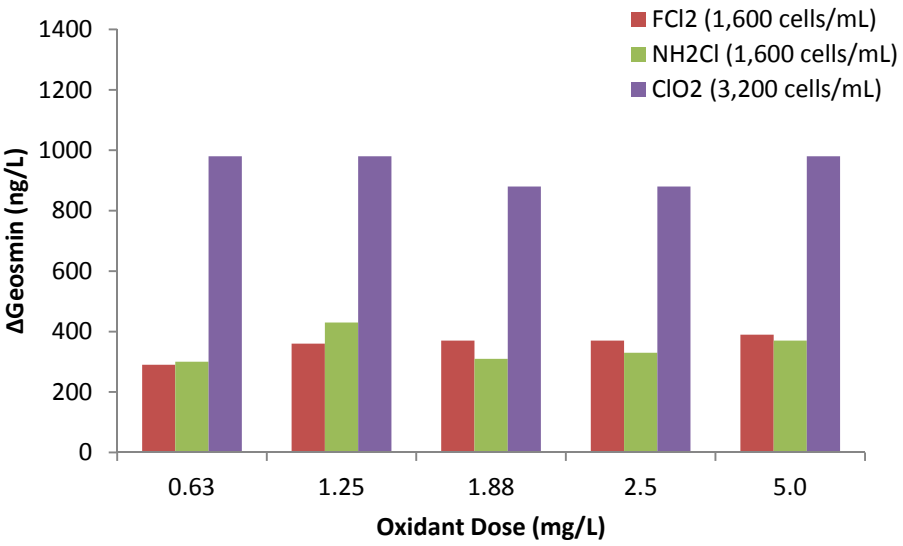

Figure 3.3. ΔGeosmin after oxidation of LYN cells by free chlorine, chlorine dioxide, and chloramines

Results among all of the oxidants were similar to those for MIB release from OSC. In the case of ozone, there was no apparent increase in the extracellular concentration of geosmin under any of the dose conditions. These results indicate that there was likely sufficient oxidation of any released geosmin by hydroxyl radicals. During oxidation by free chlorine (1,600 cells/mL), chlorine dioxide (3,200 cells/mL), and chloramine (1,600 cells/mL), the Δgeosmin was between 290-980 ng/L. The minimum oxidant exposures resulting in geosmin release were as follows: free chlorine (21 mg-min/L), chlorine dioxide (262 mg-min/L), and chloramine (442 mg-min/L). These concentrations exceeded the threshold odor values discussed previously (1.3-4.0 ng/L) [29], indicating that oxidative cell damage can result in objectionable tastes and odors during the drinking

water treatment process. The ΔGeosmin was within range of the amount of release expected based upon the ΔDOC (0.10-0.22 mg/L) and the expected MIB from IOM analysis (365-800 ng/L).

3.5. Conclusions

- During cell damage and lysis, cells appear to be stressed resulting in the release of metabolites, then destruction of photosynthetic pigments (chlorophyll-a), then cell lysis or fragmentation of the cell membrane.
- Under certain oxidation conditions, all oxidants were able to release MC-LR, MIB or geosmin faster than the rate of oxidation resulting in accumulation of these metabolites. All doses were too high to observe a dose response with metabolite release.
- Release of MC-LR, MIB, and geosmin was not a function of dose or CT under the conditions tested. These results indicate that lower oxidant exposures were responsible for the release of metabolites, which could have been metabolically triggered or physically released through a damaged cell membrane.
- During the oxidation of 50,000 cells/mL of MA, a measurable release of MC-LR occurred with chloramines (0.69-0.75 μg/L). There was no increase in MC-LR after oxidation by ozone, free chlorine, or chlorine dioxide. These results indicate that 50,000 cells/mL of MA did not contain enough intracellular MC-LR to produce a release exceeding the WHO guideline of 1 μg/L. However, intracellular MC-LR concentration can be dependent upon the growth phase and strain specific.

- During the oxidation of 200,000 cells/mL of MA, release of intracellular MC-LR exceeded the WHO guideline of 1 μg/L (ΔMC-LR=1.21-3.28 μg/L) during the following oxidant exposures: ozone (0 mg-min/L), free chlorine (<40 mg-min/L), chlorine dioxide (<558 mg-min/L), and chloramine (<636 mg-min/L).
- During the oxidation of OSC cells, release of intracellular MIB occurred when using free chlorine, chlorine dioxide, and chloramines (ΔMIB=370-660 ng/L). Extracellular concentrations exceeded the reported threshold odor values when exposures were less than following values: free chlorine (<38 mg-min/L), chlorine dioxide (<206 mg-min/L), and chloramine (<665 mg-min/L).
- During the oxidation of LYN cells, release of intracellular geosmin occurred when using free chlorine, chlorine dioxide, and chloramines (Δgeosmin=290-980 ng/L). Extracellular concentrations exceeded the threshold odor values at exposures less than following values: free chlorine (<21 mg-min/L), chlorine dioxide (<262 mg-min/L), and chloramine (<442 mg-min/L).
- During ozone oxidation of OSC and LYN cells, an increase in the extracellular MIB or geosmin concentration may be expected during low ozone exposures when hydroxyl radical concentration is insufficient.
- The results for ΔMC-LR, ΔMIB, and Δgeosmin should be viewed with caution as many factors contribute the intracellular metabolite concentration. A qualitative interpretation of results illustrates the risk of metabolite release during low exposures to all oxidants.

3.6. References

1. Paerl, H. W.; Paul, V. J., Climate change: Links to global expansion of harmful cyanobacteria. *Water Res.* 2012, *46*, (5), 1349-1363.

2. Sinclair, J. L.; Hall, S., Chapter 3: Occurrence of cyanobacterial harmful algal blooms workgroup report. In *Cyanobacterial Harmful Algal Blooms: State of the Science and Research Needs*, Hudnell, H. K., Ed. Springer-Verlag Berlin: Berlin, 2008; Vol. 619, pp 45-103.

3. Pearson, L.; Mihali, T.; Moffitt, M.; Kellmann, R.; Neilan, B., On the Chemistry, Toxicology and Genetics of the Cyanobacterial Toxins, Microcystin, Nodularin, Saxitoxin and Cylindrospermopsin. *Mar. Drugs* 2010, *8*, (5), 1650-1680.

4. Hitzfeld, B. C.; Hoger, S. J.; Dietrich, D. R., Cyanobacterial toxins: Removal during drinking water treatment, and human risk assessment. *Environmental Health Perspectives* 2000, *108*, 113-122.

5. WHO, Cyanobacterial toxins: Microcystin-LR in drinking water. Background document for preparation of WHO guidleines for drinking-water quality. . In Organization, W. H., Ed. Geneva, 2003; Vol. WHO/SDS/WSH/03.04/57.

6. Canada, H., Guidelines for Canadian Drinking Water Quality: Supporting Documentation, Cyanobacterial Toxins - Microcystin-LR. In Water, F.-P.-T. C. o. D., Ed. 2002.

7. USEPA, Drinking Water Contaminant Candidate List 3 - Final. In 2009; Vol. Fed. Reg. 74(194):51850-51862.

8. Carmichael, W. W. *Assessment of Blue-Green Algal Toxins in Raw and Finished Drinking Water*; Water Research Foundation: 2001.

9. Graham, J. L.; Loftin, K. A.; Meyer, M. T.; Ziegler, A. C., Cyanotoxin Mixtures and Taste-and-Odor Compounds in Cyanobacterial Blooms from the Midwestern United States. *Environ. Sci. Technol.* 2010, *44*, (19), 7361-7368.

10. Haddix, P. L.; Hughley, C. J.; Lechevallier, M. W., Occurence of microcystins in 33 US water supplies. *American Water Works Association* 2007, *99*, (9), 118-125.

11. Izaguirre, G.; Jungblut, A.-D.; Neilan, B. A., Benthic cyanobacteria (Oscillatoriaceae) that produce microcystin-LR, isolated from four reservoirs in southern California. *Water Res.* 2007, *41*, (2), 492-498.

12. Kotak, B. G.; Zurawell, R. W., Cyanobacterial toxins in Canadian freshwaters: A review. *Lake and Reservoir Management* 2007, *23*, (2), 109-122.

13. Westrick, J. A.; Szlag, D. C.; Southwell, B. J.; Sinclair, J., A review of cyanobacteria and cyanotoxins remova/inactivation in drinking water treatment. *Analytical and Bioanalytical Chemistry* 2010, *397*, (5), 1705-1714.

14. Ho, L.; Sawade, E.; Newcombe, G., Biological treatment options for cyanobacteria metabolite removal - A review. *Water Res.* 2012, *46*, (5), 1536-1548.

15. Rodriguez, E.; Onstad, G. D.; Kull, T. P. J.; Metcalf, J. S.; Acero, J. L.; von Gunten, U., Oxidative elimination of cyanotoxins: Comparison of ozone, chlorine, chlorine dioxide and permanganate. *Water Res.* 2007, *41*, (2007), 3381-3393.

16. Onstad, G. D.; Strauch, S.; Meriluoto, J.; Codd, G. A.; von Gunten, U., Selective Oxidation of Key Functional Groups in Cyanotoxins during Drinking Water Ozonation. *Environ. Sci. Technol.* 2007, *41*, (12), 4397-4404.

17. Rositano, J.; Newcombe, G.; Nicholson, B.; Sztajnbok, P., Ozonation of NOM and Algal Toxins in Four Treated Waters. *Water Res.* 2001, *35*, (1), 23-32.

18. Acero, J. L.; Rodriguez, E.; Meriluoto, J., Kinetics of reactions between chlorine and the cyanobacterial toxins microcystins. *Water Res.* 2005, *39*, (8), 1628-1638.

19. Kull, T. P. J.; Sjovall, O. T.; Tammenkoski, M. K.; Backlund, P. H.; Meriluoto, J. A. O., Oxidation of the cyanobacterial hepatotoxin microcystin-LR by chlorine dioxide: Influence of natural organic matter. *Environmental Science & Technology* 2006, *40*, (5), 1504-1510.

20. Kull, T. P. J.; Backlund, P. H.; Karlsson, K. M.; Meriluoto, J. A. O., Oxidation of the cyanobacterial hepatotoxin microcystin-LR by chlorine dioxide: Reaction kinetics, characterization, and toxicity of reaction products. *Environmental Science & Technology* 2004, *38*, (22), 6025-6031.

21. Ho, L.; Kayal, N.; Trolio, R.; Newcombe, G., Determining the fate of Microcystis aeruginosa cells and microcystin toxins following chloramination. *Water Science and Technology* 2010, *62*, (2), 442-450.

22. Juttner, F.; Watson, S. B., Biochemical and Ecological Control of Geosmin and 2-Methylisoborneol in Source Waters. *Applied and Environmental Microbiology* 2007, *73*, (14), 4395-4406.

23. Smith, J. L.; Boyer, G. L.; Zimba, P. V., A review of cyanobacterial odorous and bioactive metabolites: Impacts and management alternatives in aquaculture. *Aquaculture* 2008, *280*, (1-4), 5-20.

24. Watson, S. B., Cyanobacterial and eukaryotic algal odour compounds: signals or by-products? A review of their biological activity. *Phycologia* 2003, *42*, (4), 332-350.

25. Watson, S. B., Aquatic taste and odor: A primary signal of drinking-water integrity. *J. Toxicol. Env. Health Part A* 2004, *67*, (20-22), 1779-1795.

26. Young, W. F.; Horth, H.; Crane, R.; Ogden, T.; Arnott, M., Taste and Odour Threshold Concentrations of Potential Potable Water Contaminants. *Water Res.* 1996, *30*, (2), 331-340.

27. Glaze, W. H.; Schep, R.; Chauncey, W.; Ruth, E. C.; Zarnoch, J. J.; Aieta, E. M.; Tate, C. H.; McGuire, M. J., Evaluating Oxidants for the Removal of Model Taste and Odor Compounds From a Municipal Water Supply. *J.-Am. Water Works Assoc.* 1990, *82*, (5), 79-84.

28. Lalezary, S.; Pirbazari, M.; McGuire, M. J., Oxidation of Five Earthy-Musty Taste and Odor Compounds. *J.-Am. Water Works Assoc.* 1986, *78*, (3), 62-69.

29. Peter, A.; von Gunten, U., Oxidation Kinetics of Selected Taste and Odor Compounds During Ozonation of Drinking Water. *Environmental Science & Technology* 2007, *41*, (2), 626-631.

30. Ding, J.; Shi, H.; Timmons, T.; Adams, C., Release and Removal of Microcystins from Microcystis during Oxidative-, Physical-, and UV-Based Disinfection. *Journal of Environmental Engineering* 2010, *136*, (1), 2-11.

31. Peterson, H. G.; Hrudey, S. E.; Cantin, I. A.; Perley, T. R.; Kenefick, S. L., Physiological toxicity, cell membrane damage and the release of dissolved organic carbon and geosmin by aphanizomenon flos-aquae after exposure to water treatment chemicals. *Water Res.* 1995, *29*, (6), 1515-1523.

32. Ramseier, M. K.; Peter, A.; Traber, J.; von Gunten, U., Formation of assimilable organic carbon during oxidation of natural waters with ozone, chlorine dioxide, chlorine, permanganate, and ferrate. *Water Res.* 2011, *45*, (5), 2002-2010.

33. Zamyadi, A.; Ho, L.; Newcombe, G.; Daly, R. I.; Burch, M.; Baker, P.; Prevost, M., Release and Oxidation of Cell-Bound Saxitoxins during Chlorination of Anabaena circinalis Cells. *Environ. Sci. Technol.* 2010, *44*, (23), 9055-9061.

34. Daly, R.; Ho, L.; Brookes, J. D., Effect of Chlorination on Microcystis aeruginosa Cell Integrity and Subsequent Microcystin Release and Degradation. *Environ. Sci. Technol.* 2007, *41*, (12), 4447-4453.

35. Lin, T.-F.; Chang, D.-W.; Lien, S.-K.; Tseng, Y.-S.; Chiu, Y.-T.; Wang, Y.-S., Effect of chlorination on the cell integrity of two noxious cyanobacteria and their releases of odorants. *Journal of Water Supply: Research and Technology-AQUA* 2009, *58*, (8), 539-551.

36. Zamyadi, A.; Ho, L.; Newcombe, G.; Bustamante, H.; Prevost, M., Fate of toxic cyanobacterial cells and disinfection by-products formation after chlorination. *Water Res.* 2012, *46*, (5), 1524-1535.

37. Zamyadi, A.; Fan, Y.; Daly, R. I.; Prevost, M., Chlorination of Microcystis aeruginosa: Toxin release and oxidation, cellular chlorine demand and disinfection by-products formation. *Water Res.* 2012.

38. Wert, E. C.; Dong, M. M.; Rosario-Ortiz, F. L., Using digital flow cytometry to assess the degradation of *Microcystis aeruginosa*, *Oscillatoria sp*., and *Lyngbya sp*. cells after oxidation processes. *Water Res.* 2013, *Submitted*.

39. Watanabe, M. F.; Harada, K.-I.; Matsuura, K.; Watanabe, M.; Suzuki, M., Heptapeptide toxin production during the batch culture of two microcystis species. *Journal of Applied Phycology* 1989, *1*, 161-165.

40. Watanabe, M. F.; Oishi, S., Effects of environmental factors on toxicity of a cyanobacterium (*Microcystis aeruginosa*) under culture conditions. *Applied and Environmental Microbiology* 1985, *49*, (5), 1342-1344.

41. Pietsch, J.; Bornmann, K.; Schmidt, W., Relevance of Intra- and Extracellular Cyanotoxins for Drinking Water Treatment. *Acta Hydrochimica et Hydrobiologica* 2002, *30*, (1), 7-15.

42. Li, L.; Gao, N.; Deng, Y.; Yao, J.; Zhang, K., Characterization of intracellular & extracellular algae organic matters (AOM) of Microcystic aeruginosa and formation of AOM-associated disinfection byproducts and odor & taste compounds. *Water Res.* 2012, *46*, (4), 1233-1240.

43. Wert, E. C.; Rosario-Ortiz, F. L., Intracellular Organic Matter from Cyanobacteria as a Precursor for Carbonaceous and Nitrogenous Disinfection Byproducts. *Environ. Sci. Technol.* 2013, *Submitted*.

44. Chorus, I.; Bartram, J., *Toxic Cyanobacteria in Water*. WHO, E & FN Spon: London, 1999.

45. APHA; AWWA; WEF, *Standard Methods for the Examination of Water and Wastewater*. 20th ed.; American Public Health Association, American Water Works Association, Water Environment Federation: Washington D.C., 1998.

CHAPTER 4. Intracellular Organic Matter from Cyanobacteria as a Precursor for Carbonaceous and Nitrogenous Disinfection Byproducts

(This Chapter was submitted to Environmental, Science & Technology)

4.1. Abstract

The formation of total organic halogen (TOX), carbonaceous disinfection byproducts (DBPs) (i.e. trihalomethanes (THMs) and haloacetic acids (HAAs)) and nitrogenous DBPs (i.e. trichloronitromethane (TCNM) or chloropicrin, haloacetonitriles (HANs) and nitrosamines) was examined during the chlorination or chloramination of intracellular organic matter (IOM) extracted from *Microcystis aeruginosa*, *Oscillatoria sp*., and *Lyngbya sp*. The percentage of unknown TOX (22-38%) during chlorination indicated the majority of DBPs were identified among THMs, HAAs, TCNM, and HANs. Bromide was readily incorporated into DBPs with speciation shifting slightly from dihalogenated species to trihalogenated species. During formation potential (FP) testing with chloramines, nitrosamine yields from IOM were measured for *N*-nitrosodimethylamine (NDMA, 10-52 ng/mg$_C$), *N*-nitrosopyrrolidine (NPYR, 14 ng/mg$_C$), *N*-nitrosopiperidine (NPIP, 3.7-5.5 ng/mg$_C$), and *N*-nitrosomethylethylamine (NMEA, 2.1-2.6 ng/mg$_C$). When IOM was added to a natural water matrix, the nitrosamine yields were not realized likely due to competition from natural organic matter. Ozonation increased NDMA and NMEA formation and reduced NPYR and NPIP formation during subsequent chloramination. In addition, ozone oxidation of IOM

formed detectable concentration of aldehydes, which may contribute to DBP formation. Finally, >99% of the IOM extracted from OSC and LYN was considered to be assimilable organic carbon (AOC). Therefore, a biological treatment process could minimize this source of DBP precursor material during drinking water treatment.

4.2. Introduction

Blooms of cyanobacteria (also referred to as blue-green algae) can generate a variety of organic metabolites of concern to drinking water utilities, including taste and odor compounds, cyanotoxins, and disinfection byproduct (DBP) precursors. Cyanobacteria cells may excrete these substances during normal cell activity or cell decay. Most literature has focused on the treatment of these compounds present as extracellular organic matter (EOM) in drinking water supplies[1-3]. However, the intracellular (or cell bound) organic matter (IOM) may also contribute to the presence of these metabolites during drinking water treatment.

Many utilities initially use an oxidation process (referred to preoxidation) to meet water quality objectives such as disinfection, control of invasive species, or biofilm control. During a bloom of cyanobacteria, preoxidation may damage or lyse cells resulting in the release of intracellular cyanotoxins or taste and odor compounds[4-7]. In addition to these specific metabolites, the bulk release of IOM may introduce another source of precursor material for carbonaceous DBPs (C-DBPs) or nitrogenous DBPs (N-DBPs) due to the dissolved organic carbon (DOC) and dissolved organic nitrogen (DON) content found in cyanobacteria cells[8-10].

The composition of IOM and EOM has been examined with respect to amino acids, proteins, carbohydrates, hydrophobicity, aromaticity, and molecular weight distribution[9, 11-13]. In general, cyanobacteria-derived organic matter is considered to have low aromaticity (characterized by specific UV absorbance at 254 nm ($SUVA_{254}$) less than 1.7 L cm^{-1} mg_C^{-1}) and contain mostly hydrophilic substances[11, 12]. Other characteristics of IOM are different from EOM. For example, Fang et. al. (2010) showed that IOM contained greater concentrations of amino acids (e.g. arginine, lysine, and glycine) than the corresponding EOM[9]. The same study also showed IOM to have large fraction of unidentified organic nitrogen that was not accounted for by the analysis of 5 aliphatic amines (i.e. methylamine, dimethylamine, ethylamine, diethylamine, and methylethylamine). Li et. al. (2012) showed the molecular weight of IOM was characterized by a distribution from < 1 kDa to > 800 kDa, while that of EOM was between 1-100 kDa[12]. These results indicate that IOM likely contains more carbohydrates and proteins than EOM. Furthermore, a large portion of the IOM can be considered to be assimilable organic carbon (AOC)[14, 15], which is readily biodegradable[16]. Additional information is needed regarding the DOC and DON composition among different cyanobacteria species, growth phases, and environmental conditions.

Cyanobacteria and green algae have been identified for decades as a potential source of trihalomethane (THM) and haloacetic acid (HAA) precursor material[17]. The United States Environmental Protection Agency (USEPA) established a maximum contaminant level (MCL) of 80 µg/L for the sum of four THMs (i.e. chloroform ($CHCl_3$),

chlorodibromomethane ($CHBr_2Cl$), bromodichloromethane ($CHBrCl_2$), and bromoform ($CHBr_3$)), and an MCL of 60 µg/L for the sum of five HAAs (i.e. monochloroacetic acid (CAA), dichloroacetic acid (DCAA), trichloroacetic acid (TCAA), monobromoacetic acid (BAA), and dibromoacetic acid (DBAA))[18]. Several components within the IOM and EOM are known to be precursors for THM and HAA formation including specific amino acids[19], proteins[20], and carbohydrates[21]. Precursor production has also been shown to vary based upon the growth phase. During studies of *Anabaena* and *Microcystis*, the precursor content increased throughout the growth cycle with maximum production during the stationary phase[10, 22]. Several other studies have showed that the yield of THMs and HAAs (from cells and EOM) vary with the strain of cyanobacteria[12, 13, 22-25]. Total organic halogen (TOX) formation from cyanobacteria-derived sources has not been widely evaluated regarding the contribution of IOM as precursor material for other classes of C-DBPs and unknown halogenated byproducts.

Cyanobacteria-derived DON may also provide precursor material for N-DBPs (e.g. haloacetonitriles (HANs), haloacetamides (HAcAms), halonitromethanes (HNMs), cyanogen halides, and nitrosamines)[8, 26, 27], which are considered to be more toxic than the regulated THMs and HAAs[28, 29]. Reaction mechanisms involving N-DBP formation from chlorination and chloramination have been identified with different model compounds (e.g. amines, amino acids, aldehydes, and nucleic acids)[30]. Furthermore, cyanobacteria have been identified as a source of precursors for HANs[10, 25, 31] and trichloronitromethane (TCNM) also referred to as chloropicrin[10, 25]. Nitrosamine formation (specifically *N*-Nitrosodimethylamine (NDMA)) has also been reported from

cyanobacteria-derived sources after chlorination[7, 9, 32] or chloramination[9, 12]. Typically, NDMA yield was greater during chloramination, since chloramines provide the most important pathway toward NDMA formation[30]. Additional information is needed regarding the formation of N-nitrosamines from cyanobacteria-derived organic matter due to rising interest in this class of DBPs[26].

There are also C-DBP and N-DBP implications from aldehyde formation during ozone oxidation. For example, Krasner et. al. (2012) found that ozonation increased the formation of trihalogenated acetaldehydes during subsequent chlorination in natural waters[33]. Pedersen et. al. (1999) found that formaldehyde reacts with monochloramine to form cyanogen chloride[34]. Aldehydes may also participate in the formation of HANs and TCNM during subsequent chloramination[30, 35, 36]. Therefore, a sequential oxidation process involving ozonation may impact the release of IOM via cell damage along with subsequent C-DBP or N-DBP formation.

In this study, the first objective was to identify the yield of C-DBPs (i.e. THMs, HAAs, TOX) and N-DBPs (i.e. HANs, TCNM, nitrosamines) from extracted IOM during chlorination or chloramination. IOM was extracted from three cyanobacteria (*Microcystis aeruginosa* (MA), *Oscillatoria sp.* (OSC), and *Lyngbya sp.* (LYN)). The yields were also examined during sequential oxidation processes (ozone-chlorination (O_3/FCl_2), ozone-chloramination (O_3/NH_2Cl)) and after adding IOM to a natural water matrix (i.e. Colorado River water (CRW)). The percentages of identified TOX and unknown TOX were also identified during the chlorination of IOM. The second

objective was to evaluate the effect of bromide on THM and HAA speciation. The third objective was to quantify the AOC content in IOM and evaluate aldehyde formation during ozone oxidation. The results provide a comprehensive evaluation regarding the significance of IOM as a source of C-DBP and N-DBP precursors during drinking water treatment.

4.3. Materials and Methods

4.3.1. Selection and Culturing of Cyanobacteria

Microcystis aeruginosa (LB 2385, Culture Collection of Algae at the University of Texas, Austin, TX, USA), *Oscillatoria sp*. (LM 603d, Metropolitan Water District of Southern California (MWDSC), La Verne, CA, USA), and *Lyngyba sp*. (SDC 202d, MWDSC, La Verne, CA, USA) were selected for the study based upon their occurrence in source water supplies, availability of an axenic culture, ability to produce odorous or toxic metabolites, and different cell morphology. A batch culture method was selected due to the simplicity of the system and number of cells required. Culturing of cyanobacteria was performed inside a growth chamber (Geneva Scientific, Fontana, WI, USA) with constant light (12 hrs light followed by 12 hrs of darkness) and temperature (22°C) conditions. The cyanobacteria were cultured in either BG-11 growth media (for OSC and LYN) or Bold 3N growth media (for MA). A digital flow cytometer (FlowCAM®, Fluid Imaging Technologies, Yarmouth, ME, USA) was used to quantify the cell concentration in the stock cell suspension and monitor the growth cycle. Additional information regarding the culturing conditions, growth curve development, and digital flow cytometer settings can be found elsewhere [4].

4.3.2. Preparation of IOM Standards

MA, OSC, and LYN cells were harvested during the late exponential growth phase (28 days). The cells were separated from the growth media using a centrifuge (1900 rpm, 14 min) and the supernatant containing the growth media and extracellular organic matter (EOM) was discarded. The remaining cell pellet was rinsed with 10 mM phosphate buffered MilliQ (MQ) water (pH=7.5), followed by centrifugation and discarding the rinse water containing any residual growth media and/or EOM. In the case of OSC and LYN, a mortar and pestle was used to grind the cell pellet in order to improve the extraction of IOM from these filamentous cyanobacteria with protective outer sheaths. The cells were then exposed to (3) freeze-thaw sequences (-77°C freezer, 35°C water bath) and sonication (60 min) in order to release the IOM. The cell debris was separated from the dissolved IOM through filtration (0.7 μm). The filtrate was used as the extracted IOM standard for each MA, OSC, and LYN.

In addition, standards of the photosynthetic pigments identified from the IOM isolates were purchased including phycocyanin (#P2172, Sigma Aldrich, St. Louis, MO, USA) and phycoerythrin (#52412, Sigma Aldrich, St. Louis, MO, USA)). The phycocyanin came in the form of lyophilized powder from *Spirulina sp*., and contained 40% pigment along with sucrose, dithilerythritol, and sodium azide as preservatives. The phycoerythrin was suspended in 150 mM sodium phosphate, 60% ammonium sulfate, 1 mM EDTA, 1 mM sodium azide. The pigment standards were used to evaluate nitrosamine formation during chloramination.

4.3.3. Formation Potential Testing

Formation potential (FP) testing conditions using either free chlorine or monochloramine were similar to those described by Standard Method 5710B[37]. FP tests with free chlorine evaluated the production of TOX, THMs, HAAs, TCNM, and HANs, while FP tests with chloramines evaluated nitrosamine formation. All FP tests were conducted at room temperature (22-24°C) in head space free 1L amber glass bottles. IOM was diluted in phosphate buffered (10 mM) MQ water (pH=7.5) to achieve DOC concentrations of 1, 2, and 3 mg/L. A free chlorine standard was prepared from 5.6% liquid sodium hypochlorite (NaOCl, Fisher Scientific, USA). A preformed chloramine solution was generated by mixing ammonium hydroxide (29%, J.T Baker, USA) with sodium hypochlorite using a chlorine:ammonia ratio of 3:1. The pH of the chloramine standard was maintained above 10, which favors monochloramine speciation. All experiments were repeated with a bromide spike of 100 µg/L (1.25 µM) to evaluate bromide incorporation into THMs and HAAs.

During the MA experiments, chlorine and chloramine decay curves were used to determine the dose required to achieve a free chlorine or chloramine residual between 3-5 mg/L after 7 days following SM5710B. The free chlorine dosages were determined to be 5, 15, 25, and 35 mg/L as Cl_2 to correspond to DOC concentrations of 0, 1, 2, and 3 mg/L. The chloramine dosages were determined to be 5, 12, 19, and 25 mg/L to correspond to DOC concentrations of 0, 1, 2, and 3 mg/L. After 7 days, free chlorine residuals were measured using the DPD method (Method 8021, Hach Company,

Loveland, CO, USA). During chloramine testing, total chlorine residuals were measured after 7 days using the DPD method (Method 8167, Hach Company, Loveland, CO, USA). The same dosages were used during the FP testing of IOM extracted from OSC and LYN.

Additional FP testing was performed to evaluate the effect of pre-ozonation on IOM reactivity during subsequent chlorination (O_3/FCl_2) or chloramination (O_3/NH_2Cl). Ozone stock solutions were made by dissolving a high concentration of gaseous ozone into deionized water at 2°C. The stock solutions were typically 80 mg/L as measured by the indigo method (SM4500-O3)[37]. After IOM addition, an aliquot of ozone stock solution was added to achieve the desired dosed dose (0.6 - 2.1 mg/L). Upon completion of ozone decay, either free chlorine or chloramine was added to begin the FP test. FP testing was also performed in Colorado River water (CRW) with and without IOM addition to determine whether the yields identified in MQ water would be observed in a natural water matrix. In this case, an aliquot of IOM standard (1 mg/L DOC) was added to CRW (DOC~2.5 mg/L) followed by different oxidation scenarios including chlorination, chloramination, O_3/FCl_2, or O_3/NH_2Cl.

4.3.4. Analytical Methods

DOC and total nitrogen were measured using a TOC analyzer (Shimadzu, Columbia, MD, USA) according to SM 5310B. DON was calculated as the difference between the total dissolved nitrogen (TN) and the total dissolved inorganic nitrogen (ammonia, nitrite, and nitrate). UV absorbance at 254 nm (UV_{254}) was measured using a spectrophotometer (Lambda 45, Perkin Elmer, Waltham, MA, USA) according to SM 5910B[37]. THMs were

collected in (2) 40 mL clear glass vials, quenched with 30 μL of 10% (w/v) sodium thiosulfate, and analyzed by USEPA Method 524.2 using gas chromatography with mass spectrometry (GC/MS). Total THMs (TTHM) were reported as the sum of $CHCl_3$, $CHBrCl_2$, $CHBr_2Cl$, and $CHBr_3$. HAA samples were collected in (2) 60 mL amber glass vials, quenched with 6 mg of ammonium chloride, and analyzed by USEPA Method 552.2 with gas chromatography with electron capture detection (GC/ECD). HAA9 were reported as the sum of HAA5 (regulated HAAs) with BCAA, BDCAA, CDBAA, and TBAA. TOX samples were collected in a 500 mL amber glass bottle, quenched with 80 mg/L of sodium thiosulfate, and measured according to Standard Method 5320B using activated carbon adsorption with microcoulometric-titration detection. Samples for HANs and TCNM were collected in (2) 60 mL amber glass vials, quenched with 6 mg of ammonium chloride, and analyzed by USEPA Method 551.1 using liquid-liquid extraction and GC/ECD. HANs were reported as the sum of bromochloroacetonitrile (BCAN), dibromoacetonitrile (DBAN), dichloracetonitrile (DCAN), and trichloroacetonitrile (TCAN). Nitrosamines were collected in a 1-L amber glass bottle, quenched with 80 mg of sodium thiosulfate, preserved with 1 g of sodium azide, and analyzed using automated solid phase extraction and GC-MS/MS[38]. The following compounds were included during nitrosamine analysis: NDMA, N-nitrosomethylethylamine (NMEA), N-nitrosodiethylamine (NDEA), N-nitrosodipropylamine (NDPA), N-nitrosomorpholine (NMOR), N-nitrosopyrrolidine (NPYR), N-nitrosopiperidine (NPIP), N-nitrosodibutylamine (NDBA), and N-nitrosodiphenylamine (NDPhA). Assimilable organic carbon (AOC) samples were collected in 1L amber glass bottles, and analyzed using a bioluminescence-based test

developed by Weinrich et. al.[39]. Aldehyde samples were collected in (3) 40 mL amber glass vials, quenched with 25 mg of ammonium chloride, preserved with 22 mg of copper sulfate, and analyzed by USEPA method 556 using GC/ECD. Measured aldehydes included acetaldehyde, formaldehyde, glyoxal, propanal, M-glyoxal, pentanal, and butanal.

4.4. Results and Discussion

4.4.1. IOM Composition

The properties of the diluted IOM extracted from MA, OSC, and LYN are shown in Table 4.1. The DON/DOC content of MA (0.26) and OSC (0.24) was greater than that of OSC (0.18). The DON/DOC content of MA from this study was in agreement with that of MA identified by other research (~0.23)[9, 12]. The DON/DOC ratio also illustrates that the extracted IOM was rich in DON compared to the source water supplies of 28 drinking water utilities (average DOC/DON ratio ~ 0.055)[40]. $SUVA_{254}$ results indicated that the IOM extracted from MA (1.59) was more aromatic than either OSC (0.66) or LYN (0.26)[41].

Table 4.1. Properties of IOM extracted from MA, OSC, and LYN after dilution in MQ water.

Cyanobacteria	DOC (mg/L)	DON (mg/L)	DON/DOC	UV_{254} (1/cm)	$SUVA_{254}$ (L/mg-m)	AOC (µg/L)	AOC/DOC (%)
MA	2.04	0.52	0.26	0.033	1.59	380	19
OSC	1.00	0.18	0.18	0.007	0.66	1000	>99
LYN	1.07	0.27	0.24	0.003	0.26	1100	>99

Visual observations of the IOM standards (Figure S2.1) indicated the presence of the photosynthetic pigments phycocyanin (a blue pigment) and phycoerythrin (a red pigment). MA and LYN had a blue appearance indicative of the presence of phycocyanin, while OSC had a purple appearance indicative of a mixture of phycocyanin and phycoerythrin. These pigments were evaluated for nitrosamine formation (see below).

4.4.2. Yields of C-DBPs and N-DBPs during Chlorination

The average yields of detected C-DBPs and N-DBPs after chlorination of IOM extracted from MA, OSC, and LYN are reported in Figure 4.1 (MQ water, pH=7.5, T=22°C, no bromide addition). The errors bars indicate the relative standard deviation (RSD) of the yields calculated from testing with MA, OSC, and LYN using 1, 2, and 3 mg/L of DOC. The free chlorine residuals measured after 7 days were between 4.1 and 13.4 mg/L (Table S2.1), which indicates that sufficient exposure had been maintained throughout the 7-day reaction period. The varied free chlorine residuals had minimal effect (<3%) on $CHCl_3$ formation provided the 7-day residual was greater than 0.33 mg/L (Figure S2.2).

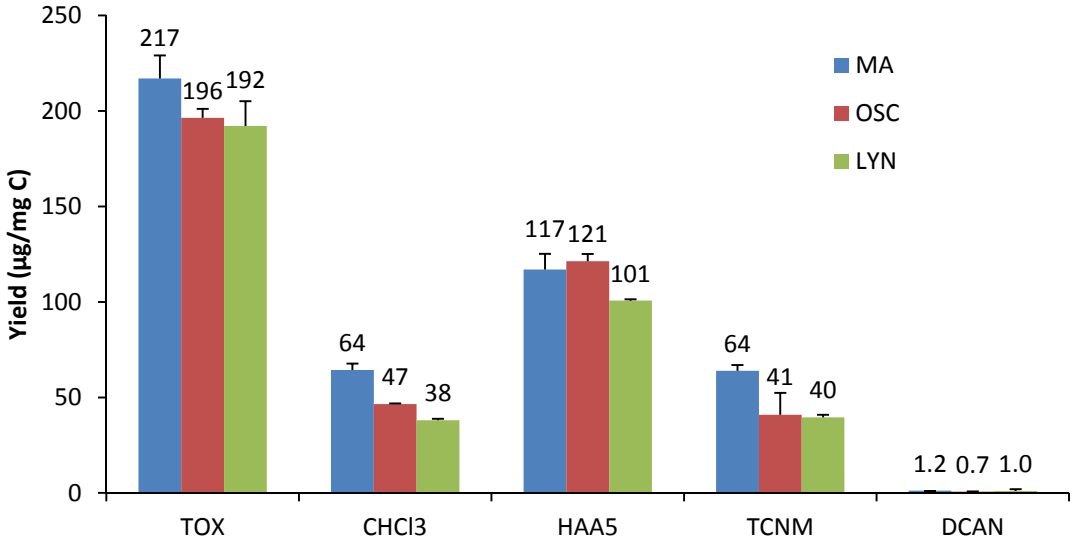

Figure 4.1. DBP yields from IOM extracts (MA, OSC, and LYN) after FP testing with free chlorine in buffered MQ water (pH=7.5, T=22-24°C, no bromide addition). (Notes: Error bars indicate 1 RSD, *TOX yield in terms of µg Cl/mg_C).

$CHCl_3$ yields ranged from 38-64 $\mu g/mg_C$ depending on the specific IOM isolate, which were well within the range (20-61 µg $CHCl_3/mg_C$) reported for other strains of cyanobacteria[13, 22, 24]. The slightly higher $CHCl_3$ production from MA may be due to greater aromaticity ($SUVA_{254}$) compared to OSC and LYN. Weishaar et. al. developed a SUVA-based model to predict THMFP using 13 organic matter isolates ($THMFP=16.30\times SUVA+34.57$, $R^2=0.54$)[41]. When applying this model using the SUVA information in Table 4.1, the predicted THMFP (MA, 61 $\mu g/mg_C$; OSC, 45 $\mu g/mg_C$; and LYN, 39 $\mu g/mg_C$) was within 5% of the measured THM yields during this study (Figure 4.1). These results illustrate that the THMFP of IOM extracted from different cyanobacteria may be accurately predicted using this model in the absence of bromide.

The HAA5 yield (i.e. CAA, DCAA, and TCAA) varied from 101-121 $\mu g/mg_C$ (Figure 4.1), which was considerably greater than the $CHCl_3$ yield. The HAA yield was dominated by DCAA (51-64%) and TCAA (29-43%). The DCAA/TCAA speciation coincides with other research showing lower TCAA production than DCAA as the pH increases from 6 to 8[42]. The fraction of hydrophobic/hydrophilic carbon in natural organic matter (NOM) can also influence the distribution of THMs and HAA with the hydrophobic fraction typically producing greater concentrations of HAAs[42]. The HAA yields from this study indicate that IOM (which tends to be hydrophilic) can still provide a significant source of precursor material.

The yield of TCNM was between 40-64 μg/mg C (Figure 4.1), which was significantly greater than yields reported during other studies of MA (<1 μg/mg C)[9, 10]. The greater yields of TCNM may be attributed to strain-specific differences in the IOM characteristics. For example, the IOM may have been rich in tryptophan and alanine, which produced the greatest concentration of TCNM among 31 different sources of organic nitrogen[43]. Furthermore, Hu et. al. (2010) proposed a TCNM formation pathway during the chlorination of aspartic acid, an aliphatic amino acid[44]. The yield of DCAN was between 0.7-1.1 $\mu g/mg_C$ (Figure 4.1), which was lower than the yield reported during another study of MA (4.6 $\mu g/mg_C$)[9]. There was no measurable formation of TCAN from the IOM extracted from MA, OSC, or LYN. HAN formation may be lower during FP testing due to DCAN degradation and possible conversion to DCAA[45].

The yield of TOX (192-217 µg Cl/mg$_C$) was similar among the IOM extracted from MA, OSC, and LYN (Figure 4.1). The fractions of identified DBPs and unknown TOX (UTOX) are compared on a chlorine-equivalent mass basis in Figure 4.2. Results also showed that MA produced greater concentrations of tri-chlorinated DBP species (61%) than OSC (46%) or LYN (42%). The portion of UTOX (22.6-38.4%) was less than that observed in natural waters (~60%)[46]. Greater proportions of UTOX are typically considered to result from the halogenation of high molecular weight organic matter[47], although fundamental differences in reactivity of the IOM could also explain the amount of UTOX.

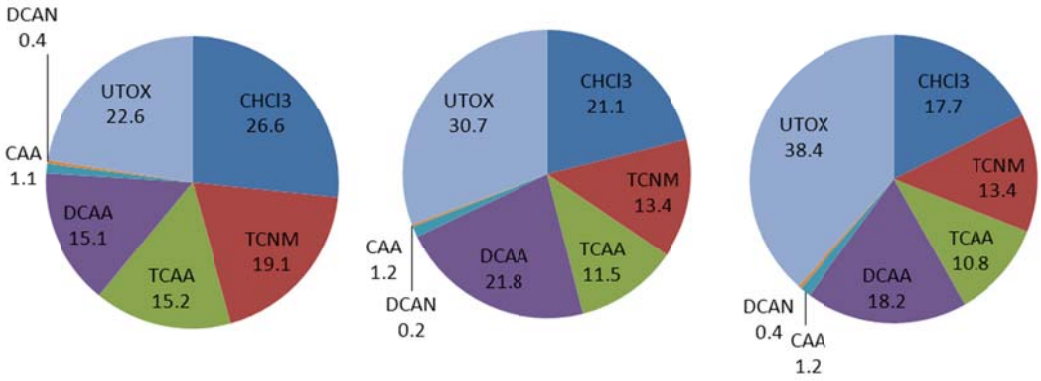

Figure 4.2. Percentages of identified DBPs and UTOX during FP testing with free chlorine using IOM extracted from MA (left), OSC (middle), and LYN (right). (Note: percentages of the identified DBPs were determined from their chlorine-equivalent mass concentration.)

FP testing in CRW showed the TOX production was greater from IOM isolates (192-217 µg/mg$_C$) than CRW (112 µg/mg$_C$) (Figure 4.3). Some changes in DBP formation may be attributed to the pH difference between MQ water (pH=7.5) and CRW (pH=8.25). When adding IOM to CRW, the additional C-DBP and N-DBP yields were measured as

expected based upon FP testing of IOM in MQ water. These results indicate that there was minimal competition from the NOM in CRW.

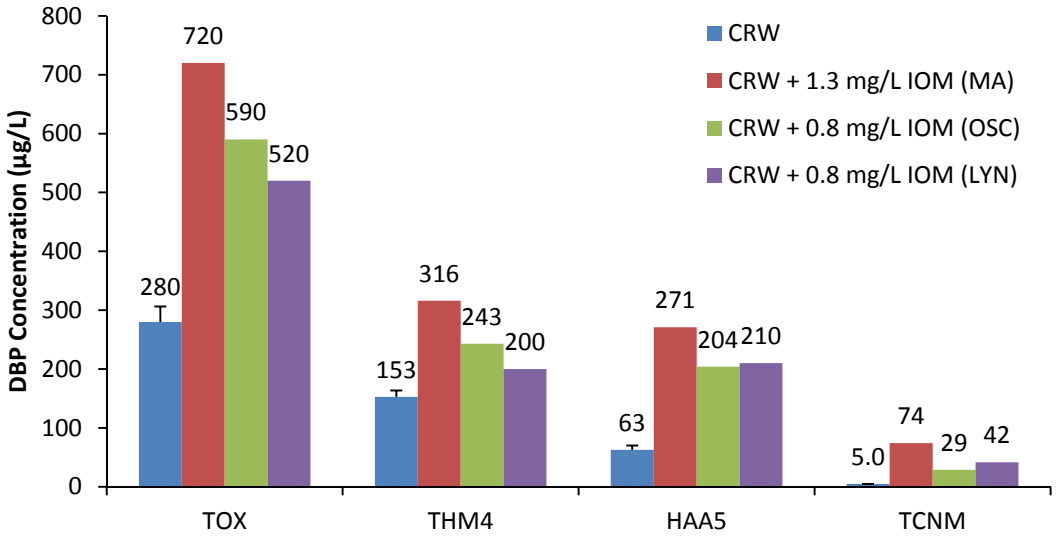

Figure 4.3. DBP formation following chlorination of CRW (pH=8.25, T=23°C) with and without the addition of IOM from MA (1.3 mg/L), OSC (0.8 mg/L), and LYN (0.8 mg/L).

Sequential testing of O_3/FCl_2 was evaluated in MQ water (Figure S2.3) and CRW (Figure S2.4). Results showed that ozone increased DBP formation by 6-40% compared to the yields identified in Figure 4.1. In the case of TCNM, ozone increased formation in MQ, which supports other literature showing greater yield of TCNM during O_3/FCl_2 treatment of lysine and glycine[48] and in natural waters[44, 46]. Furthermore, ozone has been shown to have high reactivity (k_{O3} = 10^4-10^6 M^{-1} s^{-1}) with amino acids containing aromatic rings (e.g. tryptophan, proline, phenylalanine, and histidine), and moderate reactivity (k_{O3} = 10^2-10^3 M^{-1} s^{-1}) with aliphatic amino acids (e.g. alanine, aspartic acid, and glycine)[49]. The inability of ozone oxidize precursor material with a low $SUVA_{254}$ indicates that the precursor material is more aliphatic. Dickenson et. al. demonstrated that model aliphatic

β-dicarbonyl acid compounds were capable of producing THMs and HAAs during chlorination[50].

4.4.3. Effect of Bromide on THM and HAA Speciation

During FP testing with a 100 μg/L bromide spike, bromide was readily incorporated into THMs and HAAs (Figure 4.4). Upon completion of the 7-day FP test, the measured bromide concentration decreased below the MRL (<20 μg/L), indicating that bromination may have been limited by bromide. Rapid bromination was expected since hydrophilic fractions of NOM readily incorporate bromide[42]. Bromide addition increased the overall yield of THMs by 12-29% on a mass basis (Figure S2.5), and the speciation shifted from chloroform to brominated THMs (27-47%) as shown in Figure 4.4. Bromide addition decreased the HAA5 yield by 17-26 $\mu g/mg_C$ while the HAA9 yield increased by 12-26 $\mu g/mg_C$, indicating a shift from chlorinated HAAs to brominated HAAs. The speciation indicated that formation of trihaloacetic acids increased by 7-10% while dihaloacetic acids decreased by 8-11% (Figure 4.4). A bromide mass balance accounted for 24-40% of the original bromide spike indicating that up to 60-76% of the original bromide spike may have been incorporated into unknown brominated DBPs (assuming the entire 100 μg/L of bromide was incorporated into organic matter).

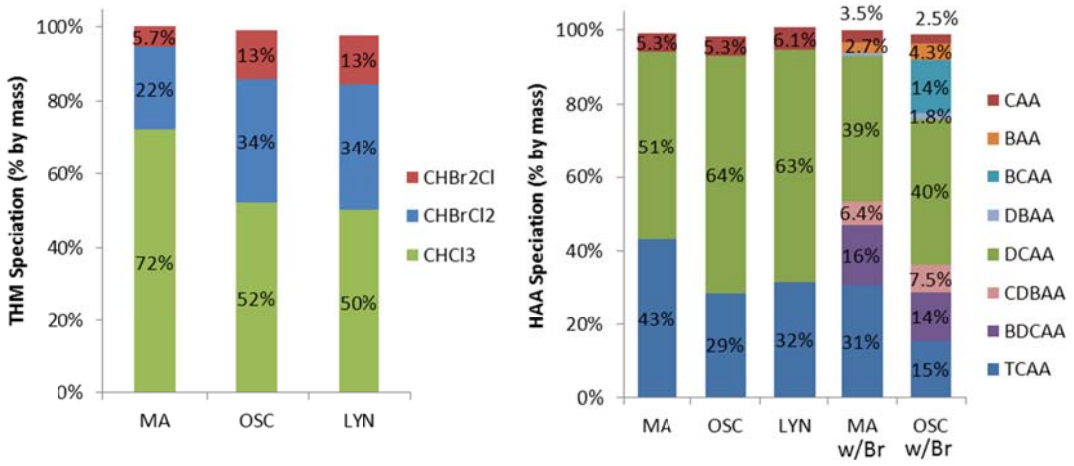

Figure 4.4. THM4 and HAA9 speciation shifts during the chlorination of IOM extracted from MA, OSC, or LYN: (a) THM4 with 100 µg/L Br, (b) HAA9 with and without 100 µg/L bromide. (Note: Percentages may not equal 100% due to rounding).

4.4.4. Nitrosamine Formation during Chloramination

The average yield of nitrosamines during chloramination of IOM are reported in Table 4.2 (MQ water, pH=7.87, T=22-24°C). Results showed that bromide addition had minimal effect on the formation of nitrosamines (Table S2.2). Therefore, all data points were used to calculate the yields shown in Table 4.2. The total chlorine residual concentration varied from 2.9-17.1 mg/L indicating that constant chloramine exposure was maintained throughout the 7-day testing period (Table S2.3).

Table 4.2. Nitrosamine yields from IOM extracts (MA, OSC, and LYN) after FP testing with chloramine in buffered MQ water (pH=7.5, T=22-24°C).

IOM Source	Nitrosamine	Yield (ng/mg C)	
		NH_2Cl	O_3/NH_2Cl
MA	NDMA	52	163
	NPYR	14	< MRL
	NPIP	5.5	< MRL
OSC	NDMA	16	NA
	NMEA	2.1	NA
LYN	NDMA	10	13
	NMEA	4.6	7.1
	NPIP	3.7	< MRL

NA=Not Analyzed

The NDMA yields reported in this study (10-52 ng/mg$_C$) were similar to those reported for MA (13.3 ng/mg C, pH=7, T=22.1 ± 1°C, 3 days of exposure to 15 mg/L of preformed chloramine)[9]. The differences in yield among MA, OSC, and LYN indicates that the quantity of precursors in the DOC/DON may be strain specific or influenced by other environmental factors (i.e. growth phase, light exposure). During a study of fractionated NOM, hydrophilic fractions (common to IOM) produced greater yields of NDMA than hydrophobic fractions[51]. $SUVA_{254}$ may also be used as a relative indicator of NDMA formation based on a linear correlation among the IOM extracted from MA, OSC, and LYN (R^2=0.97) (Figure S2.6). Other studies have shown that the loss of $SUVA_{254}$ during oxidation processes correlated well with the formation of NDMA, although correlation was not very robust among different NOM fractions[51, 52]. The $SUVA_{254}$ correlation also indicates that the precursor content may change throughout the growth cycle based on $SUVA_{254}$ data from the exponential growth phase (1.29-1.7) and stationary growth phase (0.48-0.58) among three types of phytoplankton[11]. Since the

IOM standards were visually different, nitrosamine formation was evaluated in MQ water using two photosynthetic pigments. The yields for phycocyanin (present in all 3 IOM sources) and phycoerythrin (present in only OSC) were 6 and 24 ng/mg_C, respectively, indicating that the pigments contained NDMA precursor material that could account for a fraction of the overall NDMA formation potential in IOM. It is important to note that nitrosamine formation using these standards may be influenced by the preservatives present in the stock material.

IOM specific yields of NMEA, NPYR, and NPIP were observed indicating that presence of precursor material varies by cyanobacteria strain (Table 4.2). MA experienced greater formation of NPYR and NPIP than OSC and LYN. These nitrosamines contain the hetrocyclic aromatic compounds pyrrole (5-member hetero ring) and pyridine (6-member hetero ring), respectively. Conversely, the IOM from LYN produced the greatest yield of NMEA, which is an aliphatic nitrosamine. Therefore, a higher $SUVA_{254}$ (~1.59) may be an indicator for NPYR and NPIP formation, while a low $SUVA_{254}$ (~0.26) may be an indicator for NMEA formation. The results for the other nitrosamines were below their respective MRLs: NDEA (<5 ng/L), NDPA (<10 ng/L), NMOR (<5 ng/L), NDBA (<10 ng/L), and NDPhA (< 10 ng/L).

FP testing was also conducted using CRW with 1 mg/L of IOM addition (Table S2.2). These tests produced no measurable nitrosamine formation. There are several possible explanations for this finding. First, the chloramine exposure may have been insufficient during FP testing in CRW. The dosages applied were below those recommended for

precursor analysis in other studies (45 mg/L NH_2Cl/mg DOC, 10 days of exposure)[53, 54]. Therefore, the yields shown in Table 4.2 may be conservative. Second, there could be competition from the NOM present in CRW resulting in less formation of NDMA[55, 56]. Finally, the pH difference between the experiments conducted in MQ (pH=7.5) versus CRW (pH=8.25) may also factor into the available HOCl to oxidize precursor material[55].

Sequential testing of O_3/NH_2Cl was evaluated in both MQ water and CRW using IOM extracted from MA and LYN. In MQ water, O_3/NH_2Cl increased the concentration of NDMA and NMEA, while decreasing the formation of NPYR and NPIP (Table 4.2). The decreased formation of NPYR and NPIP may be due to oxidation of the pyrrole and pyridine moieties found in each of these nitrosamines. The increase in NDMA and NMEA may be due to the formation of precursor material, although a mechanistic evaluation was not included in this study.

4.4.5. Aldehyde Formation during Ozonation of IOM

During IOM characterization, nearly all (>99%) of the DOC extracted from OSC and LYN was considered to be biodegradable as determined by AOC measurements (Table 4.1). In the case of MA, only 19% of the extracted IOM was found to be biodegradable indicating that the composition of this IOM differed from that of OSC and LYN. During ozonation of IOM in buffered MQ water, the AOC concentration fraction of the IOM extracted from MA increased to 40% when using an O3:DOC ratio of 1.0.

Aldehyde formation was measured during the ozonation of IOM extracted from MA, OSC, and LYN in buffered MQ water (Figure 4.5). Formation of acetaldehyde, formaldehyde, and glyoxal increased with O3:DOC mass ratio. In the case of propanal, an immediate increase in concentration was observed using an O3:DOC ratio of 0.25, followed by a decrease in concentration at greater O3:DOC ratios. These results indicate that propanal was further oxidized to a lower molecular weight DBP. Even though a large fraction of the IOM was found to be AOC, the aldehyde results from OSC and LYN show that the AOC composition can still change during ozonation.

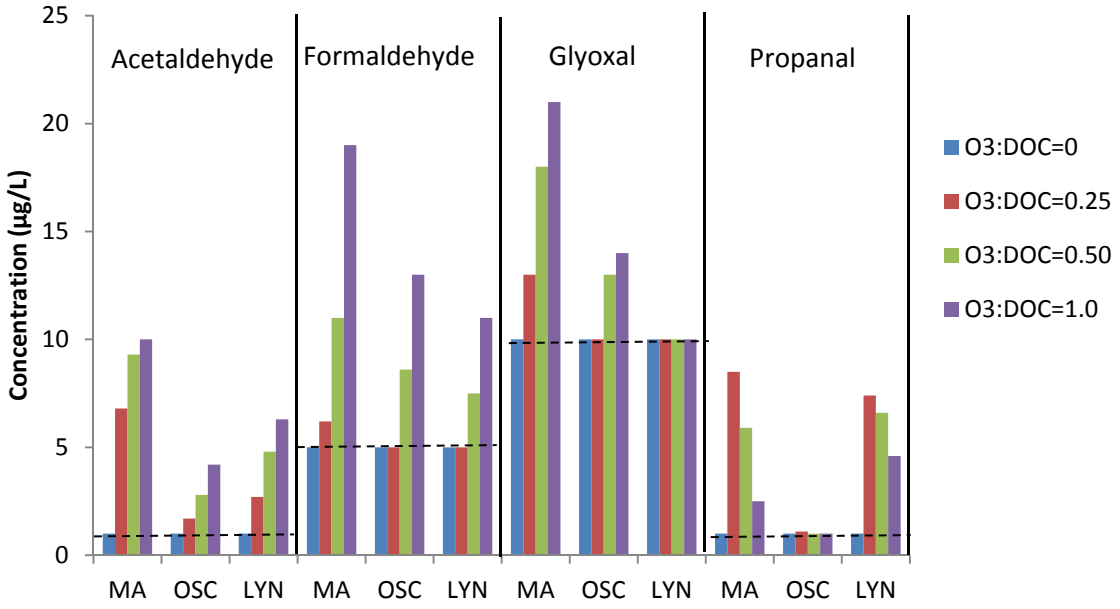

Figure 4.5. Formation of aldehydes from the IOM extracted from MA (1.5 mg/L DOC), OSC (1.0 mg/L DOC), and LYN (1.1 mg/L DOC). (Note: MRLs indicated by the dashed line).

As discussed earlier, aldehyde may contribute the formation of trihalogenated acetaldehydes, cyanogen chloride, HANs, and TCNM during chlorination[30, 33-36]. In this study, ozonation of IOM increased the formation of TCNM, possibly due to aldehyde

intermediates. However, it is also important to note that aldehydes are able to be removed via biodegradation, which would eliminate or reduce DBPs related to aldehyde formation[57].

4.5. Environmental Implications

IOM from cyanobacteria may be released during reservoir treatment with algaecides or during oxidation processes (i.e. ozone, free chlorine, chloramine, chlorine dioxide)[4]. According to the DBP yields identified in this study, IOM can contain a significant amount C-DBP or N-DBP precursors during chlorination of natural water. The yields indicate that a low release of DOC from cell lysis may impact regulatory compliance related to THM4 and HAA5 formation. Chloramine testing in MQ water clearly illustrated the potential to form nitrosamines from IOM. However, these potential nitrosamine yields may not be realized using the dosages and contact times found during drinking water treatment due to competition by background NOM[55, 56]. A sequential oxidation process using ozone (e.g. O_3/NH_2Cl) may also contribute to nitrosamine formation in natural water.

Due to low aromaticity and hydrophilic properties, the IOM precursor is not expected to easily removed by oxidation processes (such as ozonation) or by coagulation processes used during drinking water treatment. Therefore, a physical treatment process would be ideal to remove intact cyanobacteria cells before any release of IOM and corresponding DBP precursor material. Alternatively, AOC analysis of IOM has shown this material is readily biodegradable. If released in the environment during reservoir treatment with

algaecides, natural attenuation of these precursors may minimize the impact on a drinking water treatment process. If released via cell damage from oxidation, the IOM may be removed via a biological treatment process such as biofiltration. The results presented in this manuscript further the understanding of the risk of DBP production from cyanobacteria-derived organic matter, and offers treatment guidance for minimizing or eliminating this precursor pool via physical removal or biodegradation of IOM.

4.6. References

1. Westrick, J. A.; Szlag, D. C.; Southwell, B. J.; Sinclair, J., A review of cyanobacteria and cyanotoxins remova/inactivation in drinking water treatment. *Analytical and Bioanalytical Chemistry* 2010, *397*, (5), 1705-1714.

2. Glaze, W. H.; Schep, R.; Chauncey, W.; Ruth, E. C.; Zarnoch, J. J.; Aieta, E. M.; Tate, C. H.; McGuire, M. J., Evaluating Oxidants for the Removal of Model Taste and Odor Compounds From a Municipal Water Supply. *J.-Am. Water Works Assoc.* 1990, *82*, (5), 79-84.

3. Graham, N. J. D.; Wardlaw, V. E.; Perry, R.; Jiang, J.-Q., The Significance of Algae as Trihalomethane Precursors. *Water Science & Technology* 1998, *37*, (2), 83-89.

4. Wert, E. C.; Dong, M. M.; Rosario-Ortiz, F. L., Using digital flow cytometry to assess the degradation of *Microcystis aeruginosa*, *Oscillatoria sp*., and *Lyngbya sp*. cells after oxidation processes. *Water Res.* 2013, *Submitted*.

5. Ding, J.; Shi, H.; Timmons, T.; Adams, C., Release and Removal of Microcystins from Microcystis during Oxidative-, Physical-, and UV-Based Disinfection. *Journal of Environmental Engineering* 2010, *136*, (1), 2-11.

6. Zamyadi, A.; Fan, Y.; Daly, R. I.; Prevost, M., Chlorination of Microcystis aeruginosa: Toxin release and oxidation, cellular chlorine demand and disinfection by-products formation. *Water Res.* 2012.

7. Zamyadi, A.; Ho, L.; Newcombe, G.; Daly, R. I.; Burch, M.; Baker, P.; Prevost, M., Release and Oxidation of Cell-Bound Saxitoxins during Chlorination of Anabaena circinalis Cells. *Environ. Sci. Technol.* 2010, *44*, (23), 9055-9061.

8. Westerhoff, P.; Mash, H., Dissolved organic nitrogen in drinking water supplies: a review. *J. Water Supply Res Technol.-Aqua* 2002, *51*, (8), 415-448.

9. Fang, J.; Yang, X.; Ma, J.; Shang, C.; Zhao, Q., Characterization of algal organic matter and formation of DBPs from chlor(am)ination. *Water Res.* 2010, *44*, (20), 5897-5906.

10. Fang, J. Y.; Ma, J.; Yang, X.; Shang, C., Formation of carbonaceous and nitrogenous disinfection by-products from the chlorination of Microcystis aeruginosa. *Water Res.* 2010, *44*, (6), 1934-1940.

11. Henderson, R. K.; Baker, A.; Parsons, S. A.; Jefferson, B., Characterisation of algogenic organic matter extracted from cyanobacteria, green algae and diatoms. *Water Res.* 2008, *42*, (13), 3435-3445.

12. Li, L.; Gao, N.; Deng, Y.; Yao, J.; Zhang, K., Characterization of intracellular & extracellular algae organic matters (AOM) of Microcystic aeruginosa and formation of AOM-associated disinfection byproducts and odor & taste compounds. *Water Res.* 2012, *46*, (4), 1233-1240.

13. Nguyen, M.-L.; Westerhoff, P.; Baker, L.; Hu, Q.; Esparza-Soto, M.; Sommerfield, M., Characteristics and Reactivity of Algae-Produced Dissolved Organic Carbon. *Journal of Environmental Engineering* 2005, *131*, (11), 1574-1582.

14. Hammes, F.; Meylan, S.; Salhi, E.; Koster, O.; Egli, T.; von Gunten, U., Formation of assimilable organic carbon (AOC) and specific natural organic matter (NOM) fractions during ozonation of phytoplankton. *Water Res.* 2007, *41*, (2007), 1447-1454.

15. Ramseier, M. K.; Peter, A.; Traber, J.; von Gunten, U., Formation of assimilable organic carbon during oxidation of natural waters with ozone, chlorine dioxide, chlorine, permanganate, and ferrate. *Water Res.* 2011, *45*, (5), 2002-2010.

16. Huck, P. M.; Fedorak, P. M.; Anderson, W. B., Formation and removal of assimilable organic carbon during biological treatment. *Journal of American Water Works Association* 1991, *83*, (12), 69-80.

17. Hoehn, R. C.; Barnes, D. B.; Thompson, B. C.; Randall, C. W.; Grizzard, T. J.; Shaffer, P. T. B., Algae as Sources of Trihalomethane Precursors. *J.-Am. Water Works Assoc.* 1980, *72*, (6), 344-350.

18. USEPA, National Primary Drinking Water Regulations: Stage 2 Disinfectants and Disinfection Byproducts Rule; Final Rule. In 2006; Vol. Fed. Reg. 71(2):388.

19. Hong, H. C.; Wong, M. H.; Liang, Y., Amino Acids as Precursors of Trihalomethane and Haloacetic Acid Formation During Chlorination. *Archives of Environmental Contamination and Toxicology* 2009, *56*, (4), 638-645.

20. Scully, F. E.; Howell, G. D.; Kravitz, R.; Jewell, J. T.; Hahn, V.; Speed, M., Proteins in natural-waters and their relation to the formation of chlorinated organics during water disinfection. *Environmental Science & Technology* 1988, *22*, (5), 537-542.

21. Navalon, S.; Alvaro, M.; Garcia, H., Carbohydrates as trihalomethanes precursors. Influence of pH and the presence of Cl- and Br- on trihalomethane formation potential. *Water Res.* 2008, *42*, (14), 3990-4000.

22. Huang, J.; Graham, N.; Templeton, M. R.; Zhang, Y.; Collins, C.; Nieuwenhuijsen, M., A comparison of the role of two blue-green algae in THM and HAA formation. *Water Res.* 2009, *43*, (12), 3009-3018.

23. Hong, H. C.; Mazumder, A.; Wong, M. H.; Liang, Y., Yield of trihalomethanes and haloacetic acids upon chlorinating algal cells, and its prediction via algal cellular biochemical composition. *Water Res.* 2008, *42*, (20), 4941-4948.

24. Plummer, J. D.; Edzwald, J. K., Effect of Ozone on Algae as Precursors for Trihalomethane and Haloacetic Acid Production. *Environmental Science & Technology* 2001, *35*, (18), 3661-3668.

25. Yang, X.; Guo, W. H.; Shen, Q. Q., Formation of disinfection byproducts from chlor(am)ination of algal organic matter. *Journal of Hazardous Materials* 2011, *197*, 378-388.

26. Bond, T.; Templeton, M. R.; Graham, N., Precursors of nitrogenous disinfection by-products in drinking water-A critical review and analysis. *Journal of Hazardous Materials* 2012, *235*, 1-16.

27. Bond, T.; Huang, J.; Templeton, M. R.; Graham, N., Occurrence and control of nitrogenous disinfection by-products in drinking water - A review. *Water Res.* 2011, *45*, (15), 4341-4354.

28. Muellner, M. G.; Wagner, E. D.; McCalla, K.; Richardson, S. D.; Woo, Y. T.; Plewa, M. J., Haloacetonitriles vs. regulated haloacetic acids: Are nitrogen-containing DBPs more toxic? *Environmental Science & Technology* 2007, *41*, (2), 645-651.

29. Plewa, M. J.; Wagner, E. D.; Jazwierska, P.; Richardson, S. D.; Chen, P. H.; McKague, A. B., Halonitromethane drinking water disinfection byproducts: Chemical characterization and mammalian cell cytotoxicity and genotoxicity. *Environmental Science & Technology* 2004, *38*, (1), 62-68.

30. Shah, A. D.; Mitch, W. A., Halonitroalkenes, halonitriles, haloamides, and N-Nitrosamines: A critical review of nitrogenous disinfection byproduct formation pathways. *Environ. Sci. Technol.* 2012, *46*, (1), 119-131.

31. Oliver, B. G., Dihaloacetonitriles in drinking water: algae and fulvic acid as precursors. *Environ. Sci. Technol.* 1983, *17*, (2), 80-83.

32. Zamyadi, A.; Ho, L.; Newcombe, G.; Bustamante, H.; Prevost, M., Fate of toxic cyanobacterial cells and disinfection by-products formation after chlorination. *Water Res.* 2012, *46*, (5), 1524-1535.

33. Krasner, S. W.; Mitch, W. A.; Westerhoff, P.; Dotson, A., Formation and control of emerging C- and N-DBPs in drinking water. *J. Am. Water Work Assoc.* 2012, *104*, (11), 33-34.

34. Pedersen, E. J.; Urbansky, E. T.; Marinas, B. J.; Margerum, D. W., Formation of cyanogen chloride from the reaction of monochloramine with formaldehyde. *Environmental Science & Technology* 1999, *33*, (23), 4239-4249.

35. Yang, X.; Fan, C. H.; Shang, C. I.; Zhao, Q., Nitrogenous disinfection byproducts formation and nitrogen origin exploration during chloramination of nitrogenous organic compounds. *Water Res.* 2010, *44*, (9), 2691-2702.

36. Yang, X.; Shang, C.; Shen, Q. Q.; Chen, B. Y.; Westerhoff, P.; Peng, J. F.; Guo, W. H., Nitrogen Origins and the Role of Ozonation in the Formation of Haloacetonitriles and Halonitromethanes in Chlorine Water Treatment. *Environmental Science & Technology* 2012, *46*, (23), 12832-12838.

37. APHA; AWWA; WEF, *Standard Methods for the Examination of Water and Wastewater*. 20th ed.; American Public Health Association, American Water Works Association, Water Environment Federation: Washington D.C., 1998.

38. Holady, J. C.; Trenholm, R. A.; Snyder, S. A., Use of Automated Solid-Phase Extraction and GC-MS/MS to Evaluate Nitrosamines in Water Matrices. *Am. Lab.* 2012, *44*, (3), 25-30.

39. Weinrich, L. A.; Giraldo, E.; LeChevallier, M. W., Development and Application of a Bioluminescence-Based Test for Assimilable Organic Carbon in Reclaimed Waters. *Applied and Environmental Microbiology* 2009, *75*, (23), 7385-7390.

40. Lee, W.; Westerhoff, P.; Esparza-Soto, M., Occurrence and removal of dissolved organic nitrogen in US water treatment plants. *J. Am. Water Work Assoc.* 2006, *98*, (10), 102-+.

41. Weishaar, J. L.; Aiken, G. R.; Bergamschi, B. A.; Fram, M. S.; Fujii, R.; Mopper, K., Evaluation of Specific Ultraviolet Absorbance as an Indicator of the Chemical

Composition and Reactivity of Dissolved Organic Carbon. *Environmental Science & Technology* 2003, *37*, (20), 4702-4708.

42. Liang, L.; Singer, P. C., Factors Influencing the Formation and Relative Distribution of Haloacetic Acids and Trihalomethanes in Drinking Water. *Environ. Sci. Technol.* 2003, *37*, (13), 2920-2928.

43. Yang, X.; Shen, Q. Q.; Guo, W. H.; Peng, J. F.; Liang, Y. M., Precursors and nitrogen origins of trichloronitromethane and dichloroacetonitrile during chlorination/chloramination. *Chemosphere* 2012, *88*, (1), 25-32.

44. Hu, J.; Song, H.; Addison, J. W.; Karanfil, T., Halonitromethane formation potentials in drinking waters. *Water Res.* 2010, *44*, (1), 105-114.

45. Reckhow, D. A.; Platt, T. L.; MacNeill, A. L.; McClellan, J. N., Formation and degradation of dichloroacetonitrile in drinking waters. *J. Water Supply Res Technol.-Aqua* 2001, *50*, (1), 1-13.

46. Hua, G.; Reckhow, D. A., Comparison of disinfection byproduct formation from chlorine and alternative disinfectants. *Water Res.* 2007, *41*, (2007), 1667-1678.

47. Zhang, X. R.; Minear, R. A., Formation, adsorption and separation of high molecular weight disinfection byproducts resulting from chlorination of aquatic humic substances. *Water Res.* 2006, *40*, (2), 221-230.

48. Shan, J.; Hu, J.; Kaplan-Bekaroglu, S. S.; Song, H.; Karanfil, T., The effects of pH, bromide and nitrite on halonitromethane and trihalomethane formation from amino acids and amino sugars. *Chemosphere* 2012, *86*, (4), 323-328.

49. Sharma, V. K.; Graham, N. J. D., Oxidation of Amino Acids, Peptides and Proteins by Ozone: A Review. *Ozone Sci. Eng.* 2010, *32*, (2), 81-90.

50. Dickenson, E. R. V.; Summers, R. S.; Croue, J. P.; Gallard, H., Haloacetic acid and trihalomethane formation from the chlorination and bromination of aliphatic beta-dicarbonyl acid model compounds. *Environmental Science & Technology* 2008, *42*, (9), 3226-3233.

51. Chen, Z.; Valentine, R. L., Formation of N-nitrosodimethylamine (NDMA) from humic substances in natural water. *Environmental Science & Technology* 2007, *41*, (17), 6059-6065.

52. Chen, Z.; Valentine, R. L., The Influence of the Pre-Oxidation of Natural Organic Matter on the Formation of N-Nitrosodimethylamine (NDMA). *Environ. Sci. Technol.* 2008, *42*, (14), 5062-5067.

53. Lee, W.; Westerhoff, P.; Croue, J. P., Dissolved organic nitrogen as a precursor for chloroform, dichloroacetonitrile, N-Nitrosodimethylamine, and trichloronitromethane. *Environmental Science & Technology* 2007, *41*, (15), 5485-5490.

54. Mitch, W. A.; Gerecke, A. C.; Sedlak, D. L., A N-nitrosodimethylamine (NDMA) precursor analysis for chlorination of water and wastewater. *Water Res.* 2003, *37*, (15), 3733-3741.

55. Chen, Z.; Valentine, R. L., Modeling the formation of N-nitrosodimethylamine (NDMA) from the reaction of natural organic matter (NOM) with monochloramine. *Environmental Science & Technology* 2006, *40*, (23), 7290-7297.

56. Selbes, M.; Kim, D.; Ates, N.; Karanfil, T., The roles of tertiary amine structures, background organic matter and chloramine species on NDMA formation. *Water Res.* 2013, *47*, (2), 945-953.

57. Krasner, S. W.; Sclimenti, M. J.; Coffey, B. M., Testing biologically active filters from removing aldehydes formed during ozonation. *Journal of American Water Works Association* 1993, *85*, (5), 62-71.

CHAPTER 5. Research Outlook

5.1. Summary

The research presented in the previous chapters expands the knowledge base regarding cell damage/lysis during the oxidation of cyanobacteria cells, quantifies the release of intracellular organic matter (IOM), toxic metabolites, and odorous metabolites, and evaluates the formation of disinfection byproducts during the chlorination and chloramination of IOM. Interest in these issues is growing as researchers and utilities prepare for increased intensity and frequency of harmful algae/cyanobacteria blooms related to climate change (i.e. warmer temperatures, increased nutrient loadings from drought and wastewater influence).

Overall, the number of variables involved with testing cyanobacteria is seemingly endless (i.e. numerous different strains of cyanobacteria/green algae, strain variability, growth phase effects, environmental impacts (temperature, light), axenic cultures vs natural blooms, IOM/EOM characterization). Furthermore, most research has focused on *Microcystis aeruginosa*, since it commonly identified in source water supplies. As more occurrence data is collected and other toxins and DBPs are identified, the field of cyanotoxin research appears to be very wide open for further research.

5.2. Cyanobacteria Cell Lysis and Damage (Chapter 2)

There are additional opportunities to quantify the morphological changes during oxidation using digital flow cytometry (FlowCAM). Over 40 particle properties are

measured for each particle captured by the FlowCAM, which generates an abundance of quantitative information regarding morphology. We are continuing to work with Fluid Imaging Technologies to further evaluate these properties (e.g. intensity, average red, average blue, average green). Future work will include more extensive analysis of the existing FlowCAM data to better quantify morphological changes and how they may relate to metabolite release.

Many studies use staining (i.e. SYTOX green, propidium iodide) to evaluate the viability of cyanobacteria cells. There was no cell staining included in the work contained in Chapter 2, so no information was obtained regarding cell viability. Based on the results from this study and others, loss of cell viability and metabolite release appears to occur more rapidly than the degradation of chlorophyll-a or complete cell lysis/fragmentation. Future work could compare all of these aspects (i.e. loss of viability, metabolites release, potassium release, cell damage, cell lysis, and chlorophyll-a degradation) in order to better understand the sequence of how oxidants attack cyanobacteria cells and trigger metabolite release.

During this project, all of the testing was conducted using axenic cultures of cyanobacteria. The biology of cultured cyanobacteria may change with each generation of culturing. For example, some cyanobacteria have been shown to lose the ability generate toxins after a few generations in culture. Therefore, mixtures of cyanobacteria from natural blooms should be evaluated with respected to cell lysis and damage, metabolite release, and DBP formation.

5.3. Release of Toxic or Odorous Metabolites (Chapter 3)

Recent studies have evaluated concurrent intracellular and extracellular concentrations of metabolites. Although the method is intense, the grinding, freeze thaw, and sonication process worked well in this study. Microwaving cells may also prove be a more efficient way to extract IOM. Based upon these results, a testing approach could be developed to further investigate whether metabolites are released due to cell membrane damage or if near immediate release of metabolites occurs as a defense mechanism due to oxidative stress exerted on the cyanobacteria cells (reaction times of seconds to minutes).

Discussions are currently taking place regarding the inclusion of cyanotoxins on the Unregulated Contaminant Monitoring Rule 4 (UCMR4), which indicates that select toxins are under consideration for regulation by USEPA. As a result, full-scale occurrence surveys are being discussed along with appropriate sampling plans. Cyanotoxin occurrence in the raw and finished water supplies of numerous utilities would indicate the significant of intracellular release at full-scale utilities. Based upon the results collected in this study, utilities heavily reliant upon chloramine disinfection would be at the greatest risk for intracellular toxin release during drinking water treatment. Unpublished work has indicated that toxin increases are observed during drinking water treatment (personal communication - Lenore Tedesco).

Attempts were made to acquire alternative strains of cyanobacteria that produce a toxin other than microcystin-LR with no success. When a toxic cyanobacteria bloom is

identified, attempts should be made to isolate the toxin-producing strain into an axenic culture for further study. Other toxins may have greater risk of accumulation during drinking water treatment due to their second order rate constants. Furthermore, other emerging cyanotoxins may require further investigation such as BMAA, which has been linked to ALS (Lou Gehrig's disease) in Guam. There is concern that BMAA may be an intracellular specific compound due to release and rapid uptake in natural systems. We are continuing to evaluate the reaction kinetics of BMAA with oxidants including ozone, free chlorine, chloramine, and chlorine dioxide.

5.4. Formation of DBPs from IOM (Chapter 4)

The data showed the potential to form significant yields of DBPs during chlorination or chloramination of IOM. However, IOM from OSC and LYN was determined to be >99% AOC, while that of MA was only 20%. Additional characterization of other strains of cyanobacteria should be conducted. The AOC content can be significant if a utility is on the verge of exceeding Stage 2 regulations for THMs and HAAs. If cyanobacteria-derived precursor material is found to largely biodegradable, then the associated DBP formation can be minimized or eliminated through biological treatment. Furthermore, biological treatment studies would be required to evaluate the removal efficiency of cyanobacteria-derived AOC. Typically, biological processes are not completely efficient at removing the entire fraction of AOC. Emerging biological treatment processes utilizing porous plastic media may present a viable pretreatment alternative to remove EOM upon entering the plant from a surface water supply.

The role of ozone on the formation of NDMA also warrants further study. The results indicated that sequential addition of O_3/NH_2Cl could produce NDMA. However, direct formation of NDMA by ozone oxidation of IOM was not evaluated during the study. Direct formation of NDMA by ozone has been observed during wastewater treatment plants, although it is thought to be due to the oxidation of trace organic contaminants or micropollutants (i.e. ranitidine).

The relevance of nitrosamine formation from IOM and EOM is another research topic that warrants additional research, specifically the differences between ultrapure water versus CRW. The IOM could be better characterized with analysis of amino acids and hydrophobicity to better relate to literature regarding DBP yields from model compounds including amino acids, carbohydrates and proteins. IOM addition into different natural water matrices may also provide insight regarding the environmental relevance of this source of DBP precursors and NOM competition.

5.5. Practical Implications

The findings of this research have practical relevance to drinking water utilities with respect to plant operation, public health, and consumer confidence. Chapter 2 illustrates that cyanobacteria cells are damaged but not fragmented during typical drinking water treatment exposures. Therefore, oxidation of cells should have minimal impact on filterability since the cells are not degraded into smaller fragments. Chapter 3 illustrates that metabolites may be released under low oxidant exposure conditions, which may be stress induced. In the case of microcystin-LR, oxidation of the released metabolites can

be estimated based upon published kinetic information with oxidation occurring in the order of ozone>>chlorine>chlorine dioxide>chloramine. In the case of MIB and geosmin, release also occurred when using low oxidant dosages (0.63 mg/L). Release by chlorine, chloramine, or chlorine dioxide places a utility at the greatest risk of increased concentration due to slow reaction rate kinetics. Chapter 4 illustrates that IOM contains DBP precursor material during FP testing. When IOM was added to natural water, the yields of DBPs were not detectable. The findings indicate that while IOM has the potential to form C-DBPs and N-DBPs, they may not be formed under practical treatment conditions. Furthermore, a majority of IOM may be biodegradable either in the environment or during an engineering treatment process. Biological treatment may eliminate IOM and associated metabolites during a treatment process, and make the finished drinking water more biologically stable at the same time.

APPENDIX 1. Supporting Information

S.1.1 – Using Digital Flow Cytometry to Assess the Degradation of Three Cyanobacteria Species after Oxidation Processes.

Table S1.1. – Composition of BG-11 Growth Media

Component	Amount (mL)	Stock Solution (g/L)	Conc Final Medium (M)
$NaNO_3$	10	30g/200mL H_2O	17.6 mM
K_2HPO_4	10	0.8g/200mL H_2O	0.22 mM
$MgSO_4$ $7H_2O$	10	1.5g/200mL H_2O	0.03mM
$CaCl_2$ $2H_2O$	10	0.72g/200mL H_2O	0.2 mM
Citric Acid H_2O	10	0.12g/200mL H_2O	0.03 m
Ferric ammonium citrate	10	0.12g/200mL H_2O	0.02 mM
Na_2EDTA $2H_2O$	10	0.02g/200mL H_2O	0.002 mM
Na_2CO_3	10	0.4g/200mL H_2O	0.18 mM
Sodium Thiosulfate Pentahydrate	24.8 g/100mL		1 mM
Trace Metal Solution	1 mL/L		
H_3BO_3		2.86 g/L	46 uM
$MnCl_2$ $4H_2O$		1.81g/L	9 uM
$ZnSO_4$ $7H_2O$		0.22 g/L	0.77 uM
Na_2MoO_4 $2H_2O$		0.39 g/L	1.6 uM
$CuSO_4$ $5H_2O$		0.079g/L	0.3 uM
$Co(NO_3)_2$ $6H_2O$		49.4mg/L	0.17 uM

Table S1.2. – Composition of Bold 3N Growth Media

Component	Amount (mL)	Stock Solution (g/L)	Conc Final Medium (M)
$NaNO_3$	30mL/L	10g/400mL H_2O	8.82 mM
$CaCl_2$ $2H_2O$	10mL/L	1g/400mL H_2O	0.17 mM
$MgSO_4$ $7H_2O$	10mL/L	3g/400mL H_2O	0.3mM
K_2HPO_4	10mL/L	3g/400mL H_2O	0.43 mM
KH_2PO_4	10mL/L	7g/400mL H_2O	1.29 mM
NaCl	10mL/L	1g/400mL H_2O	0.43 mM
P-IV Metal Solution	6mL/L		
Na_2EDTA $2H_2O$		0.75 g/L	2 mM
FeCl3 $6H_2O$		0.097 g/L	0.36 mM
$MnCl_2$ $4H_2O$		0.041 g/L	0.21 mM
ZnCl2		0.005 g/L	0.037 mM
$CoCl_2$ $6H_2O$		0.002 g/L	0.0084 mM
Na_2MoO_4 $2H_2O$		0.004 g/L	0.017 mM
Soilwater: GR+ medium	40 mL/L	Purchase from UTEX	
Vitamin B_{12}	1mL/L		
HEPES buffer pH 7.8		2.4g/200mL	
Vitamin B_{12}		0.027g/200mL H_2O	

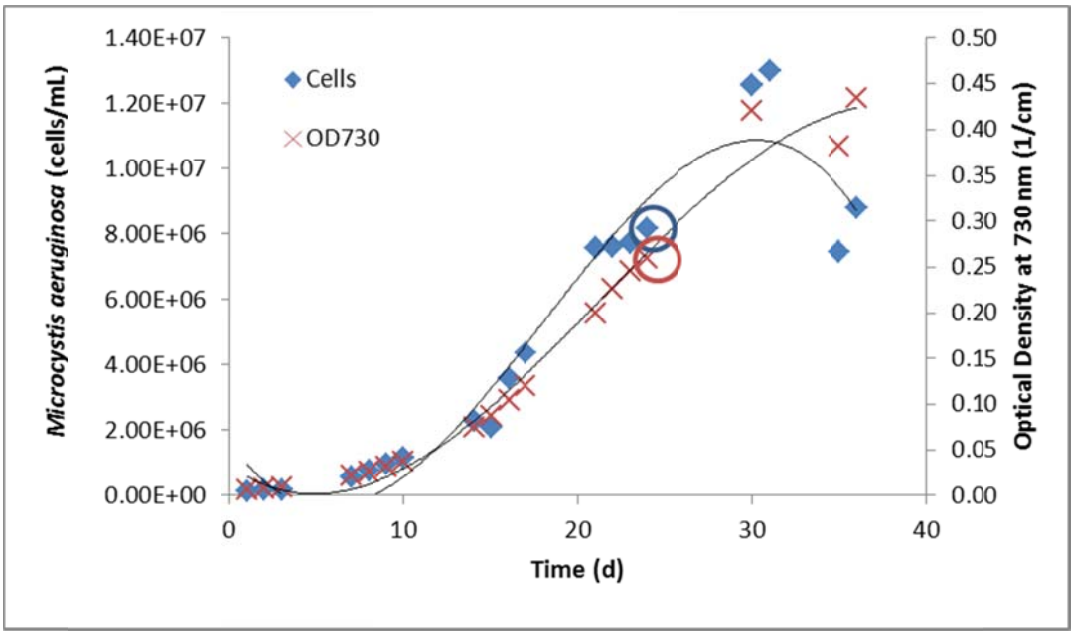

Figure S1.1. Growth curve developed for *Microcystis aeruginosa*. (Note: Circles indicate when the cells were harvested for bench-scale testing)

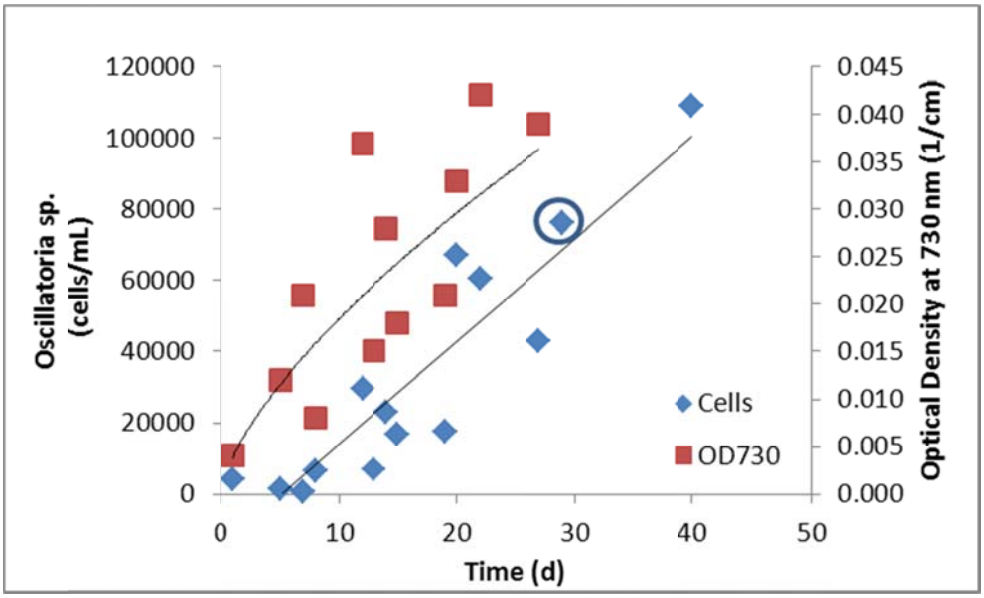

Figure S1.2. Growth curve developed for *Oscillatoria sp.* cells passing a 100 µm mesh screen. (Note: Circle indicates when the cells were harvested for bench-scale testing)

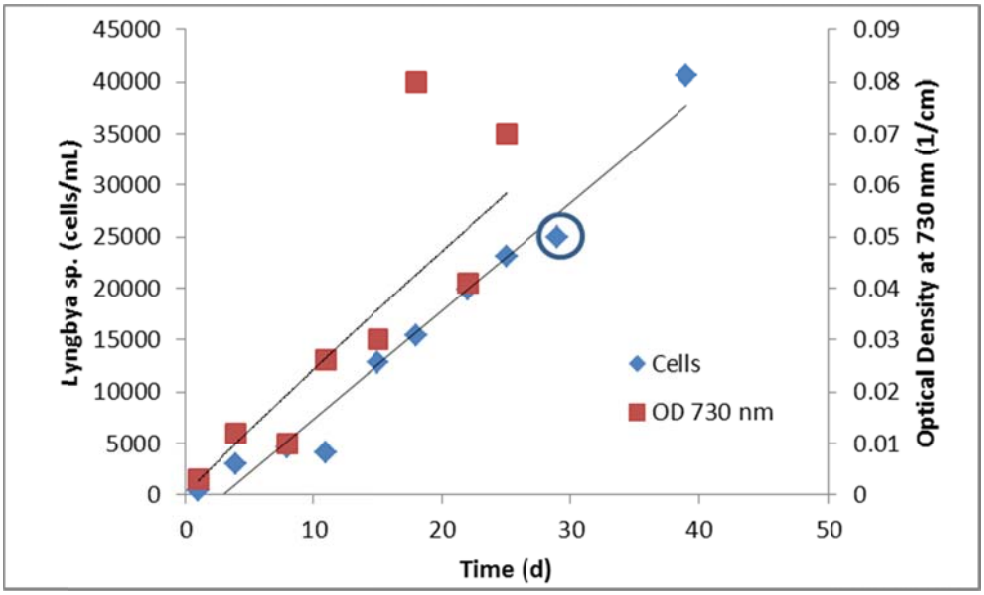

Figure S1.3. Growth curve developed for *Lyngyba sp*. cells passing a 100 µm mesh screen. (Note: Circle indicates when the cells were harvested for bench-scale testing)

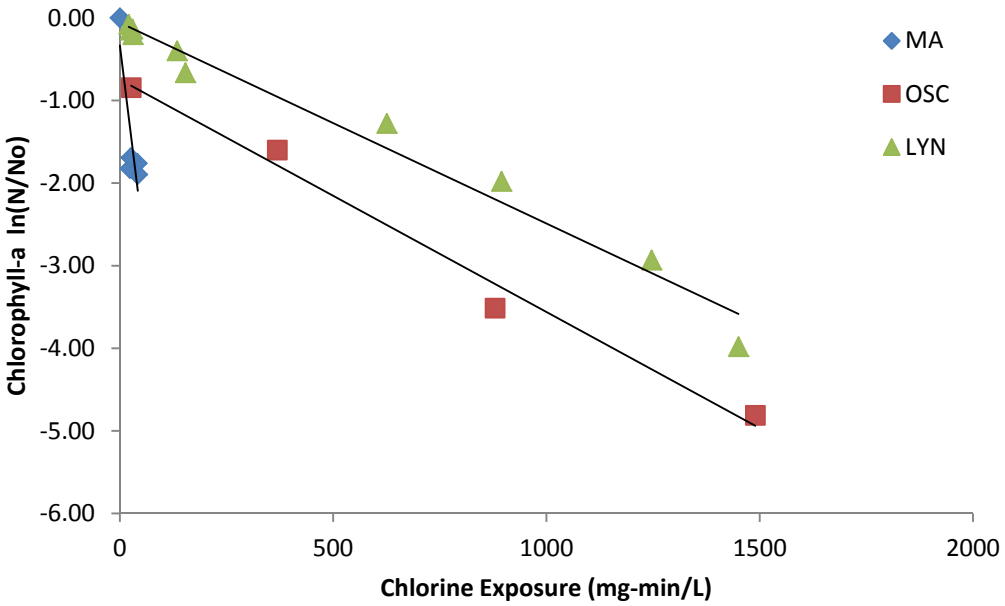

Figure S1.4. Relationship between chlorophyll-a ln(C/Co) and chlorine exposure illustrating the determination of second order rate constant for MA, OSC, and LYN in CRW at pH=8 and T=22°C. (Note: MA rate constant estimated from the slope of the line through the origin and data collected using a chlorine dose of 0.63 mg/L)

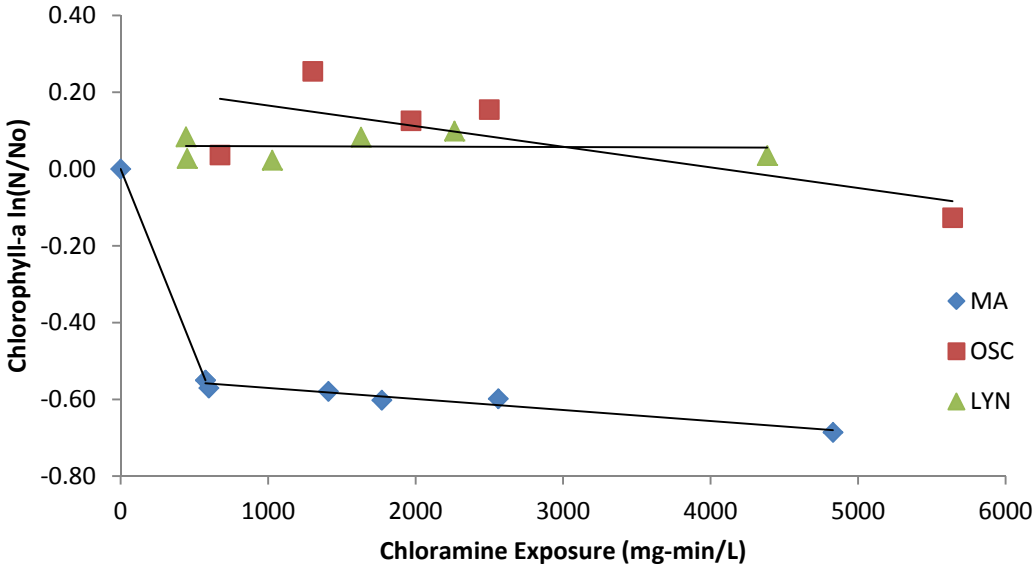

Figure S1.5. Relationship between chlorophyll-a ln(C/Co) and chloramine exposure illustrating the determination of second order rate constant for MA, OSC, and LYN in CRW at pH=8 and T=22°C

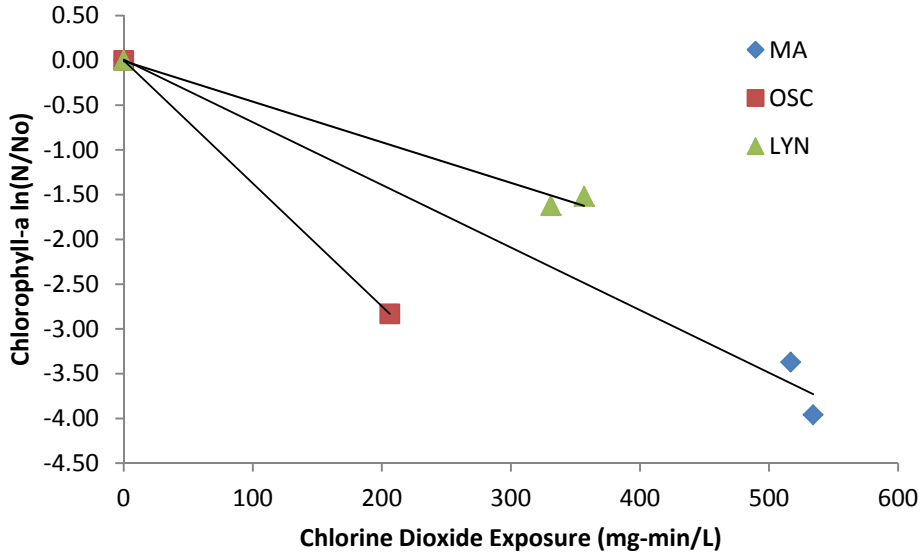

Figure S1.6. Relationship between chlorophyll-a ln(C/Co) and chlorine dioxide exposure illustrating the determination of second order rate constant for MA, OSC, and LYN in CRW at pH=8 and T=22°C. (Note: All rate constants were estimated from the slope of the line through the origin and data collected using a chlorine dioxide dose of 0.63 mg/L)

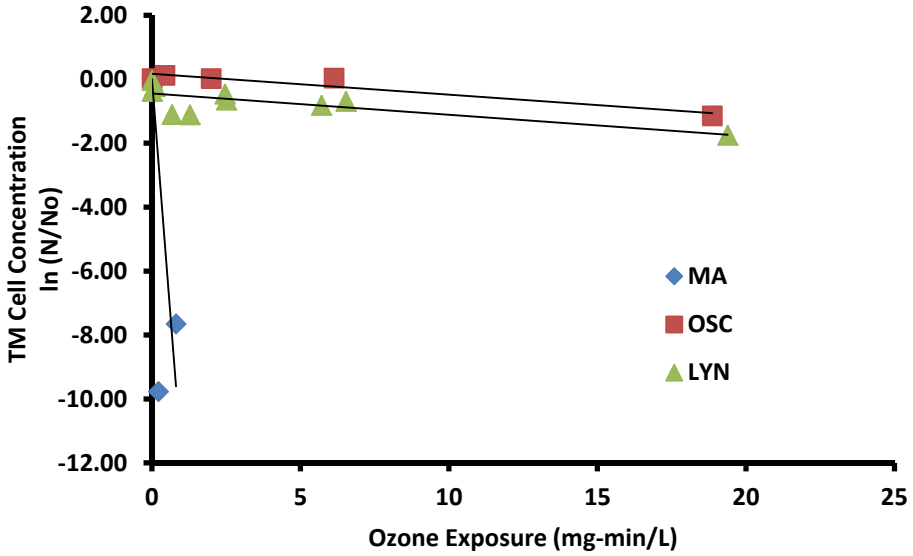

Figure S1.7. Relationship between TM cell concentration ln(C/Co) and ozone exposure illustrating the determination of second order rate constant for MA, OSC, and LYN in CRW at pH=8 and T=22°C. (Note: MA rate constant estimated from the slope of the line through the origin and data collected using an ozone dose of 0.63-1.25 mg/L)

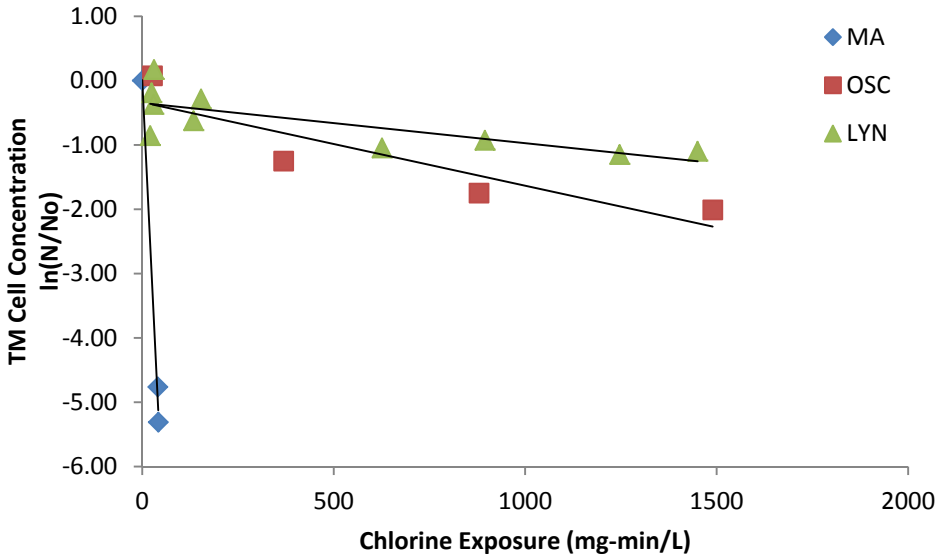

Figure S1.8. Relationship between TM cell concentration ln(C/Co) and chlorine exposure illustrating the determination of second order rate constant for MA, OSC, and LYN in CRW at pH=8 and T=22°C. (Note: MA rate constant estimated from the slope of the line through the origin and data collected using a chlorine dose of 0.63 mg/L)

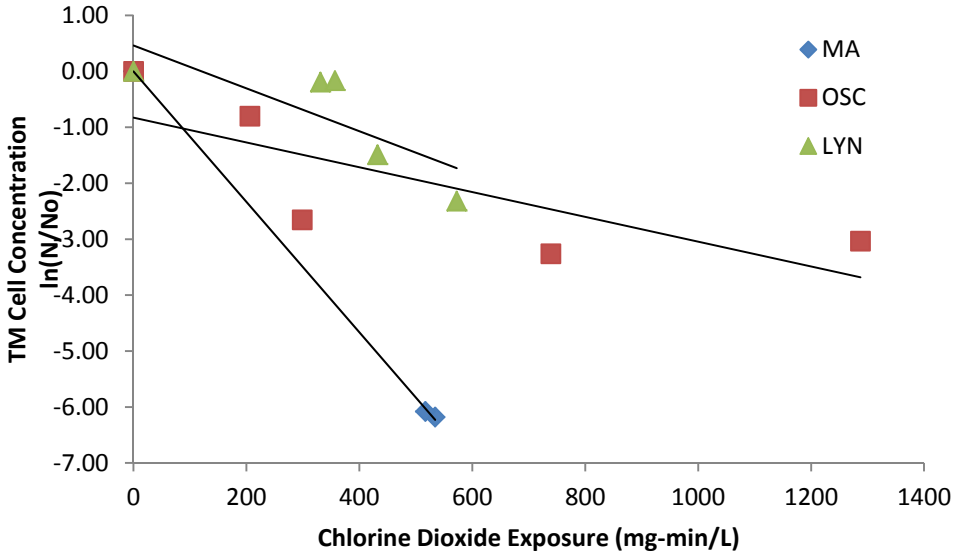

Figure S1.9. Relationship between TM cell concentration ln(C/Co) and chlorine dioxide exposure illustrating the determination of second order rate constant for MA, OSC, and LYN in CRW at pH=8 and T=22°C. (Note: MA rate constant estimated from the slope of the line through the origin and data collected using a chlorine dioxide dose of 0.63 mg/L)

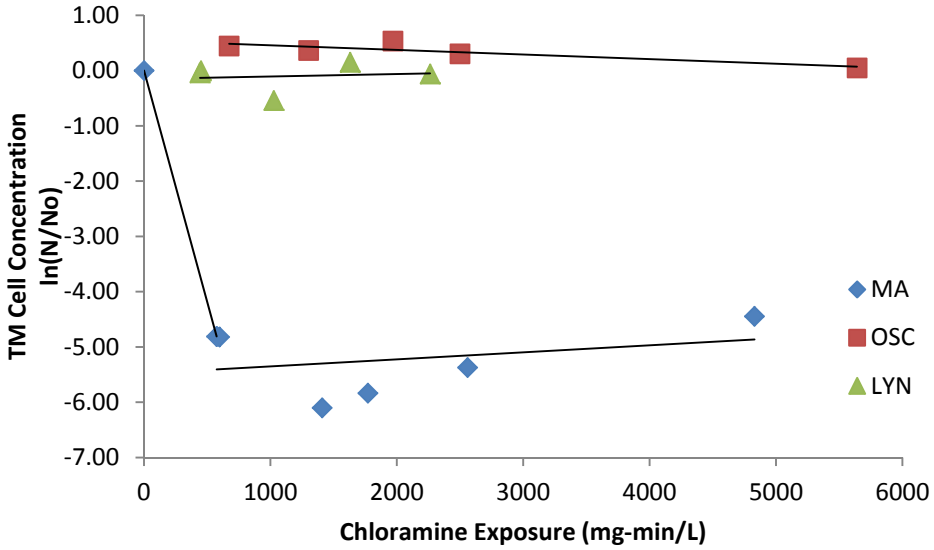

Figure S1.10. Relationship between TM cell concentration ln(C/Co) and chloramine exposure illustrating the determination of second order rate constant for MA, OSC, and LYN in CRW at pH=8 and T=22°C.

Figure S1.11. – Digital and binary images of *Microcystis aeruginosa* after oxidation by chlorine dioxide (ClO2).

(a) ClO2= 0 mg/L (Control)

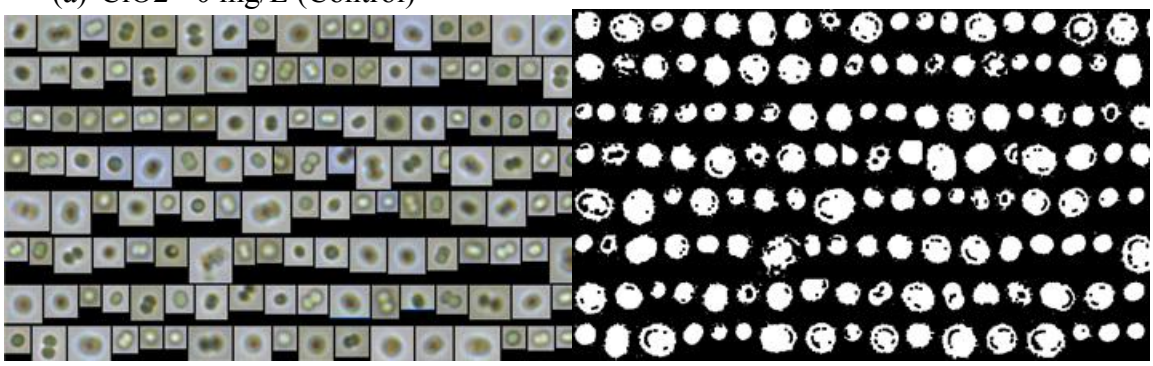

(b) ClO2=0.63 mg/L

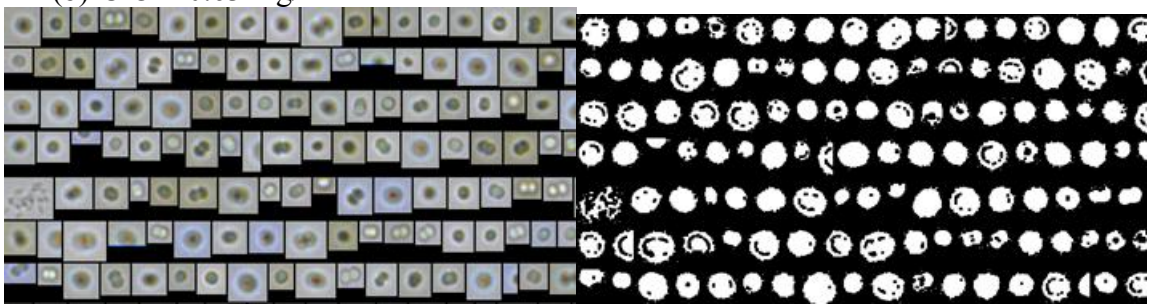

(c) ClO2=1.25 mg/L

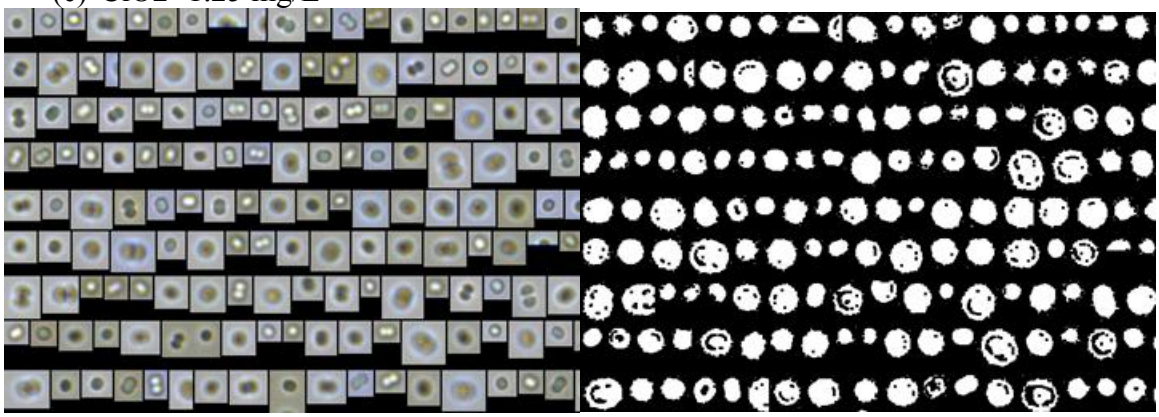

(d) ClO2=1.88 mg/L

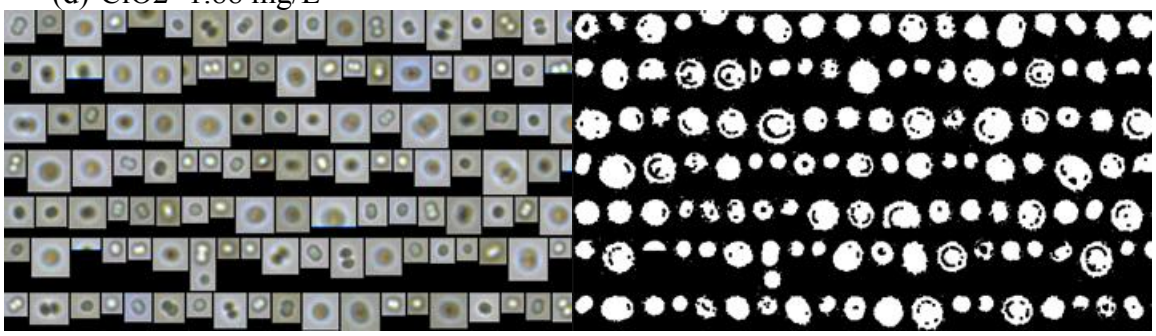

(e) ClO2=2.5 mg/L

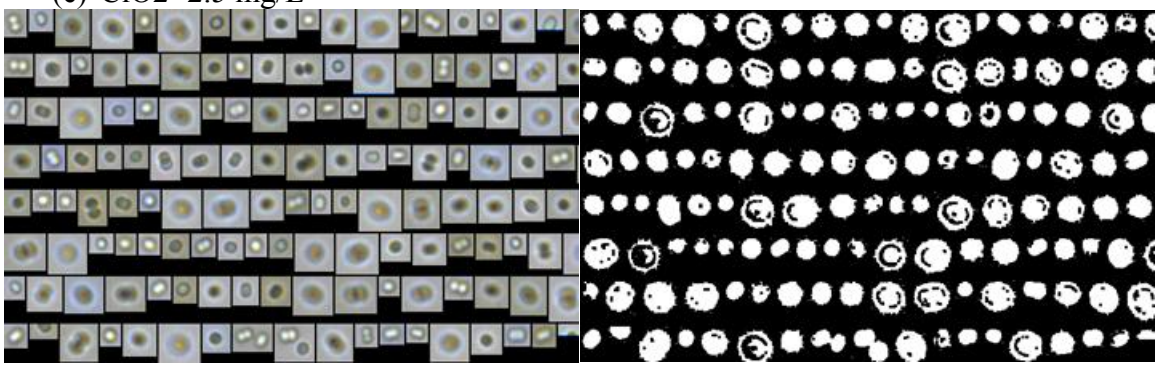

(f) ClO2=5.0 mg/L

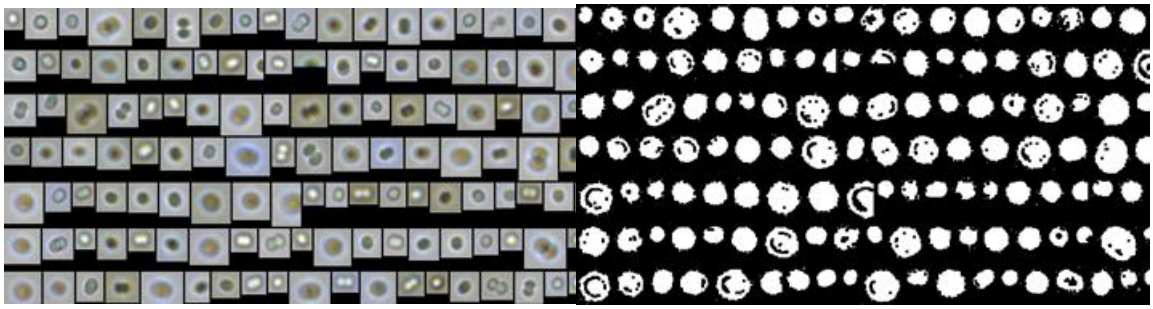

Figure S1.12. – Digital and binary images of *Microcystis aeruginosa* after oxidation by chlorine (Cl2).

(a) Cl2=0 mg/L (Control)

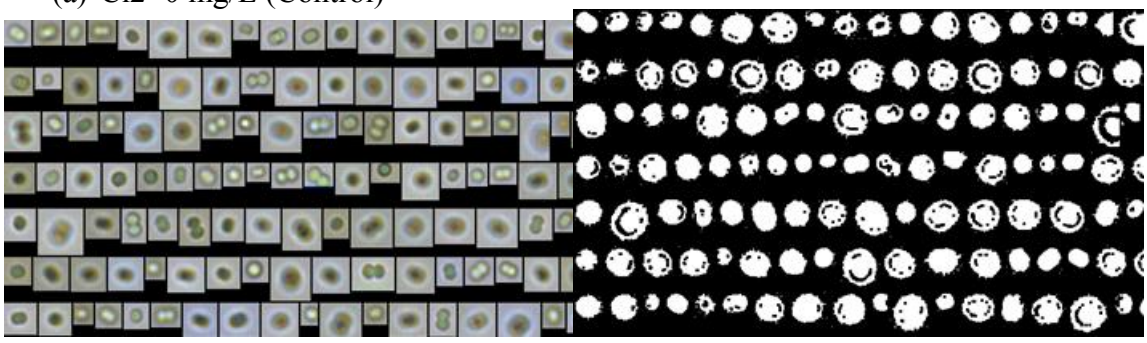

(b) Cl2=0.63 mg/L

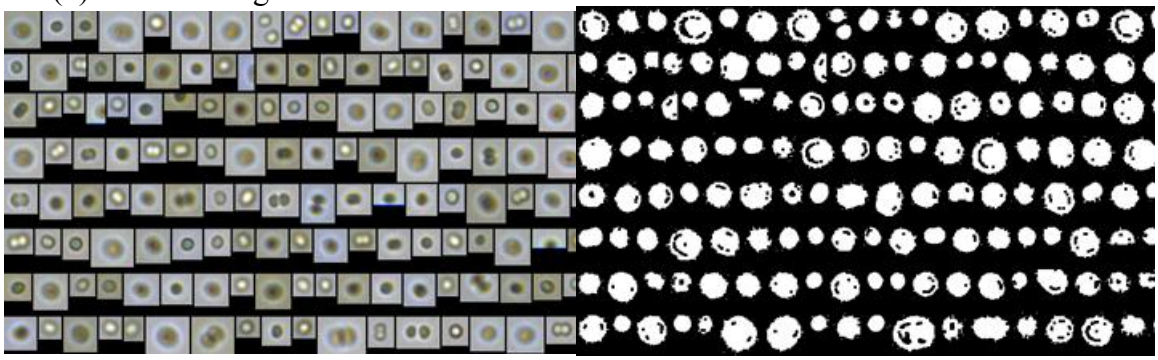

(c) Cl2=1.25 mg/L

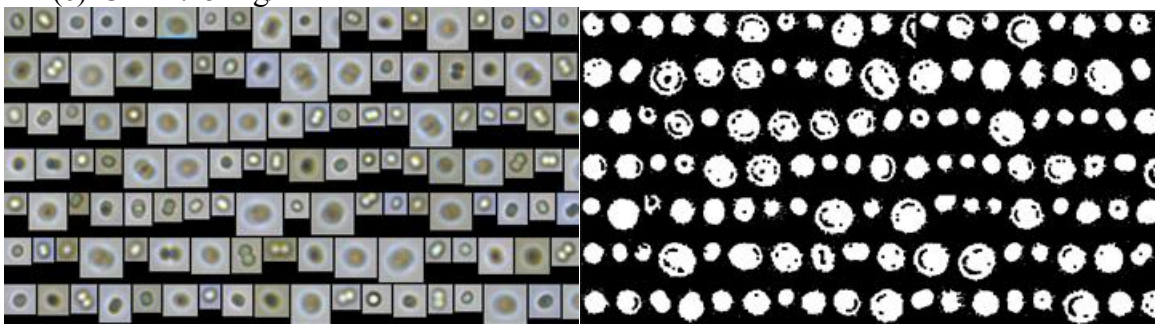

(d) Cl2=1.88 mg/L

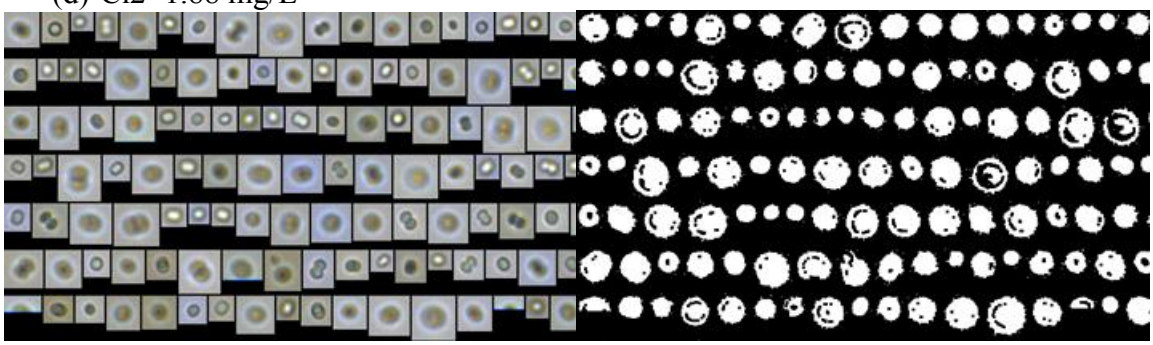

(e) Cl2=2.5 mg/L

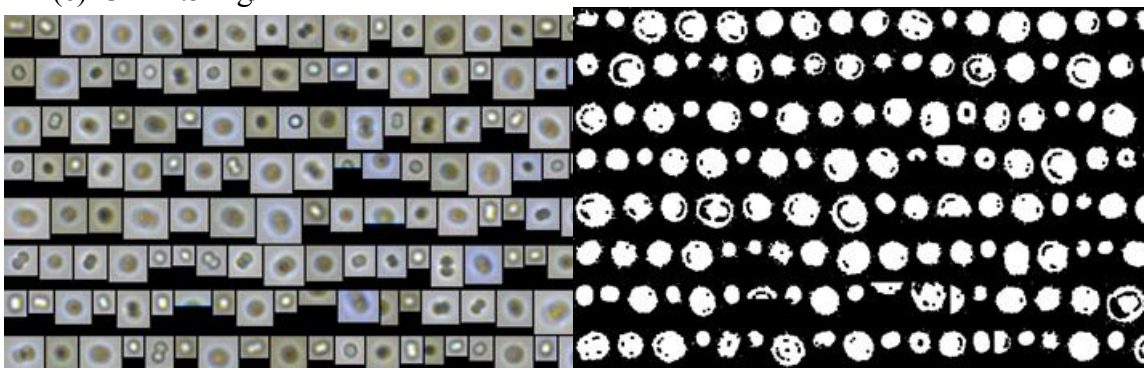

(f) Cl2=5.0 mg/L

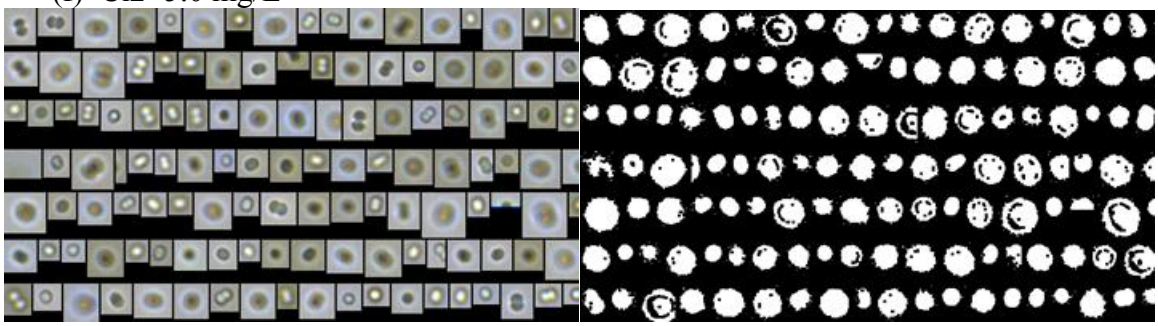

Figure S1.13. – Digital and binary images of *Microcystis aeruginosa* after oxidation by chloramine (NH2Cl).

(a) NH2Cl=0 mg/L (Control)

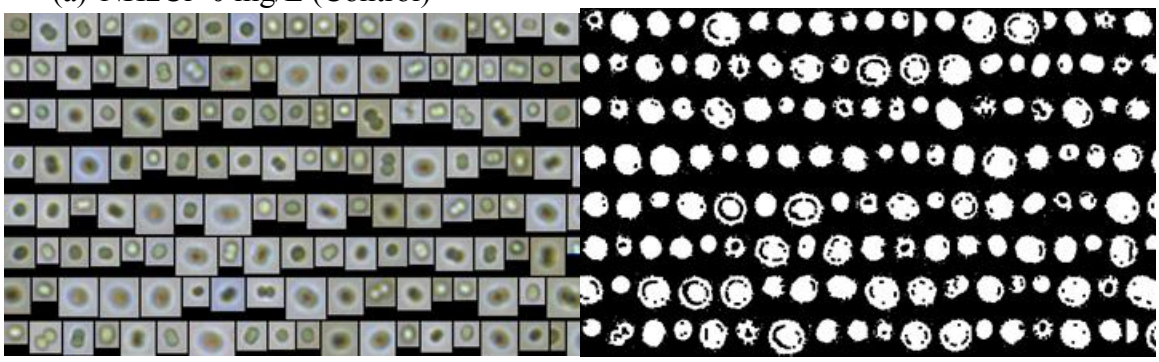

(b) NH2Cl=0.63 mg/L

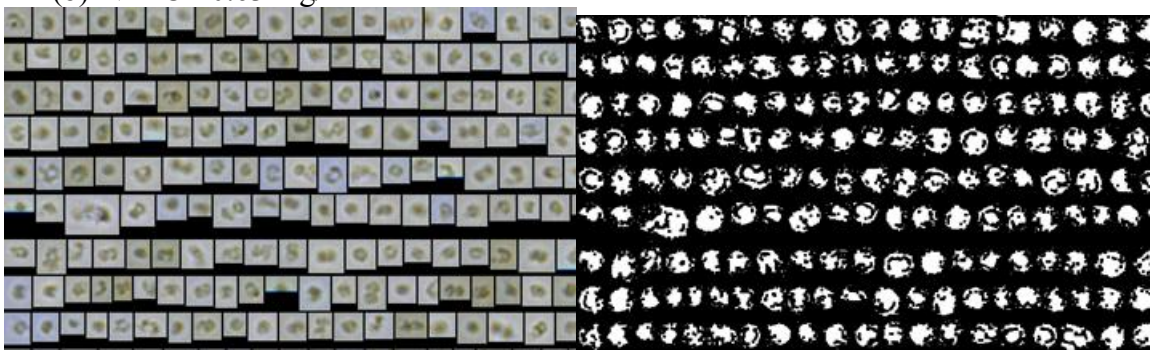

(c) NH2Cl=1.25 mg/L

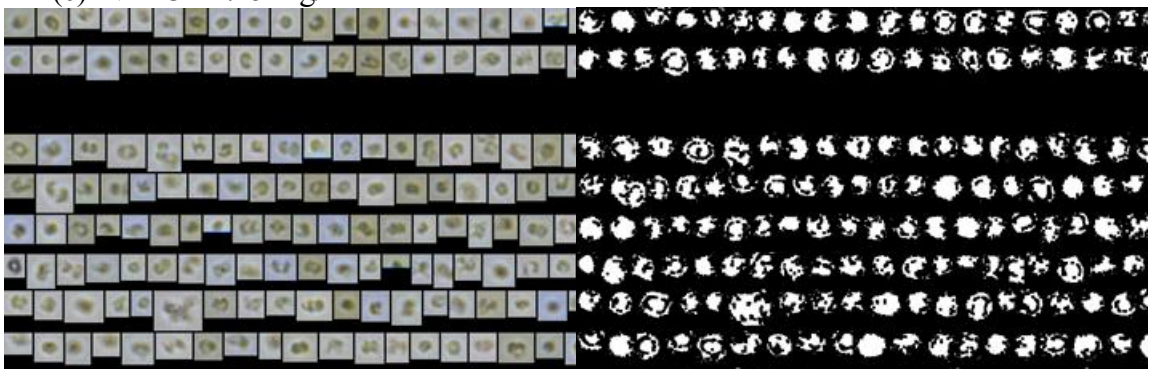

(d) NH2Cl=1.88 mg/L

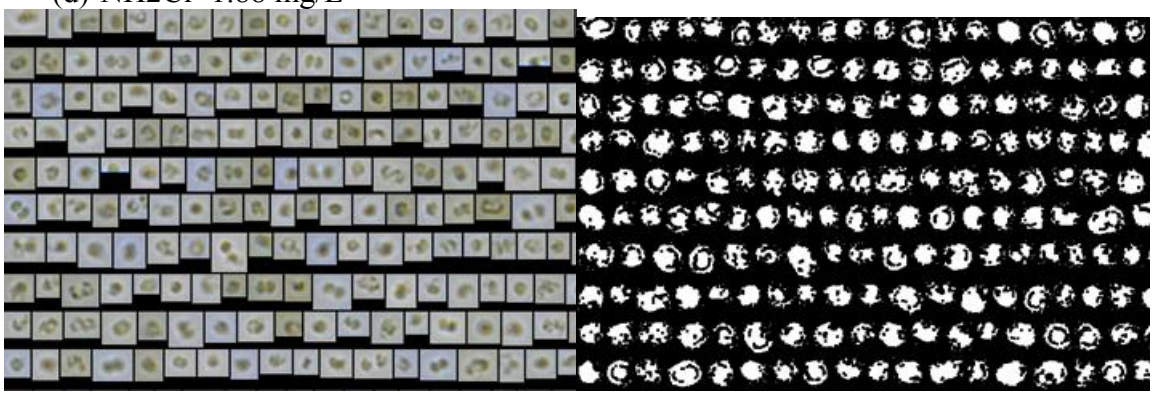

(e) NH2Cl=2.5 mg/L

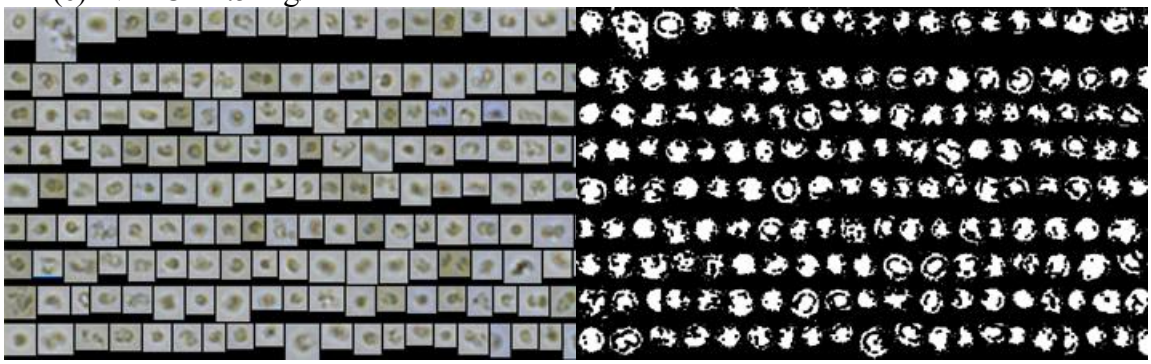

(f) NH2Cl=5.0 mg/L

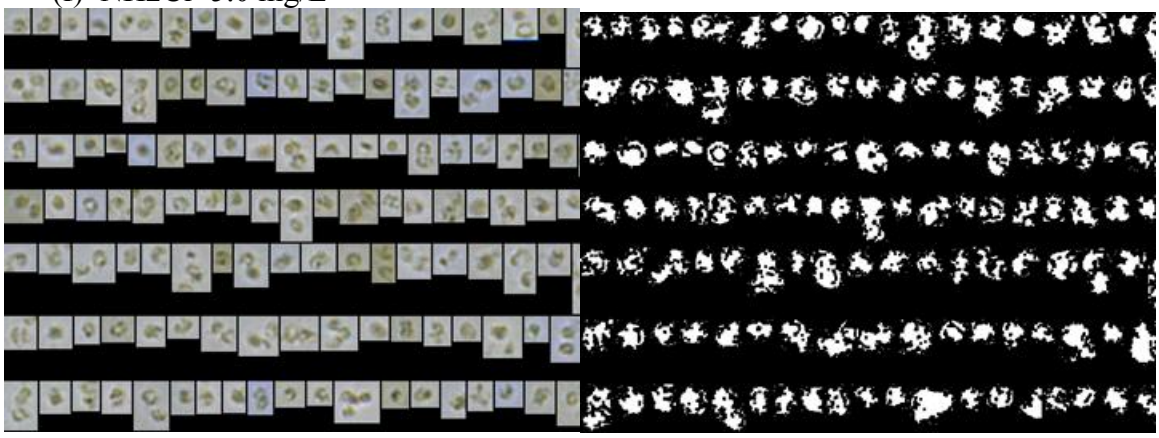

Figure S1.14. – Digital and binary images of *Microcystis aeruginosa* after oxidation by ozone (O3).

(a) O3=0 mg/L (Control)

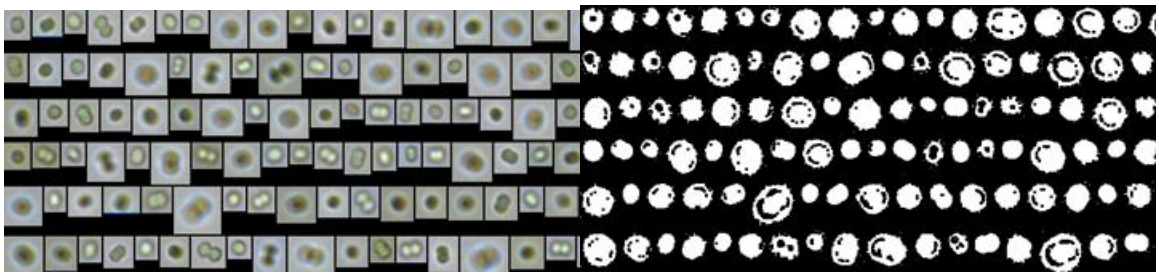

(b) O3=0.63 mg/L

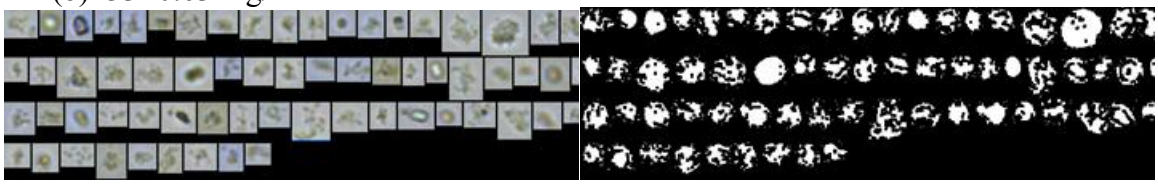

(c) O3=1.25 mg/L

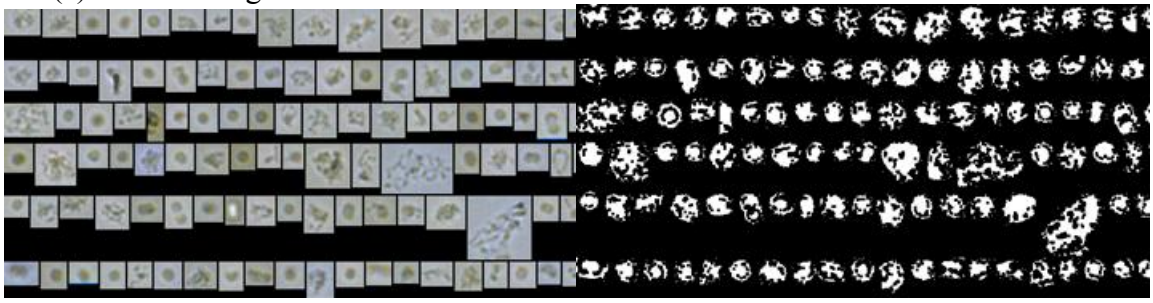

(d) O3=1.88 mg/L

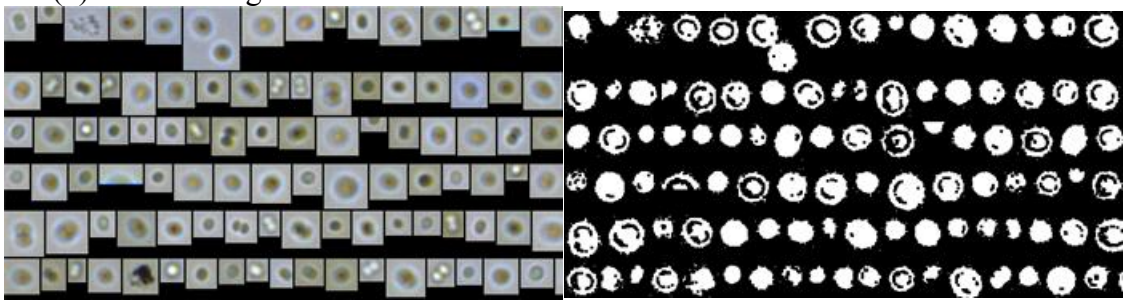

(e) O3=2.5 mg/L

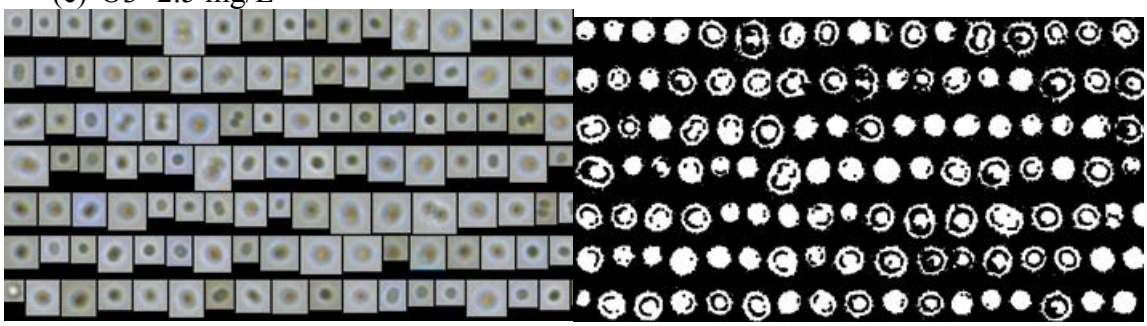

(f) O3=5.0 mg/L

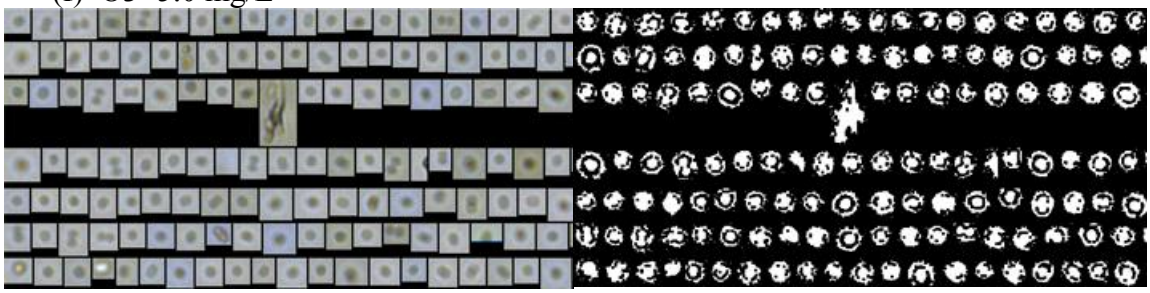

Figure S1.15. – Digital and binary images of *Oscillatoria sp.* after oxidation by chlorine dioxide (ClO2).

(a) ClO2=0 mg/L (Control)

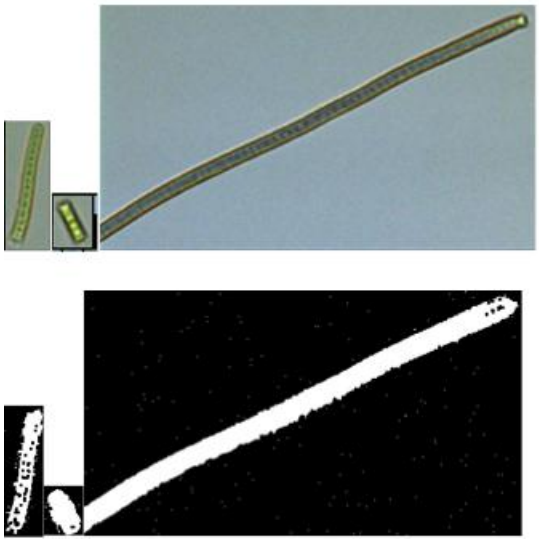

(b) ClO2=0.63 mg/L

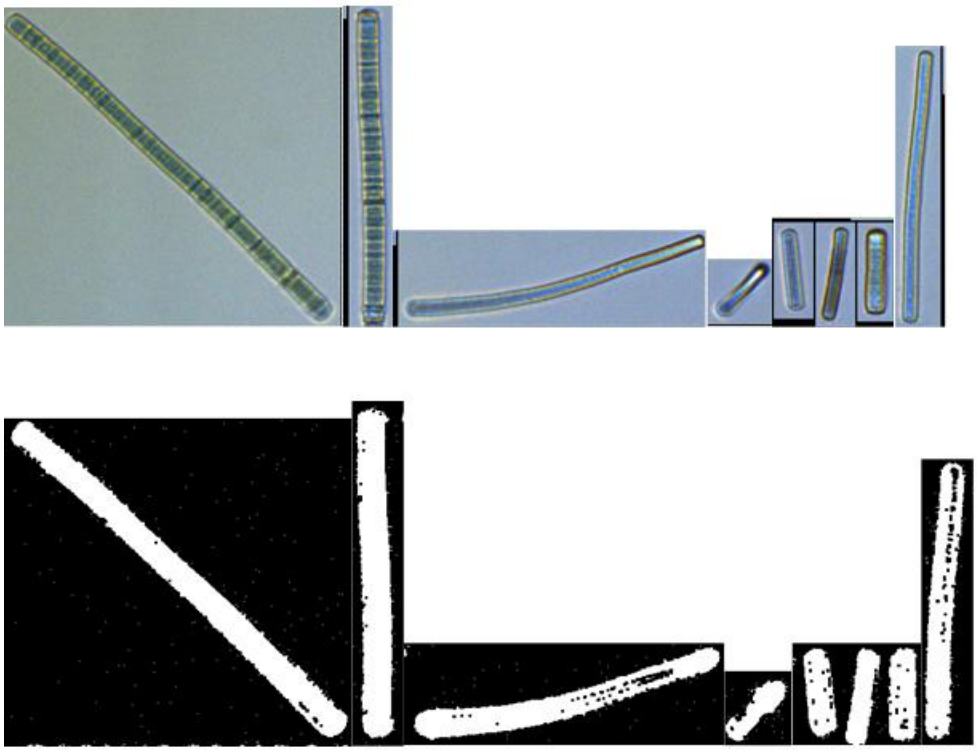

(c) ClO2=1.25 mg/L

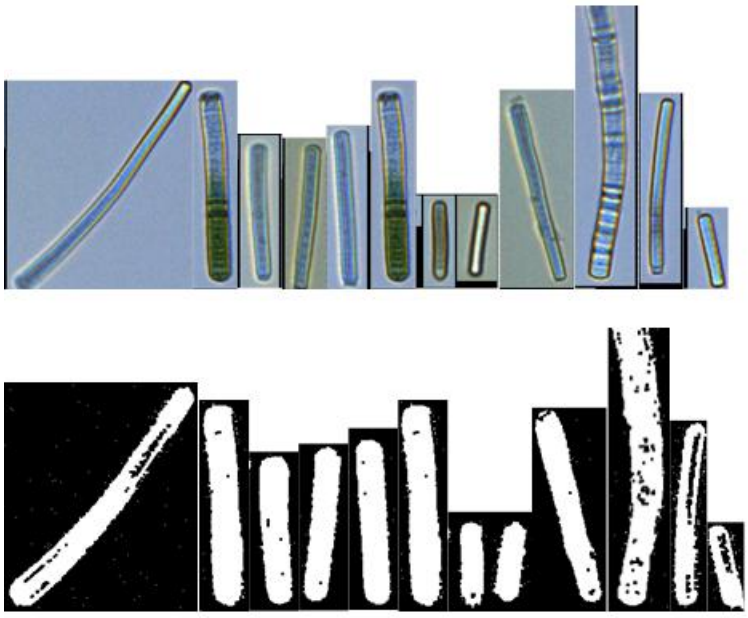

(d) ClO2=1.88 mg/L

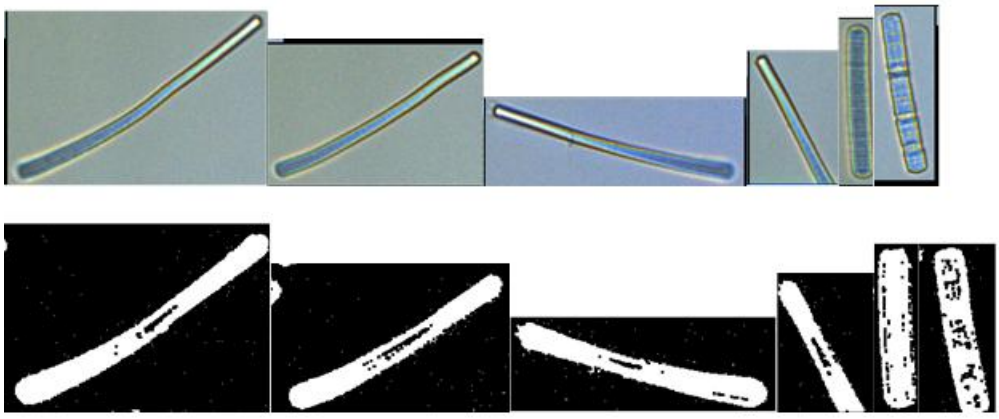

(e) ClO2=2.5 mg/L

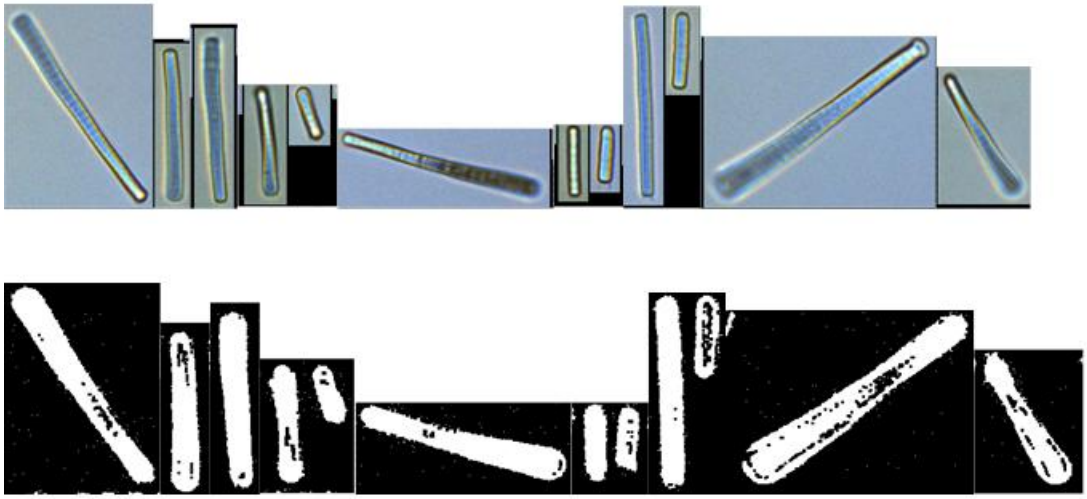

(f) ClO2=5 mg/L

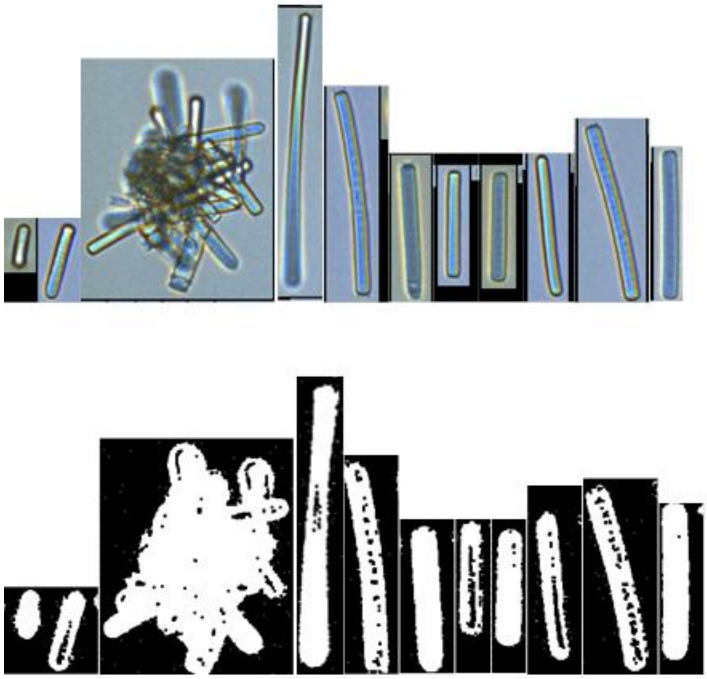

Figure S1.16. – Digital and binary images of *Oscillatoria sp.* after oxidation by chlorine (Cl2).

(a) Cl2=0 mg/L (Control)

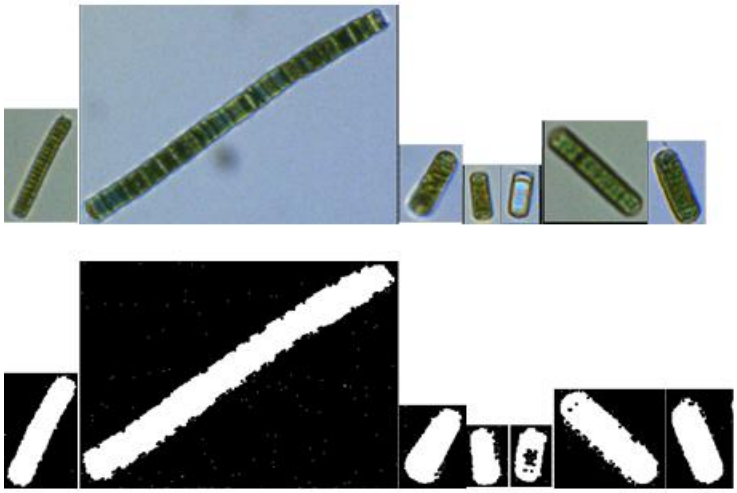

(b) Cl2=0.63 mg/L

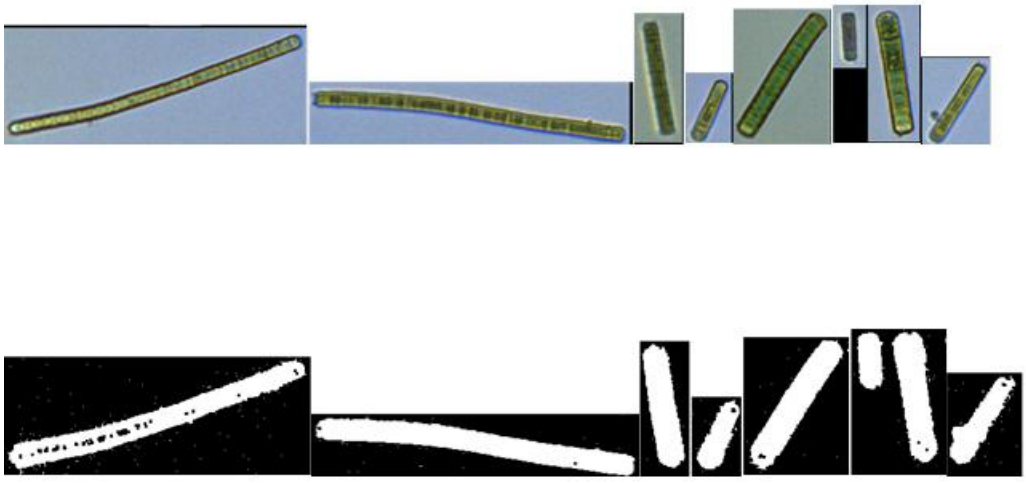

(c) Cl2=1.25 mg/L

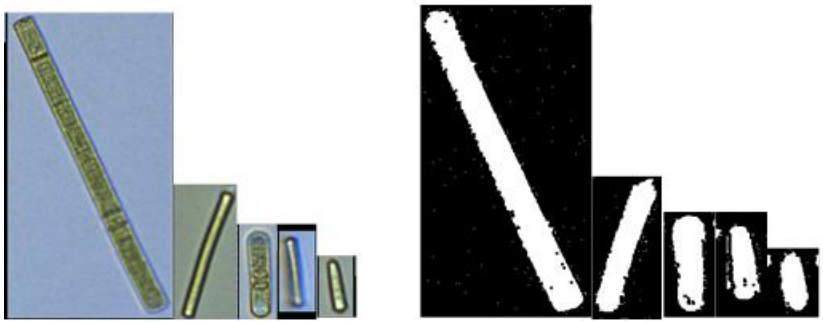

(d) Cl2=1.88 mg/L

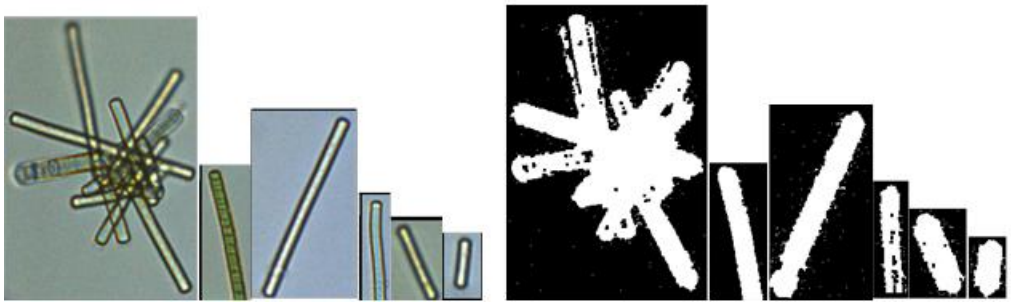

(e) Cl2=2.5 mg/L

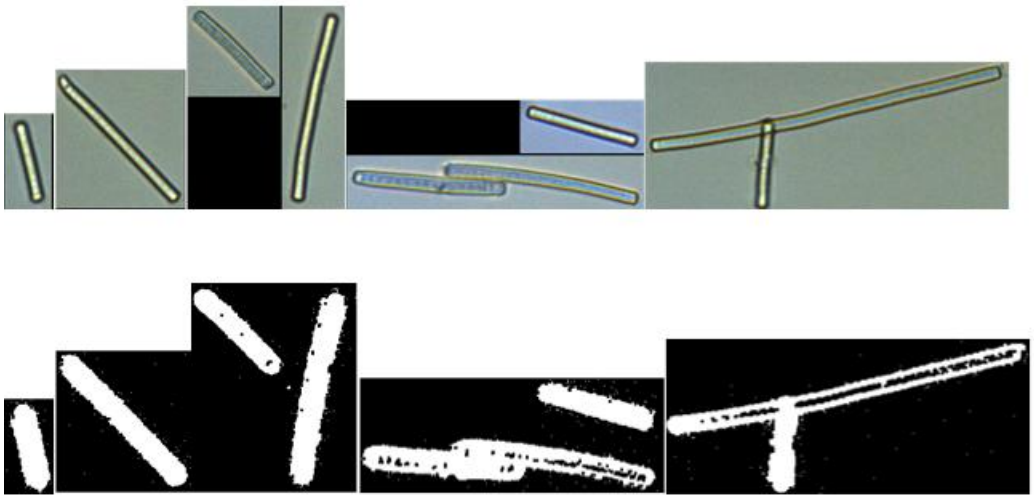

(f) Cl2=5.0 mg/L

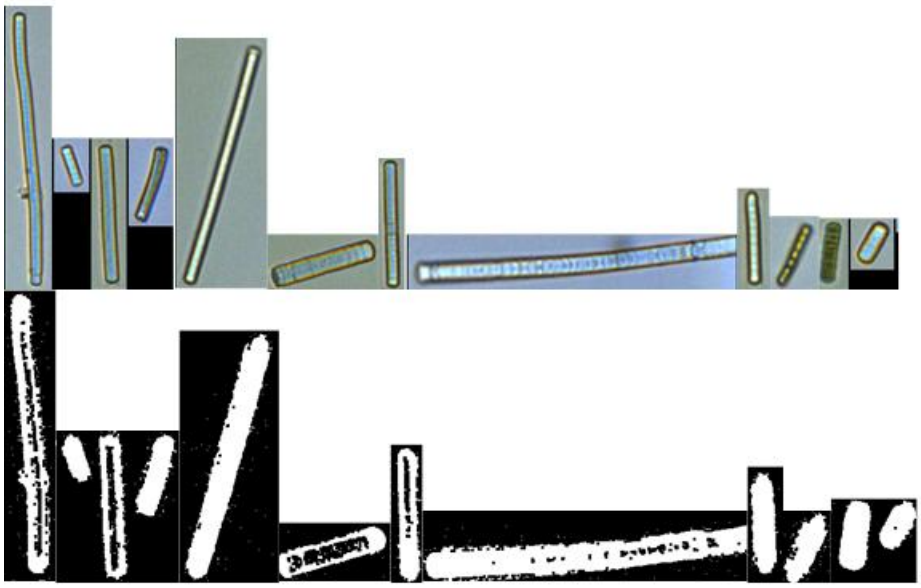

Figure S1.17. – Digital and binary images of *Oscillatoria sp.* after oxidation by chloramine (NH2Cl).

(a) NH2Cl=0 mg/L (Control)

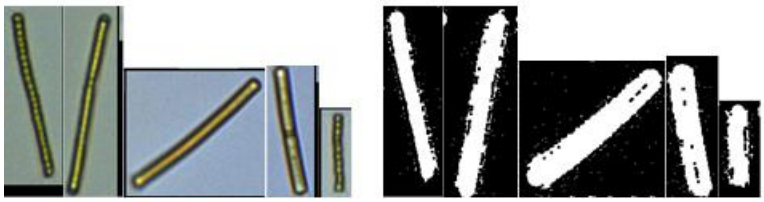

(b) NH2Cl=0.63 mg/L

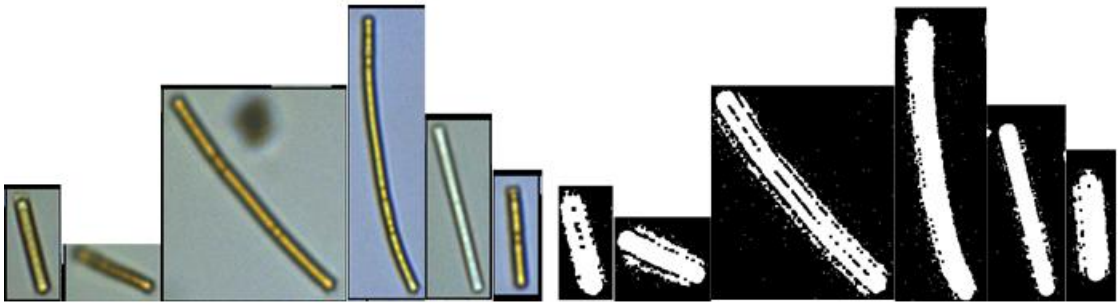

(c) NH2Cl=1.25 mg/L

(d) NH2Cl=1.88 mg/L

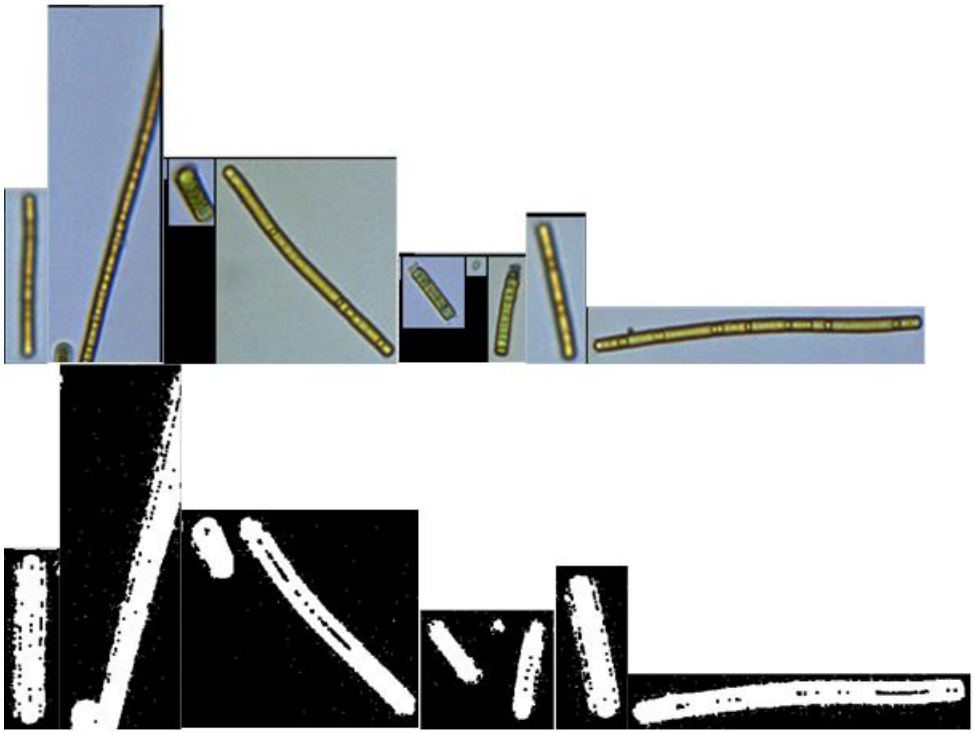

(e) NH2Cl=2.5 mg/L

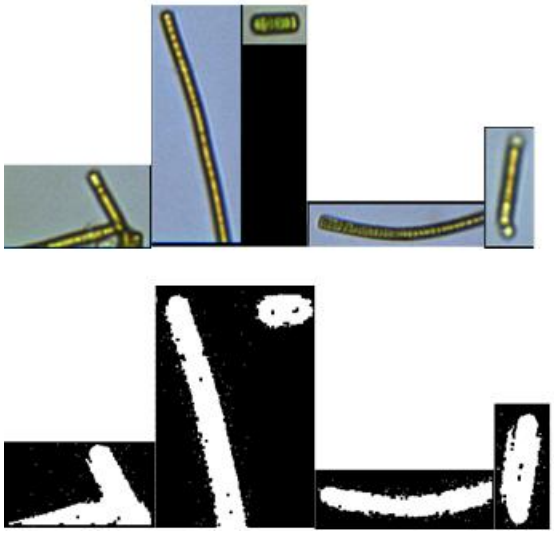

(f) NH2Cl=5.0 mg/L

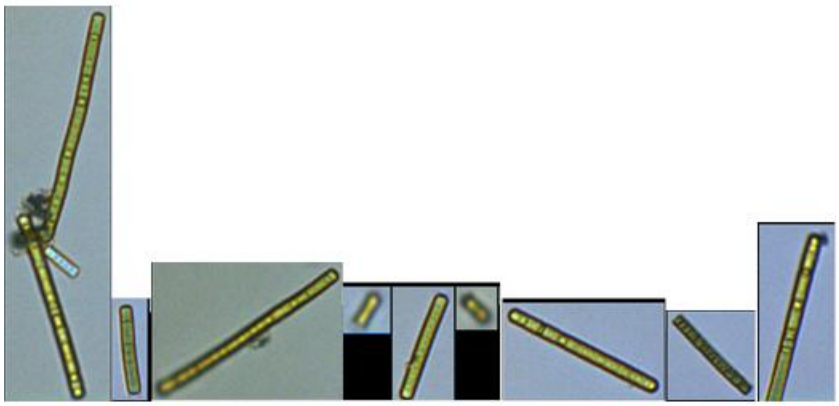

Figure S1.18. – Digital and binary images of *Oscillatoria sp.* after oxidation by ozone (O3).

(a) O3=0 mg/L (Control)

(b) O3=0.63 mg/L

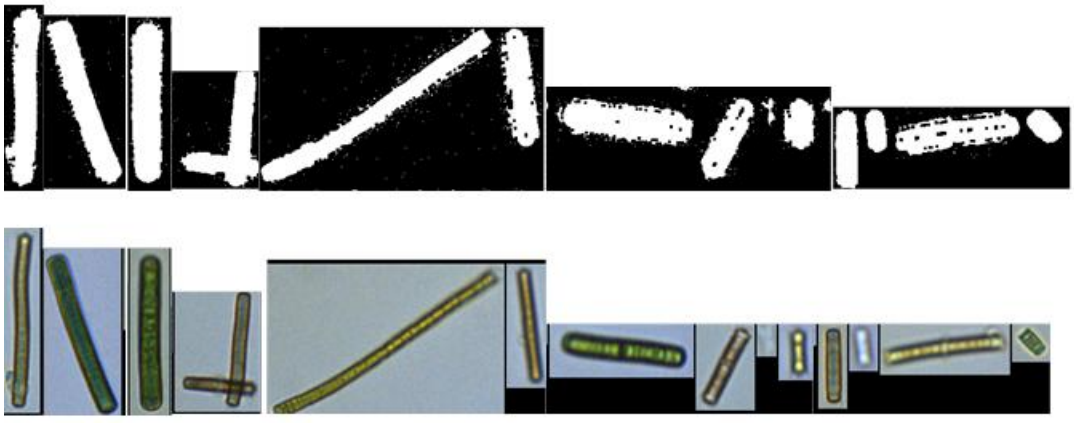

(c) O3=1.25 mg/L

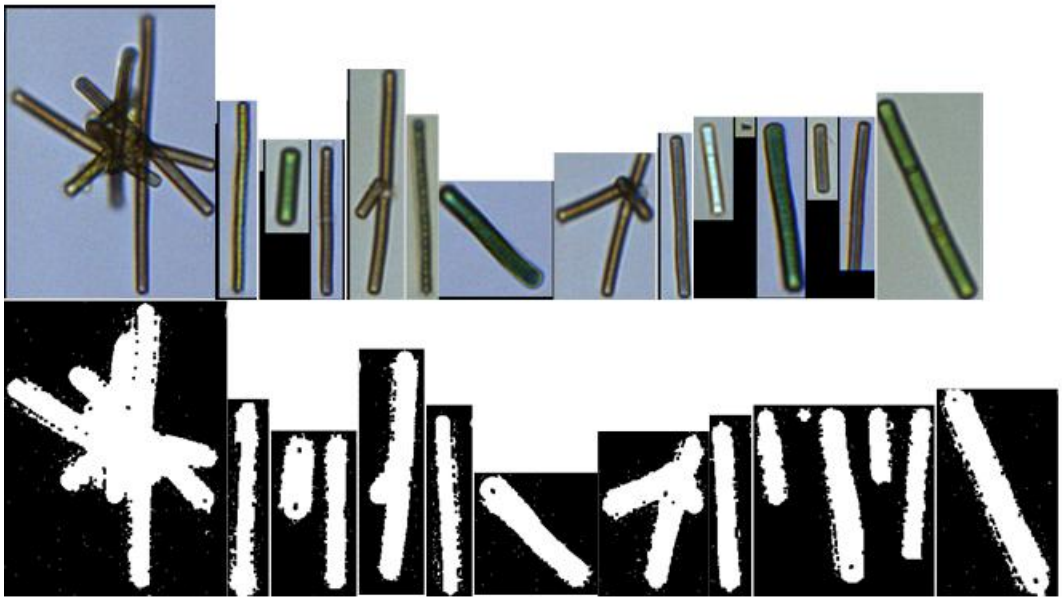

(d) O3=1.88 mg/L

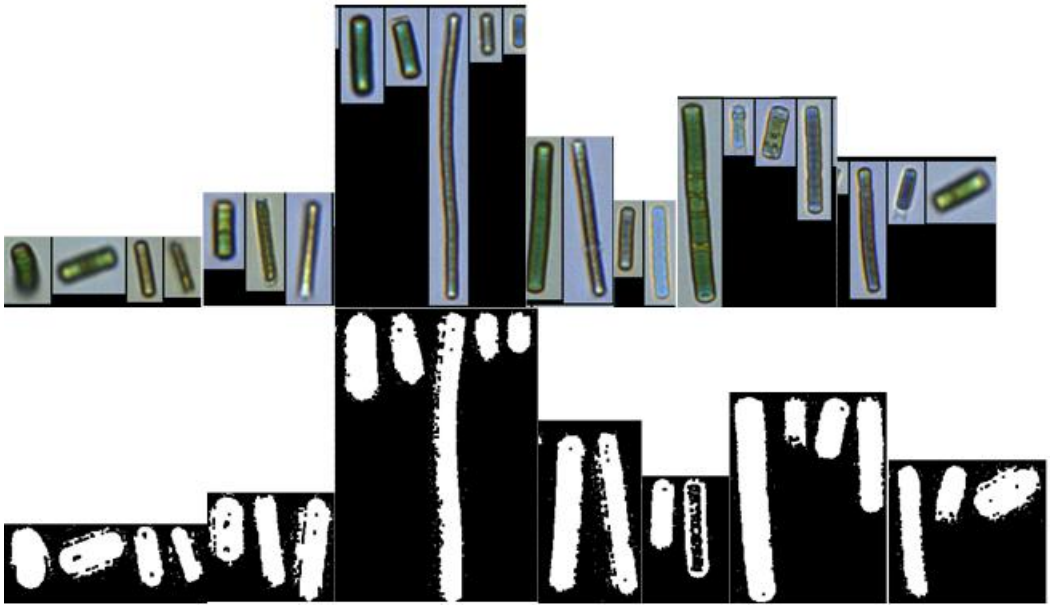

(e) O3=2.5 mg/L

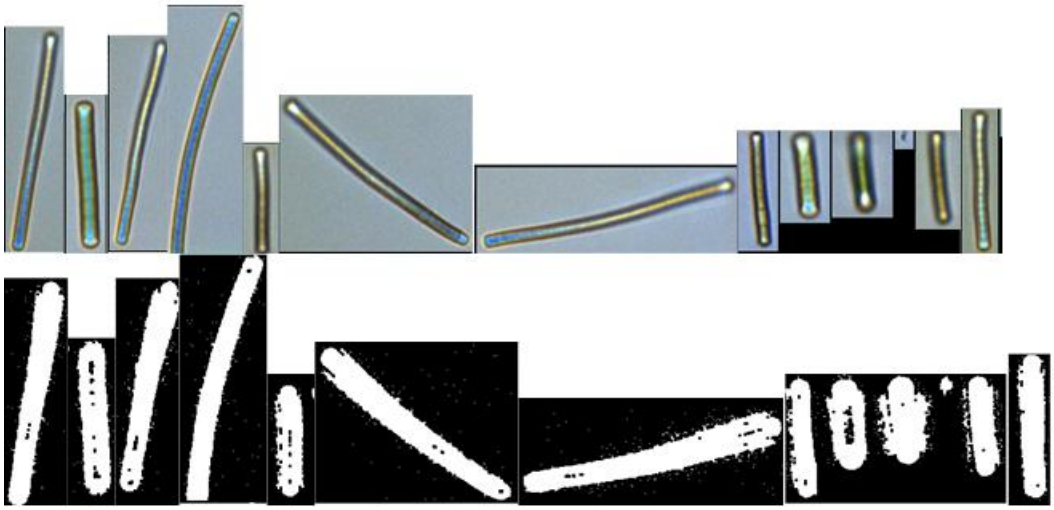

(f) O3=5.0 mg/L

Figure S1.19. – Digital and binary images of *Lyngbya sp.* after oxidation by chlorine dioxide (ClO2).

(a) ClO2=0 mg/L (Control)

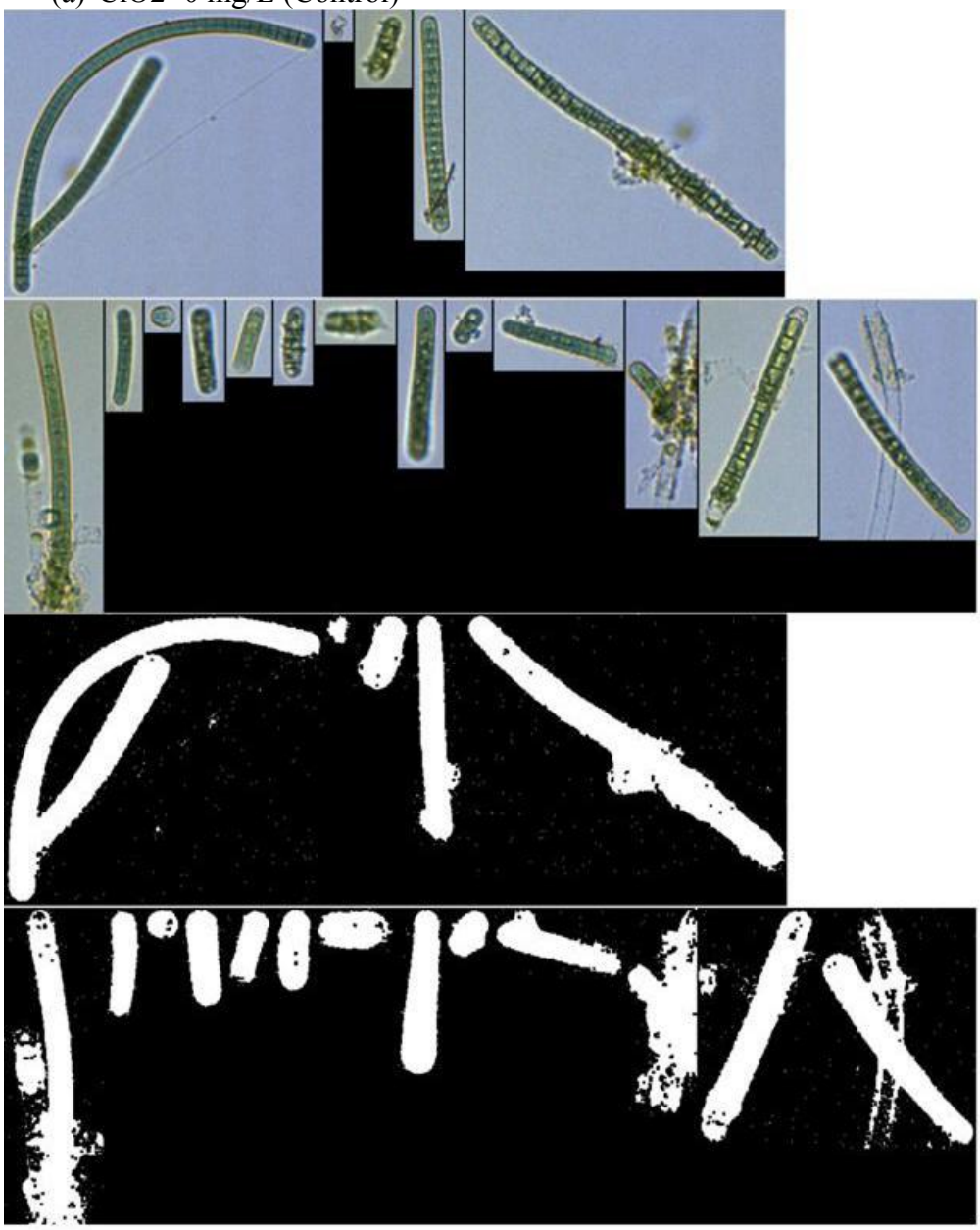

(b) ClO2=0.63 mg/L

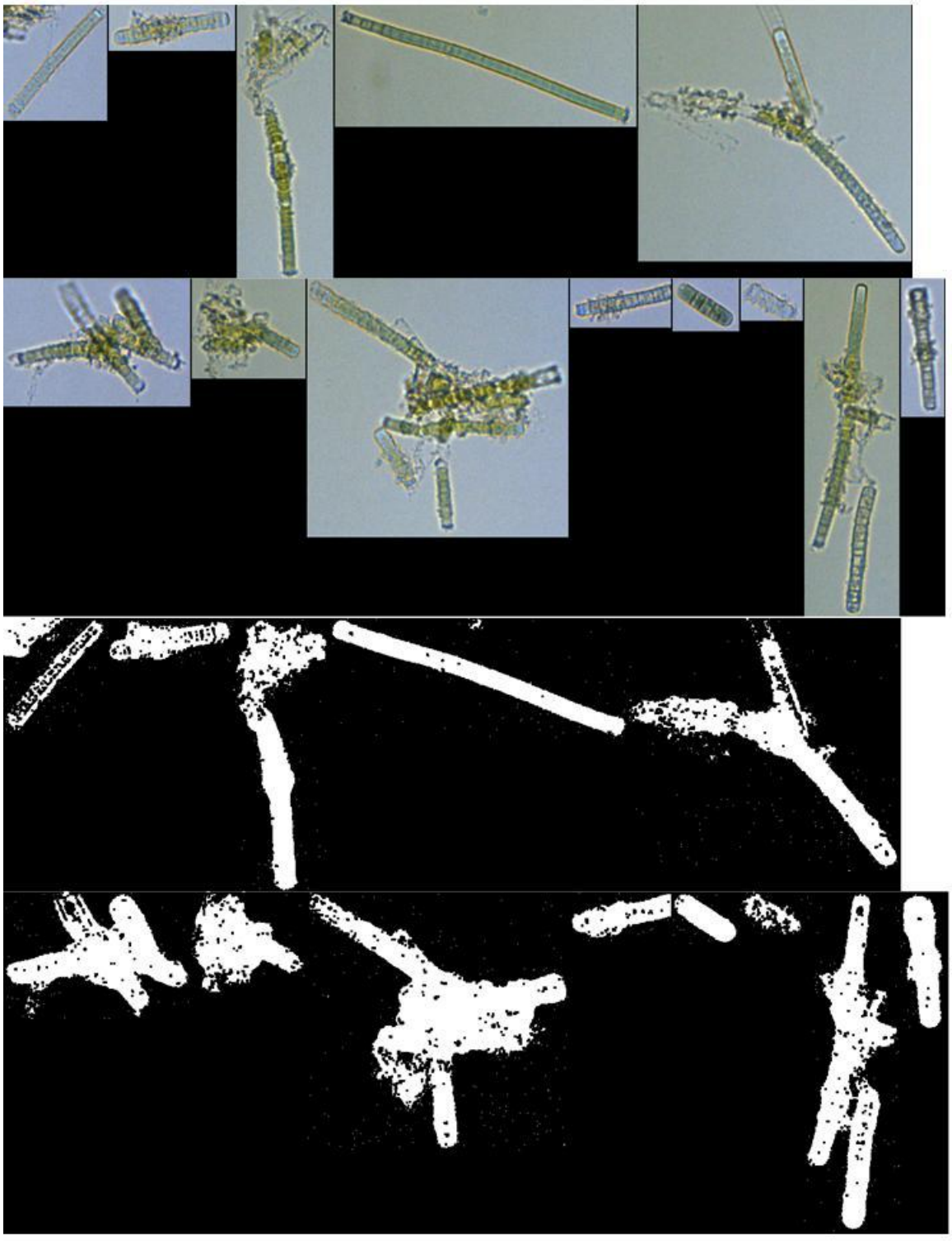

(c) ClO2=1.25 mg/L

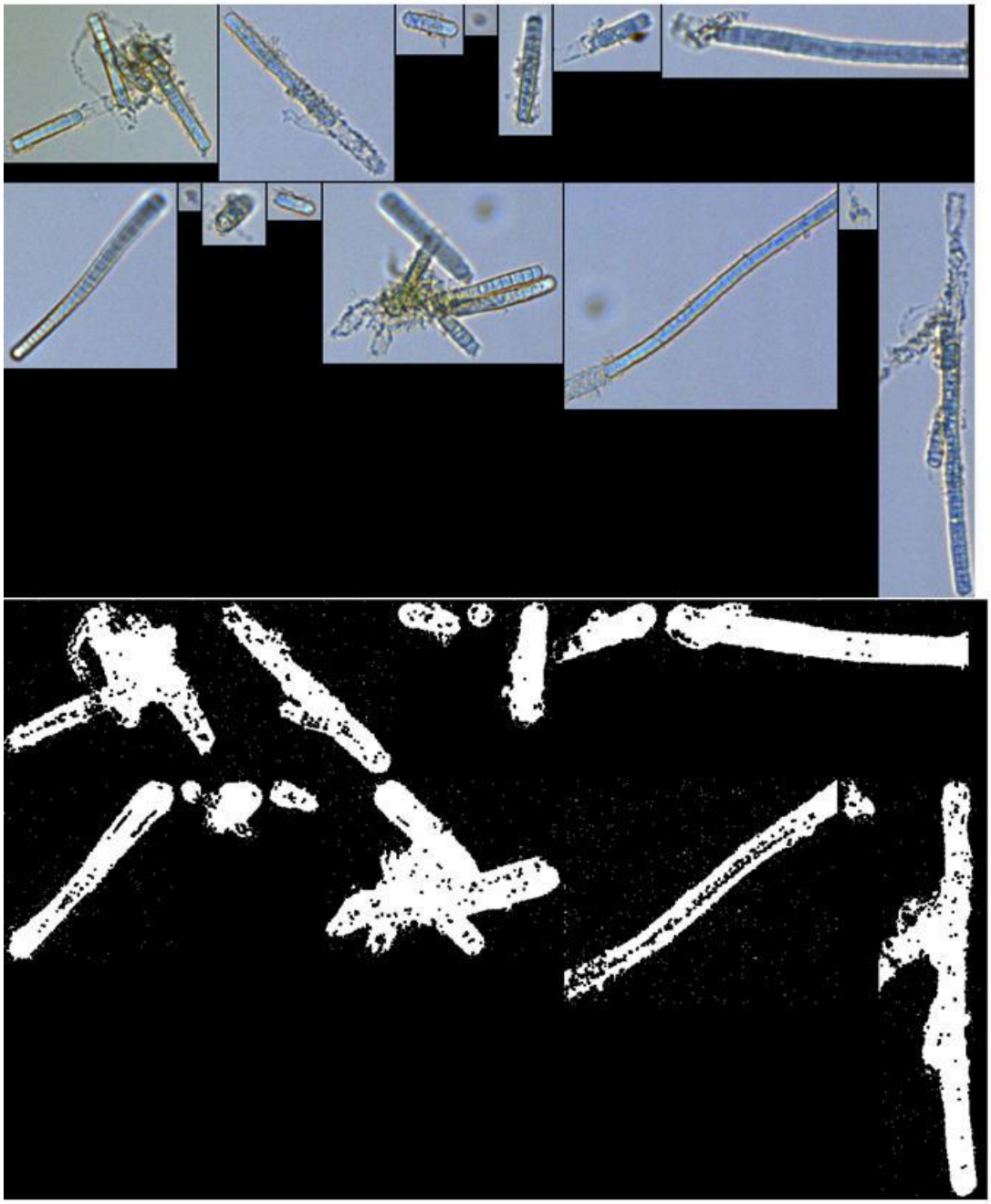

(d) ClO2=1.88 mg/L

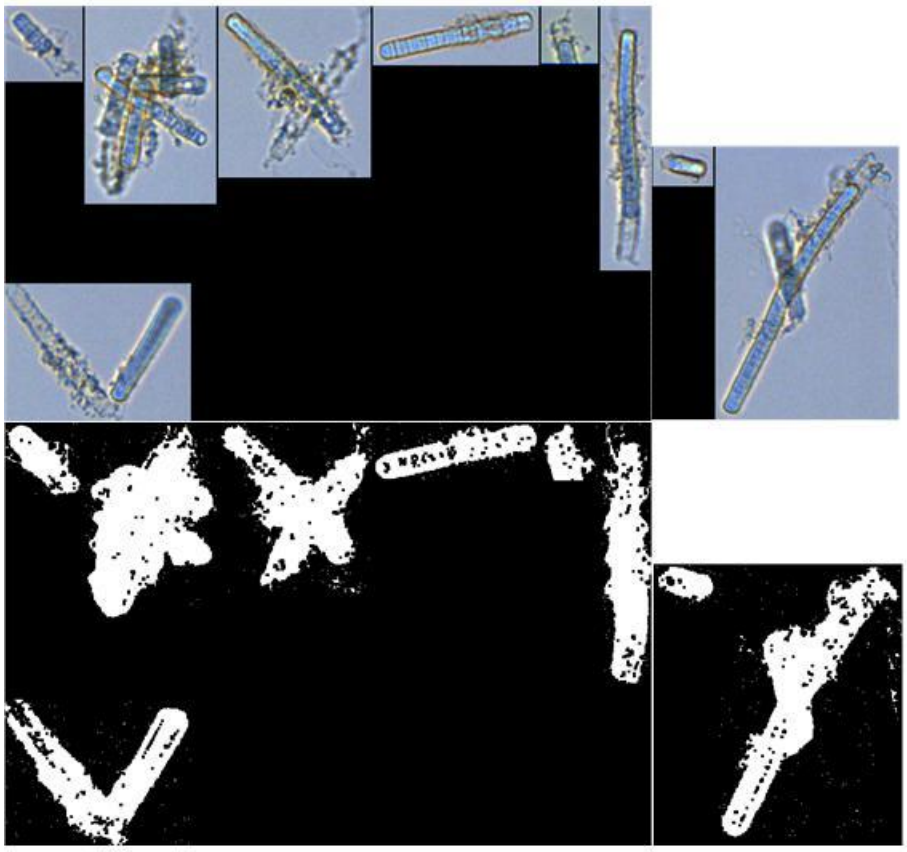

(e) ClO2=2.5 mg/L

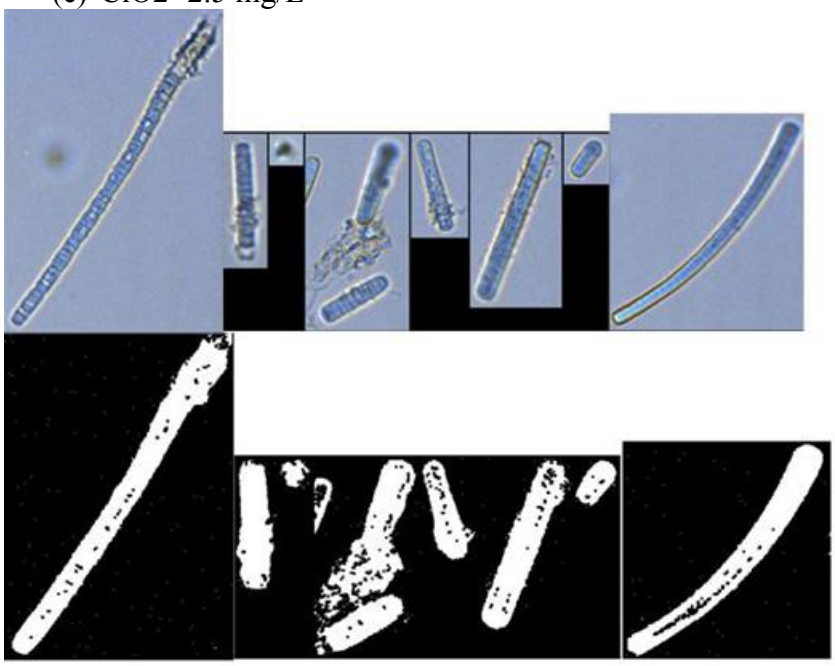

(f) ClO2=5.0 mg/L

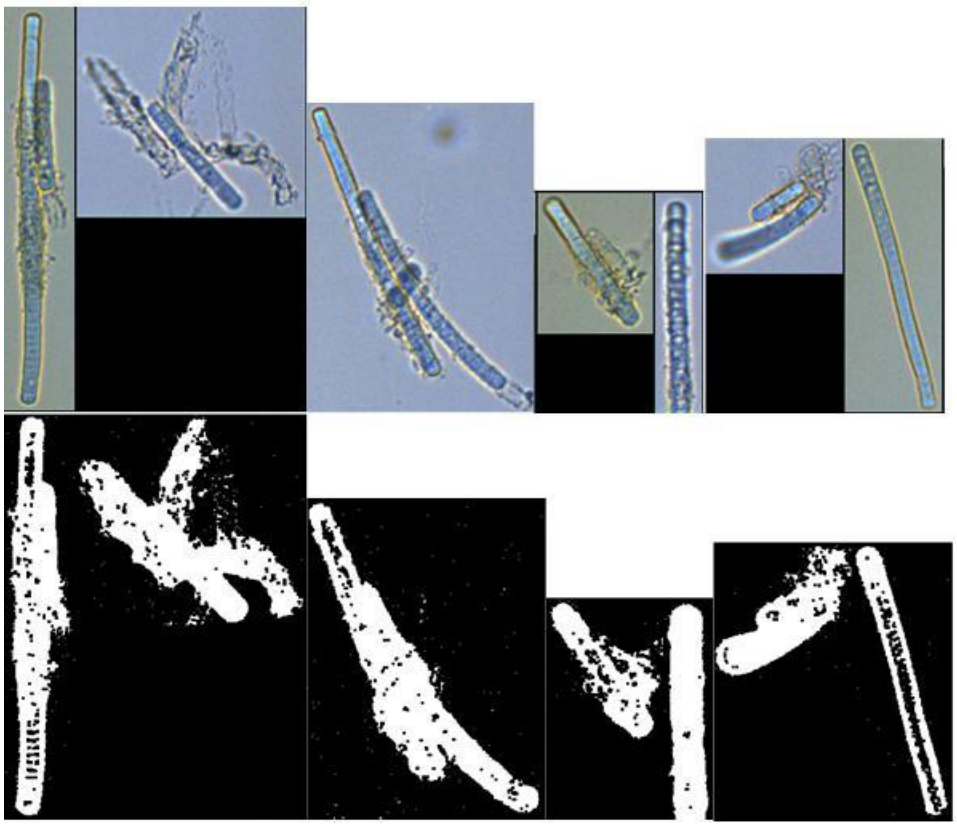

Figure S1.20. – Digital and binary images of *Lyngbya sp.* after oxidation by chlorine (Cl2).

(a) Cl2=0 mg/L (Control)

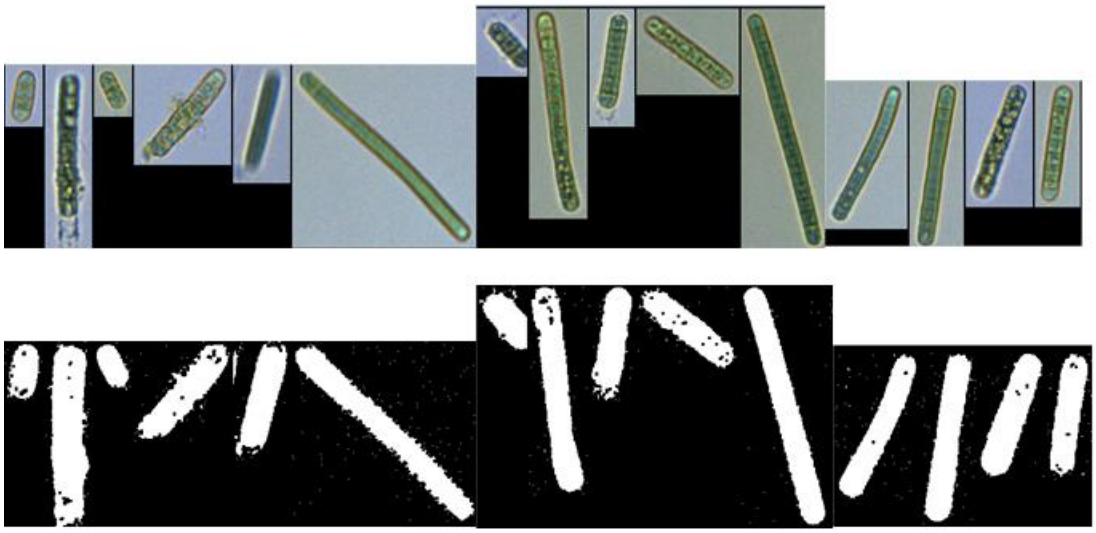

(b) Cl2=0.63 mg/L

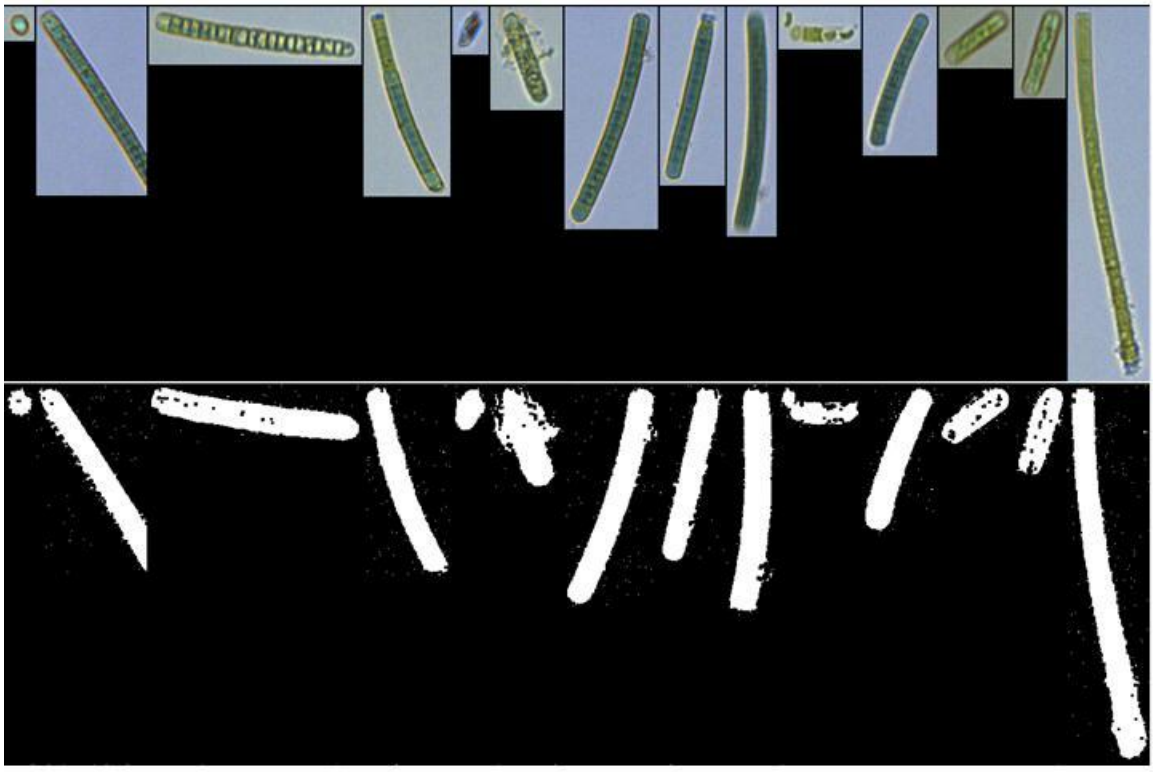

(c) Cl2=1.25 mg/L

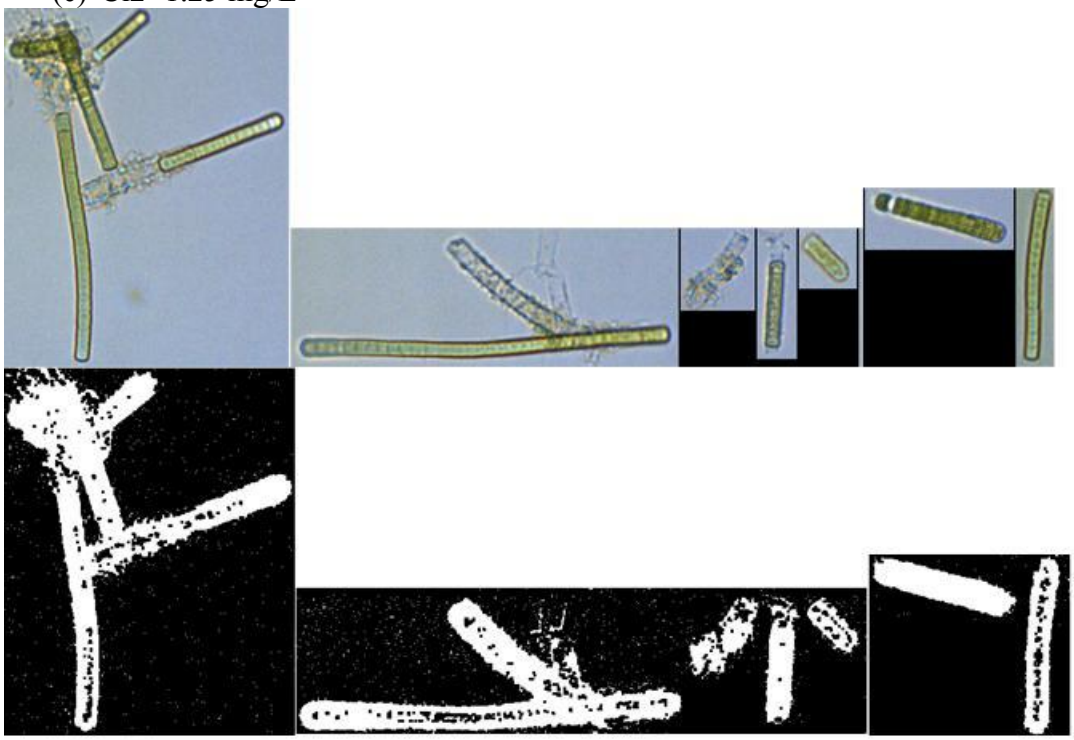

(d) Cl2=1.88 mg/L

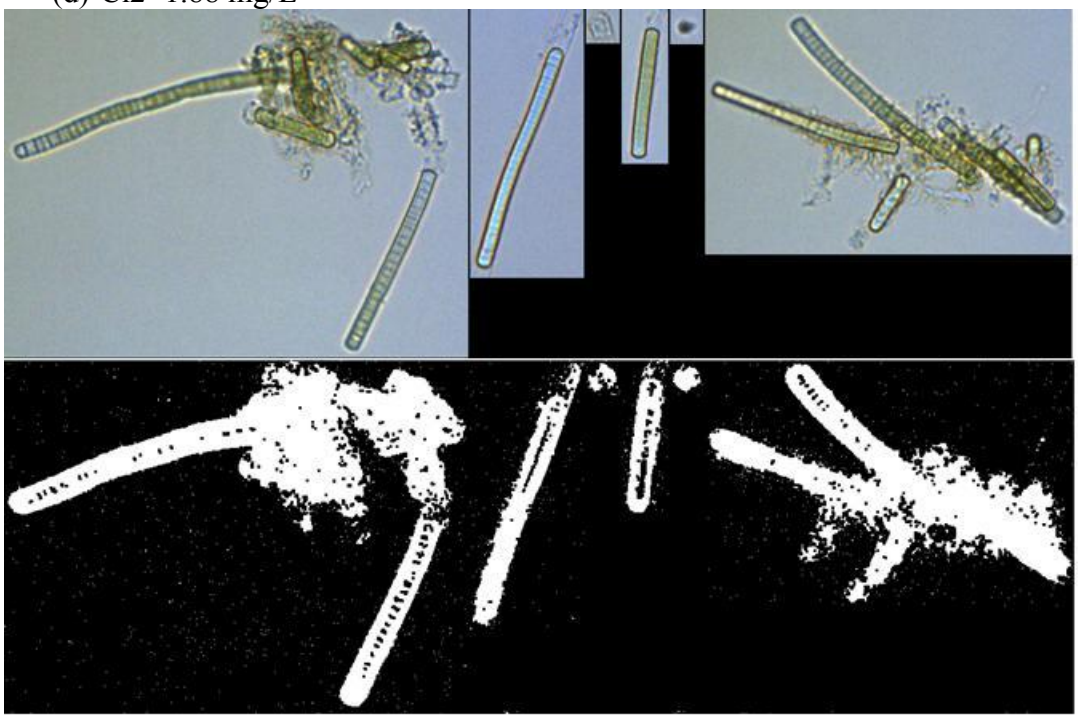

(e) Cl2=2.5 mg/L

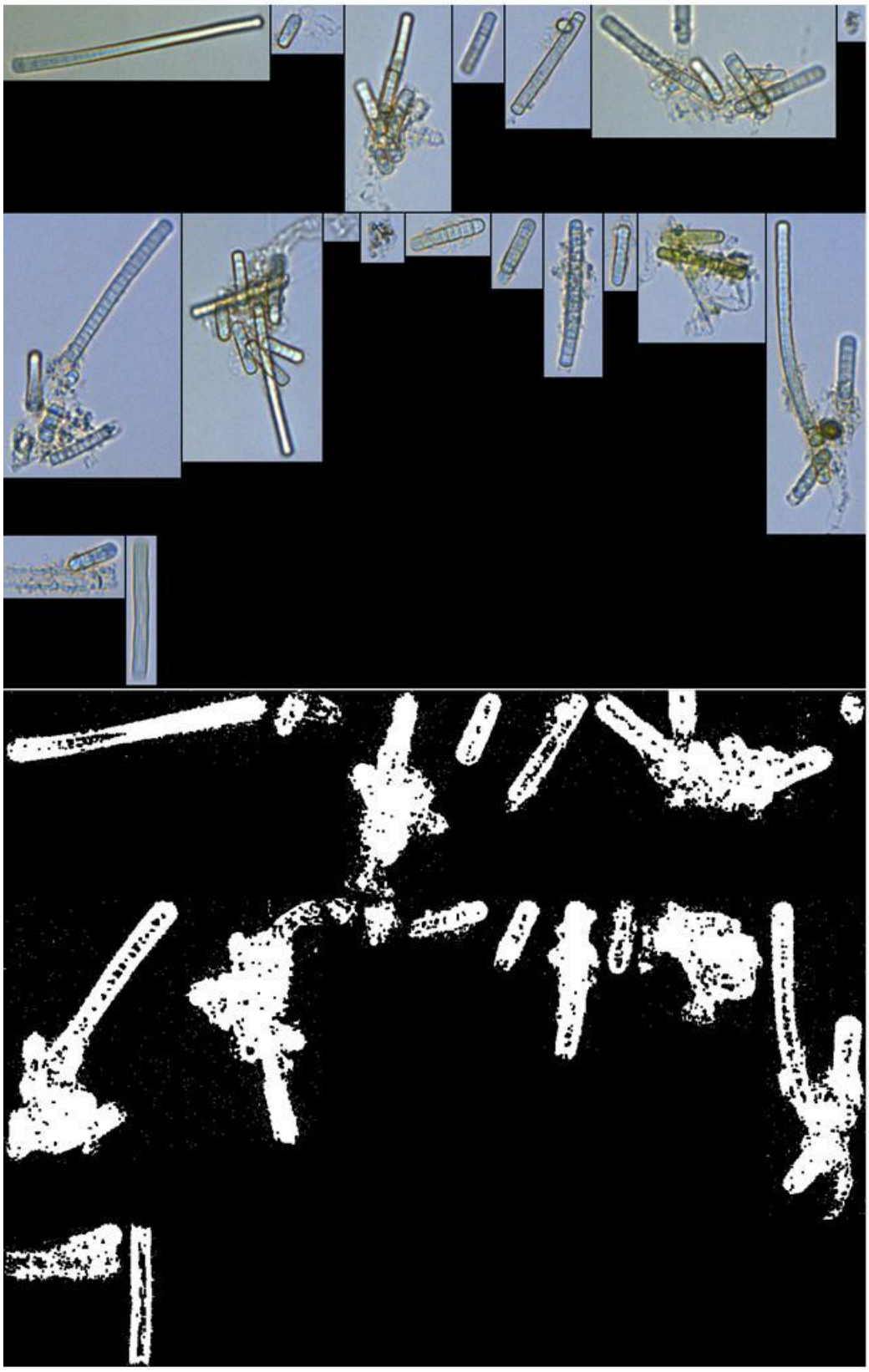

(f) Cl2=5.0 mg/L

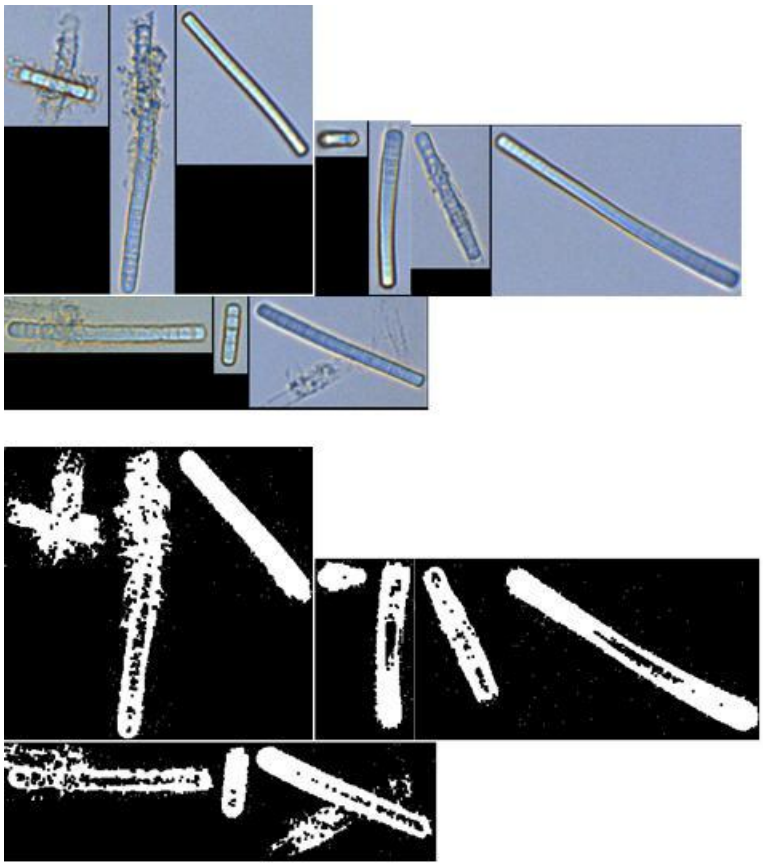

Figure S1.21. – Digital and binary images of *Lyngbya sp.* after oxidation by chloramine (NH2Cl).

(a) NH2Cl=0 mg/L (Control)

(b) NH2Cl=0.63 mg/L

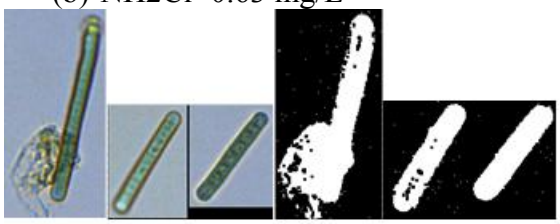

(c) NH2Cl=1.25 mg/L

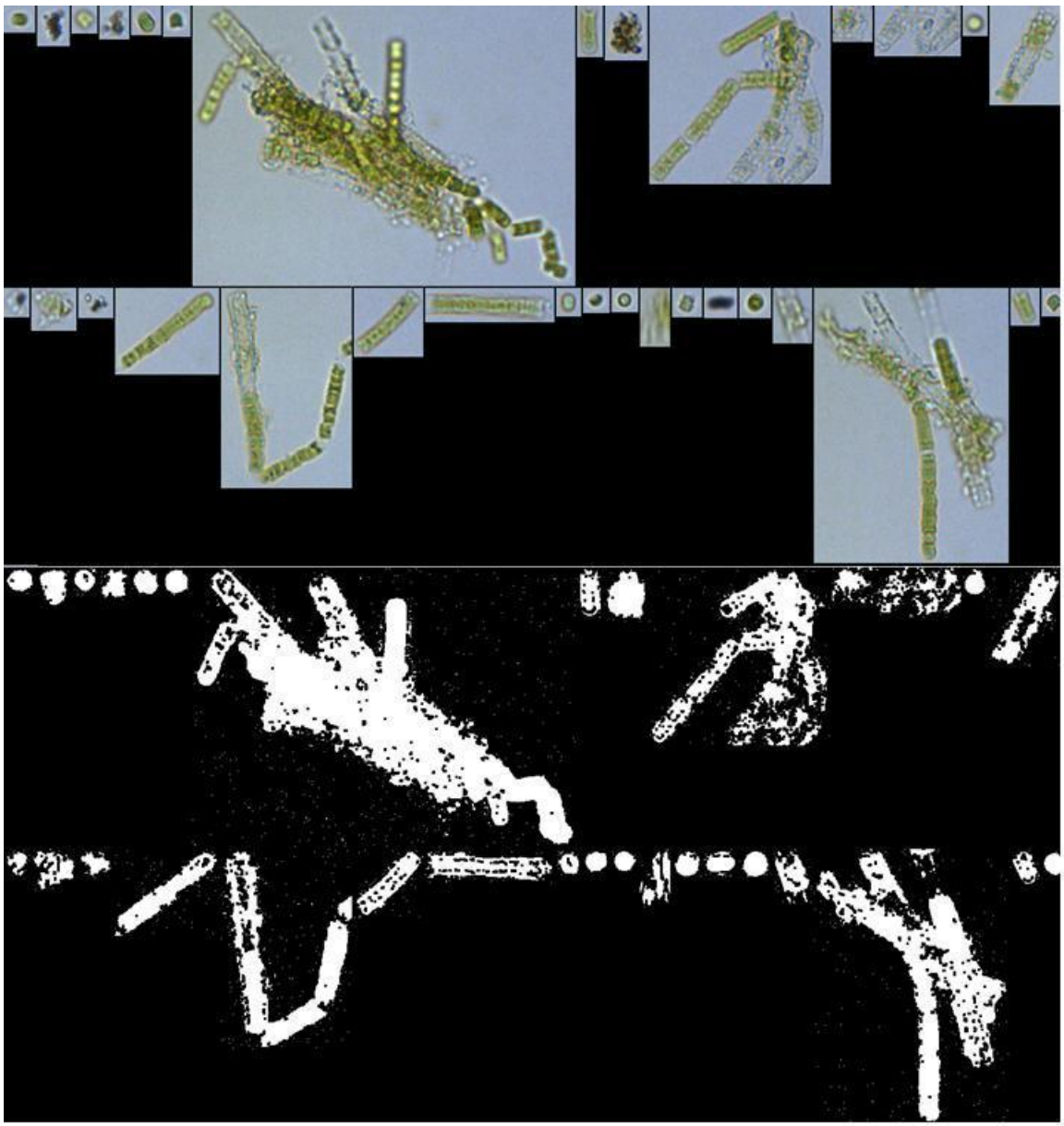

(d) NH2Cl=1.88 mg/L

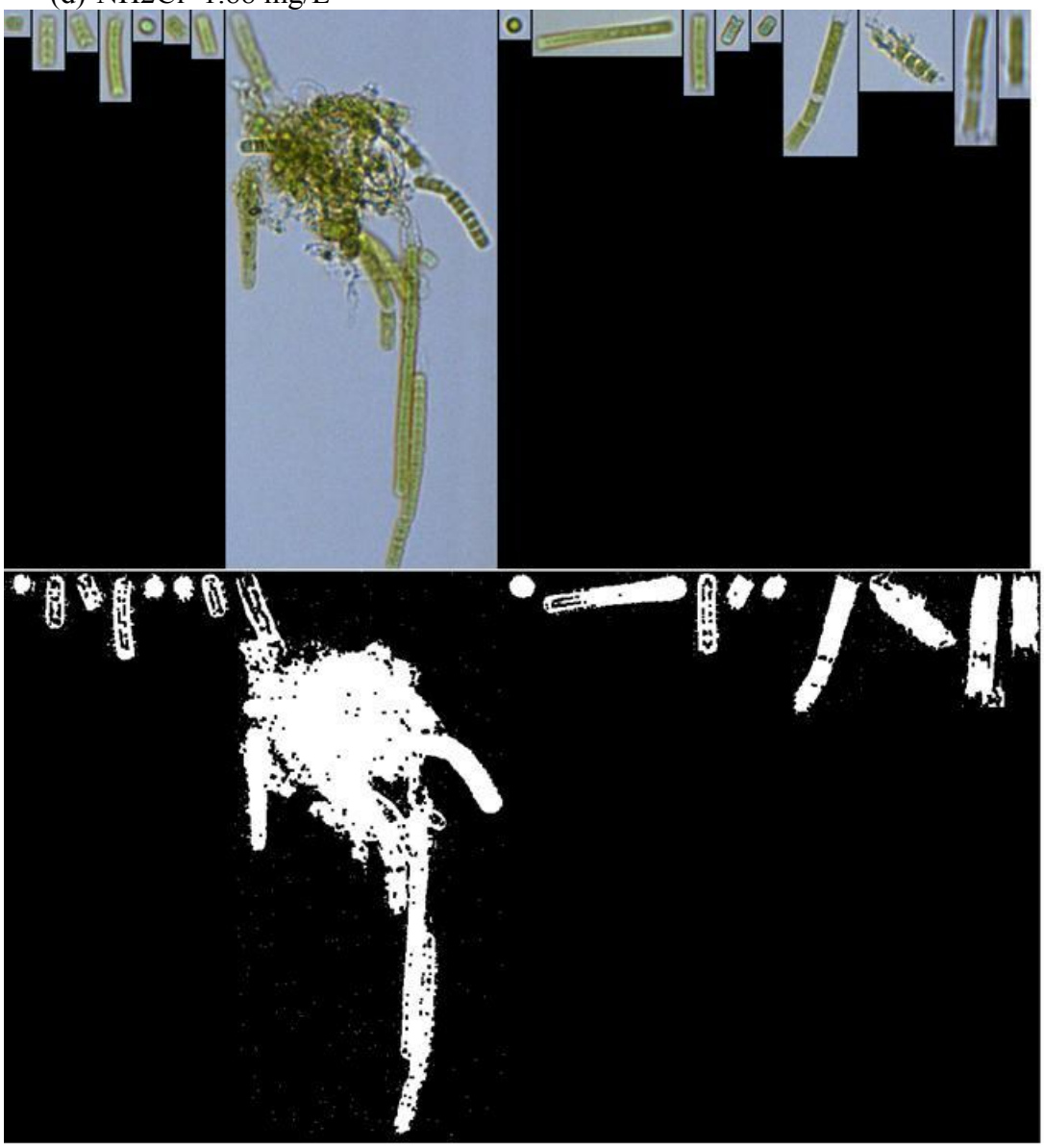

(e) NH2Cl=2.5 mg/L

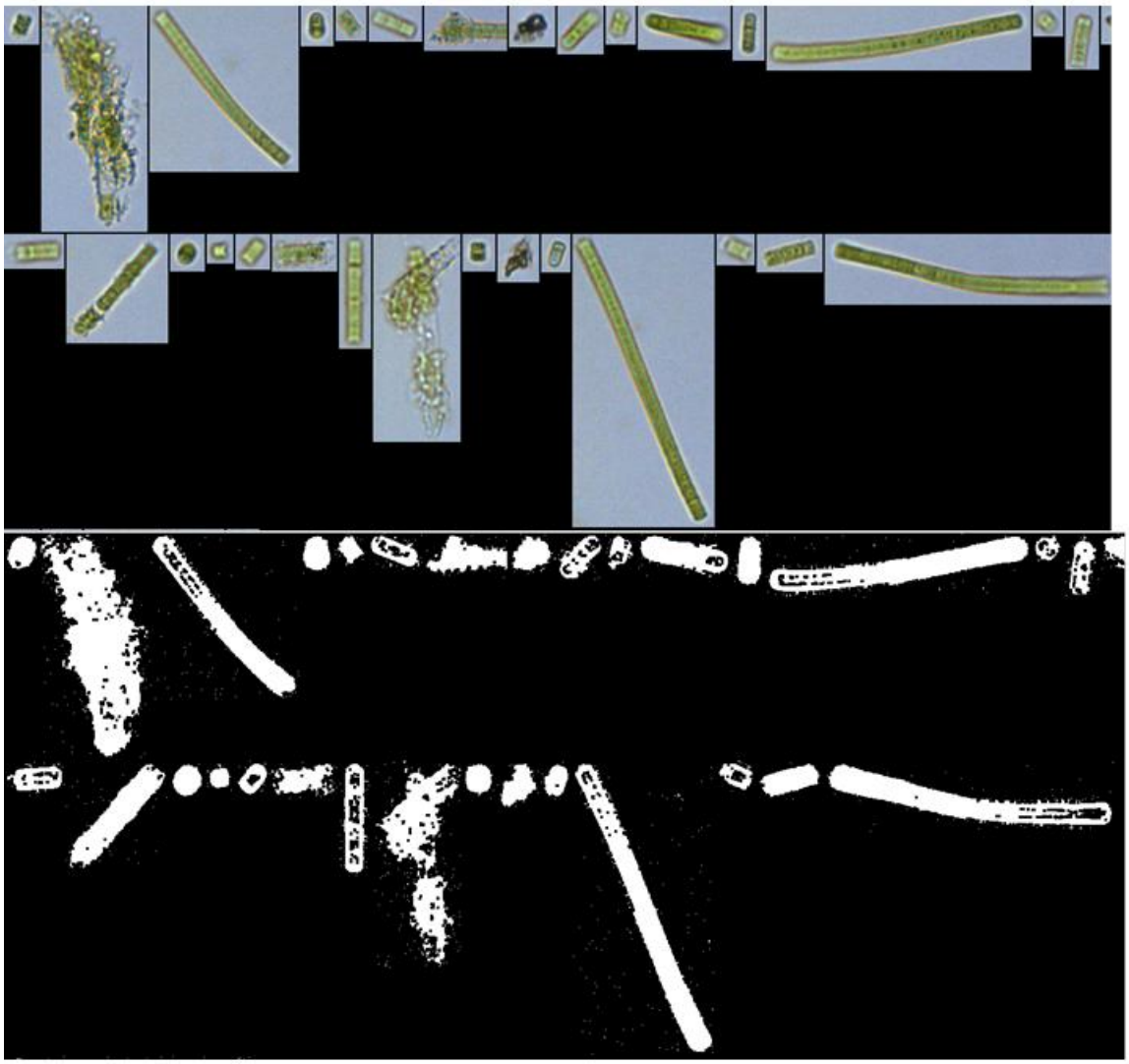

(f) NH2Cl=5.0 mg/L

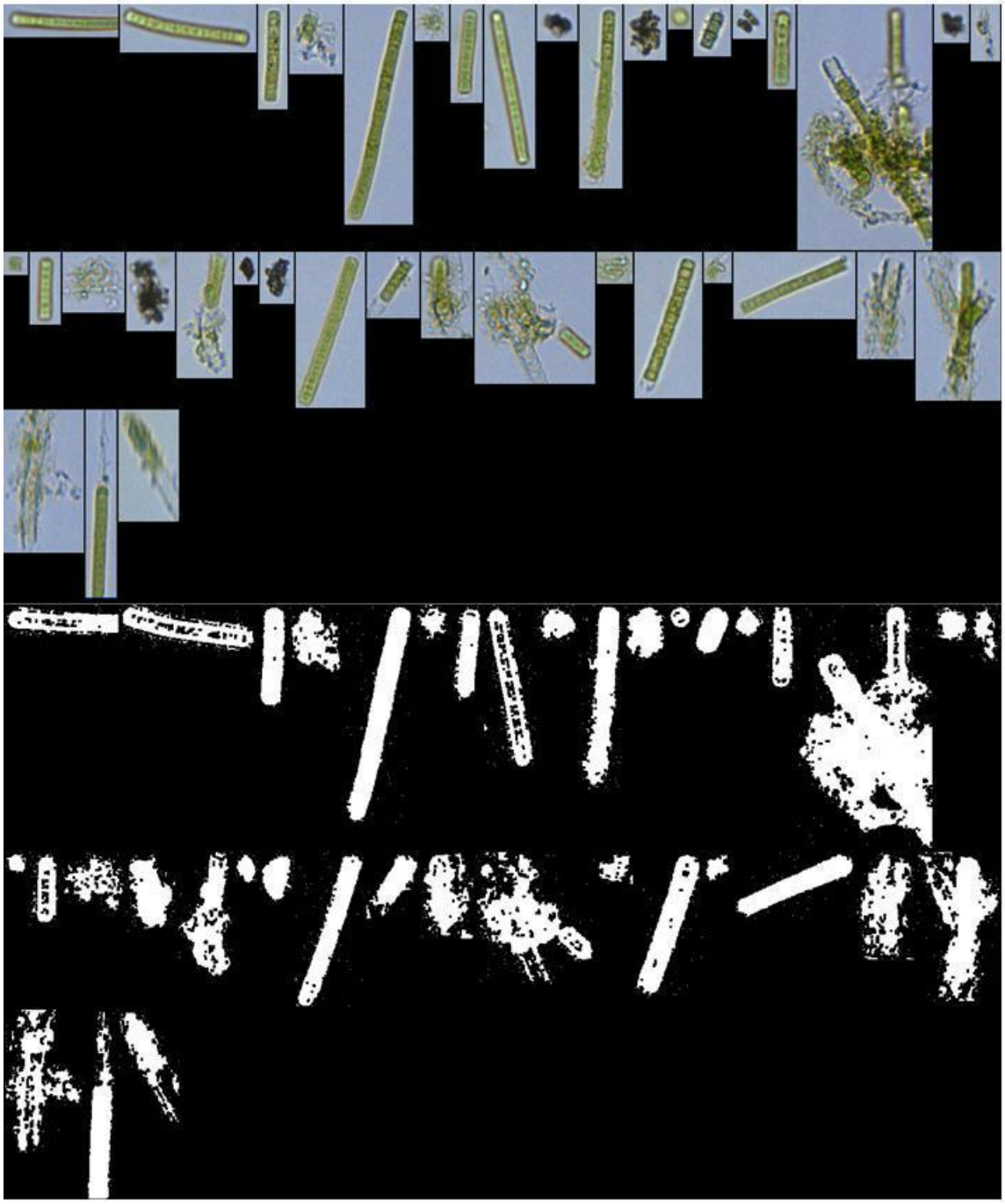

Figure S1.22. – Digital and binary images of *Lyngbya sp.* after oxidation by ozone (O3).

(a) O3=0 mg/L (Control)

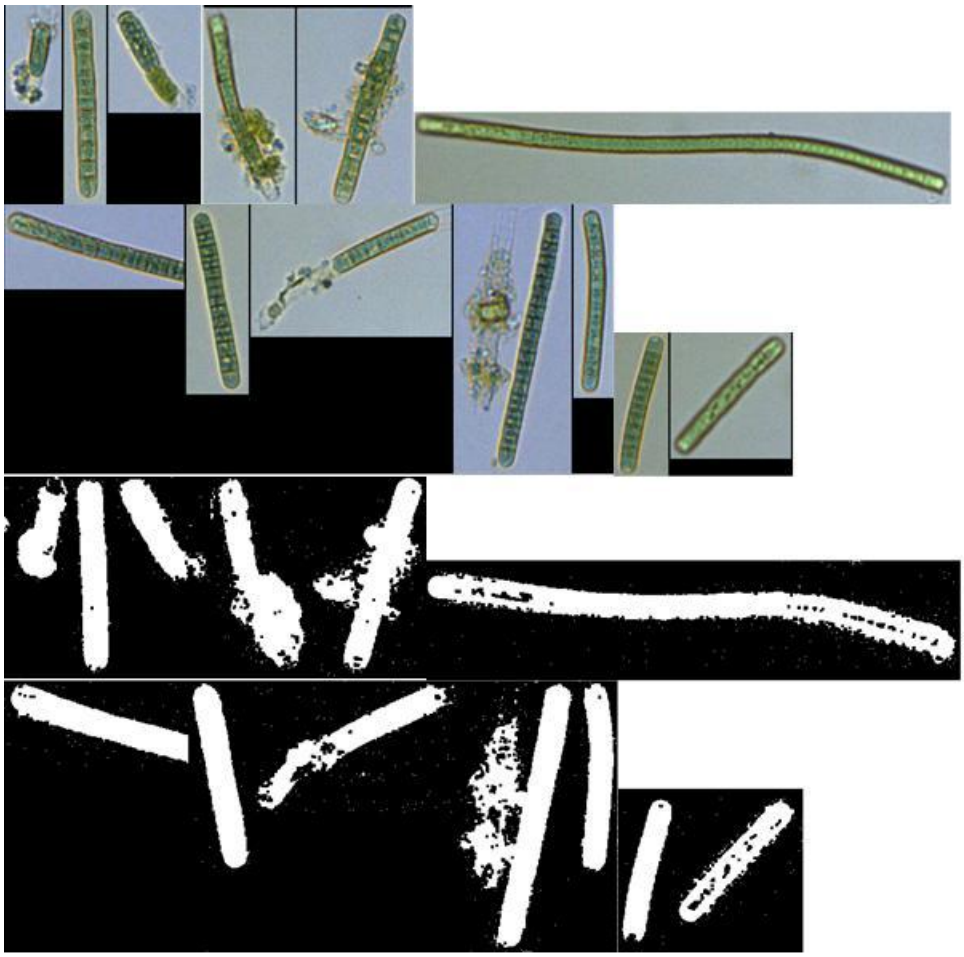

(b) O3=0.63 mg/L

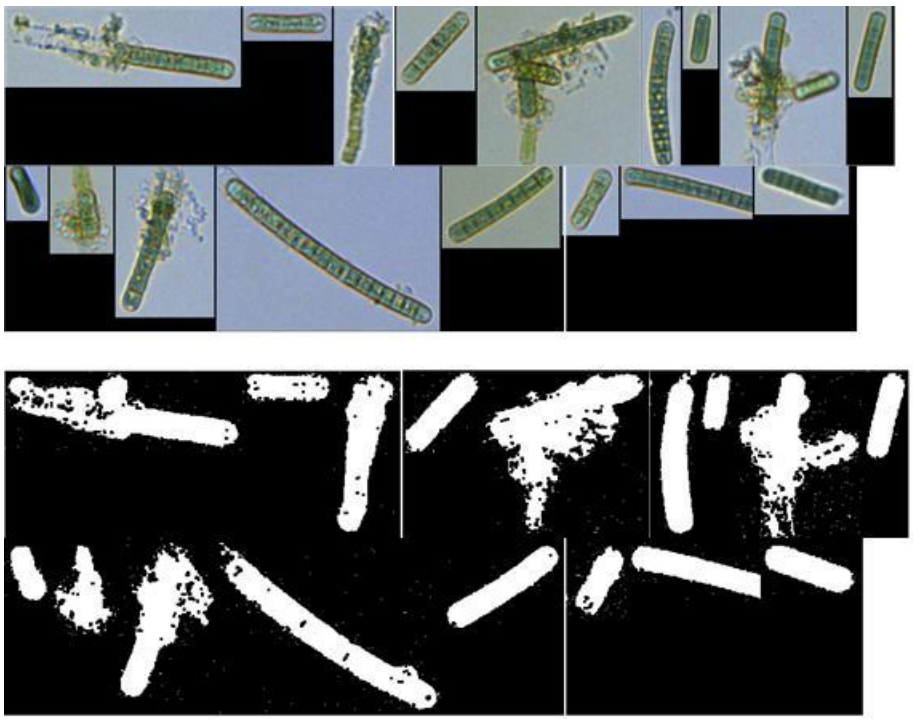

(c) O3=1.25 mg/L

(d) O3=1.88 mg/L

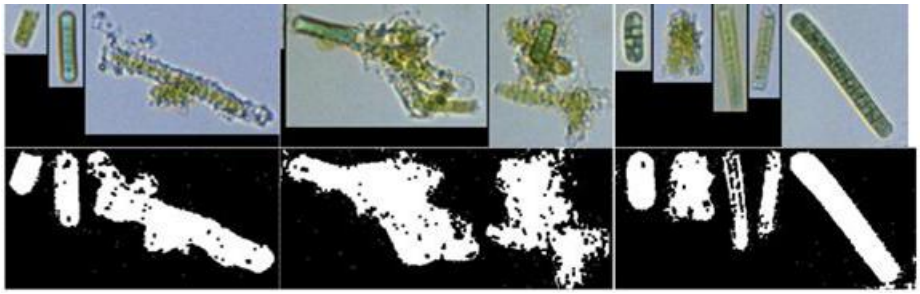

(e) O3=2.5 mg/L

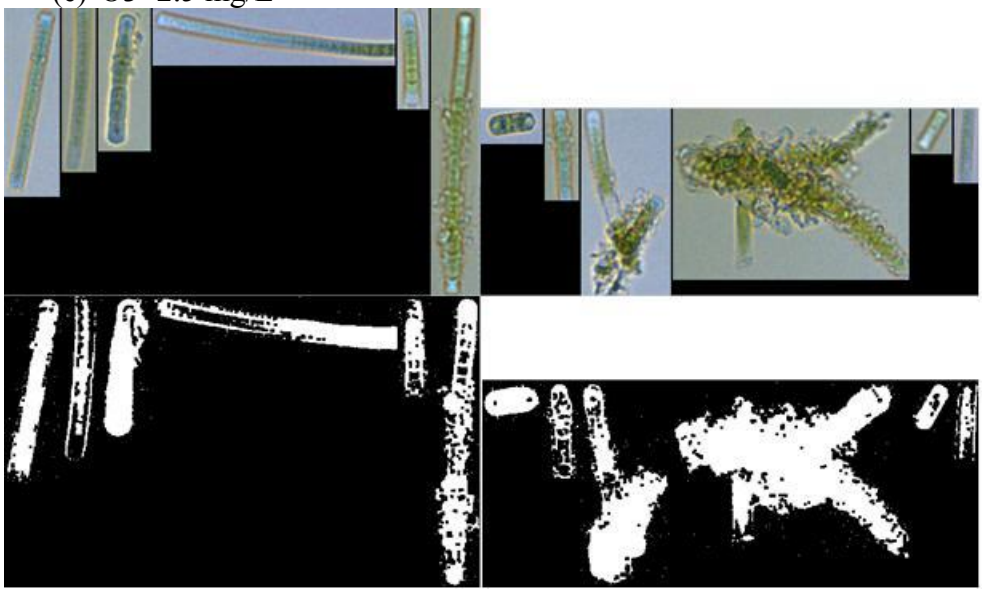

(f) O3=5.0 mg/L

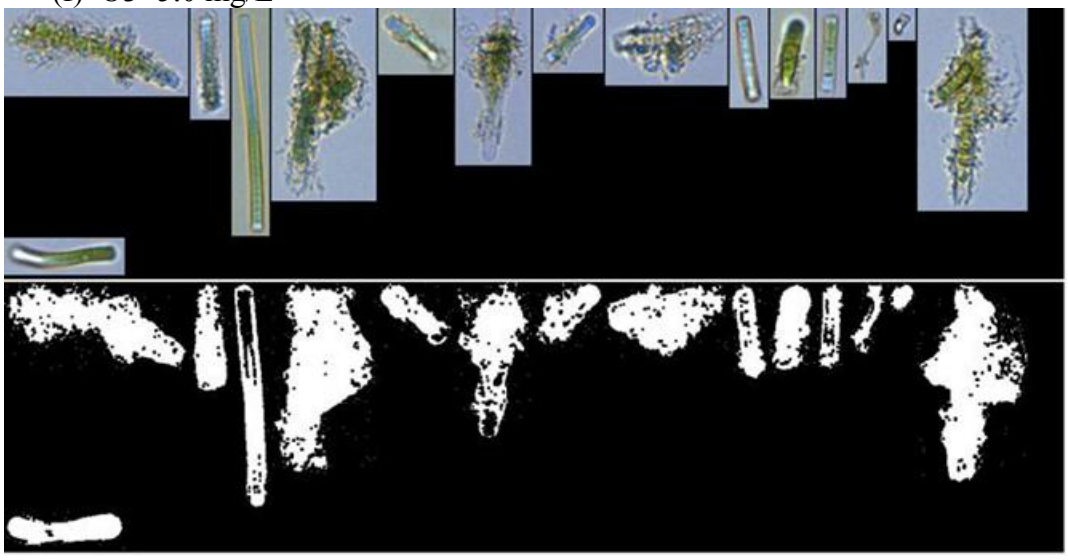

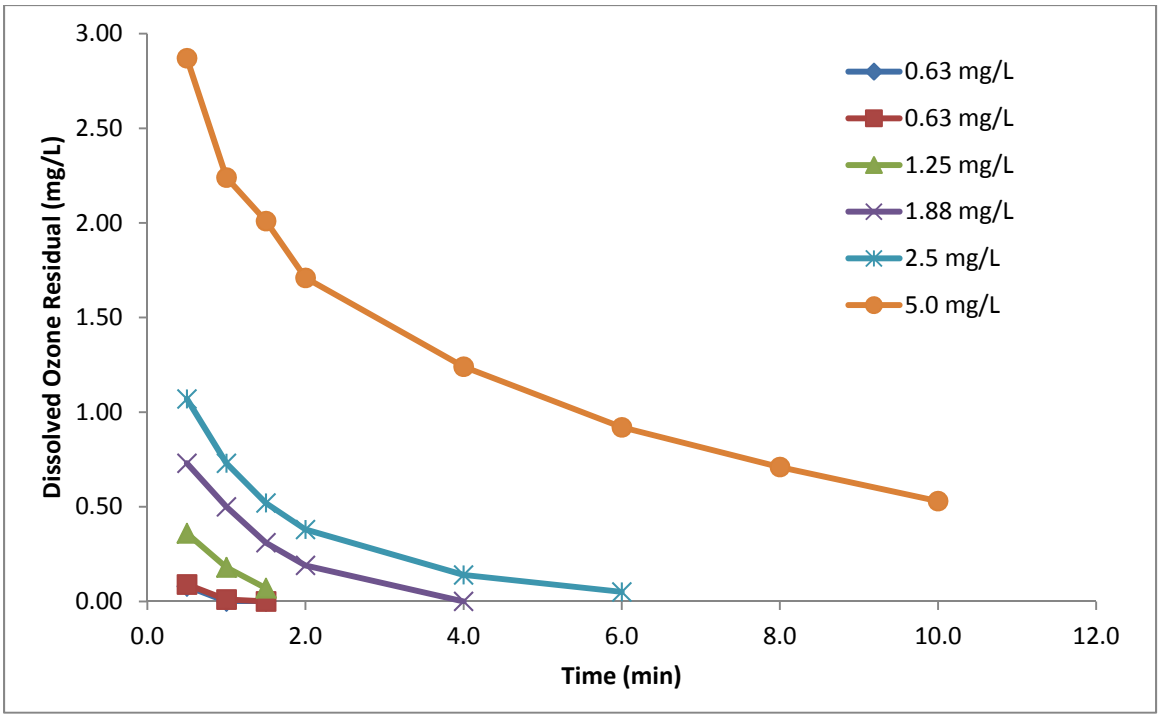

Figure S1.22. – Ozone residual decay in CRW using 200,000 cells/mL of MA.

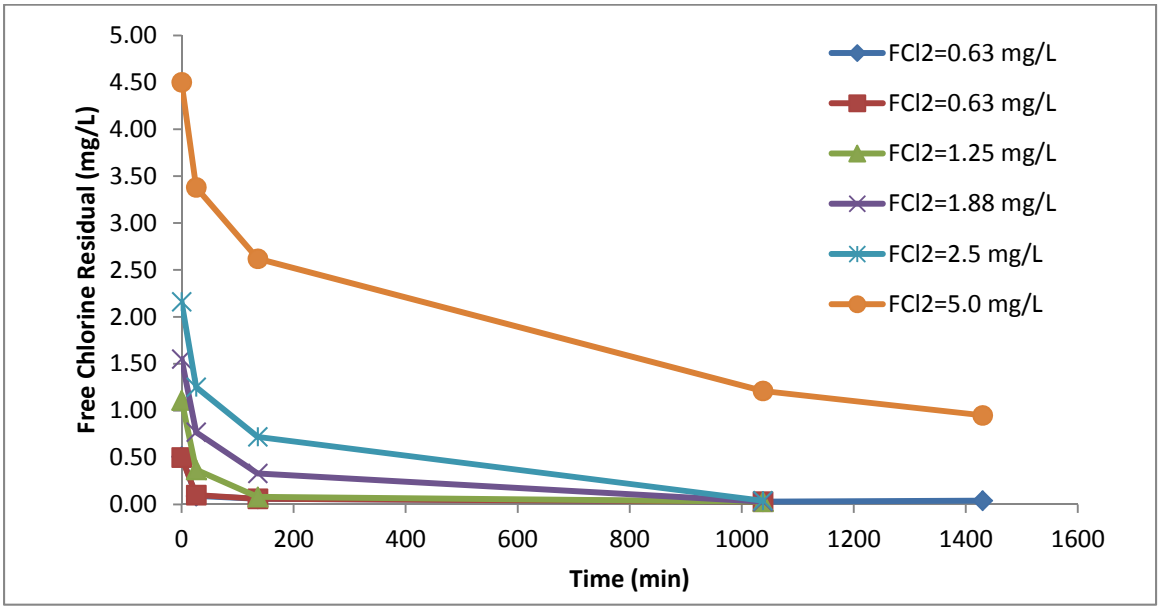

Figure S1.23. – Free chlorine residual decay in CRW using 200,000 cells/mL of MA.

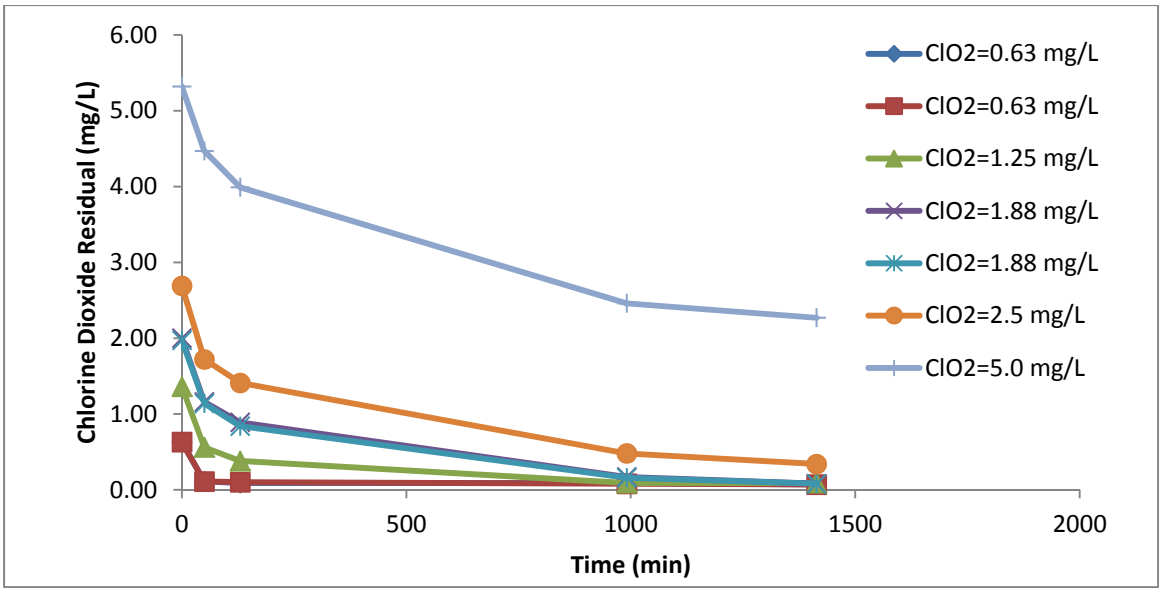

Figure S1.24. – Chlorine dioxide residual decay in CRW using 200,000 cells/mL of MA.

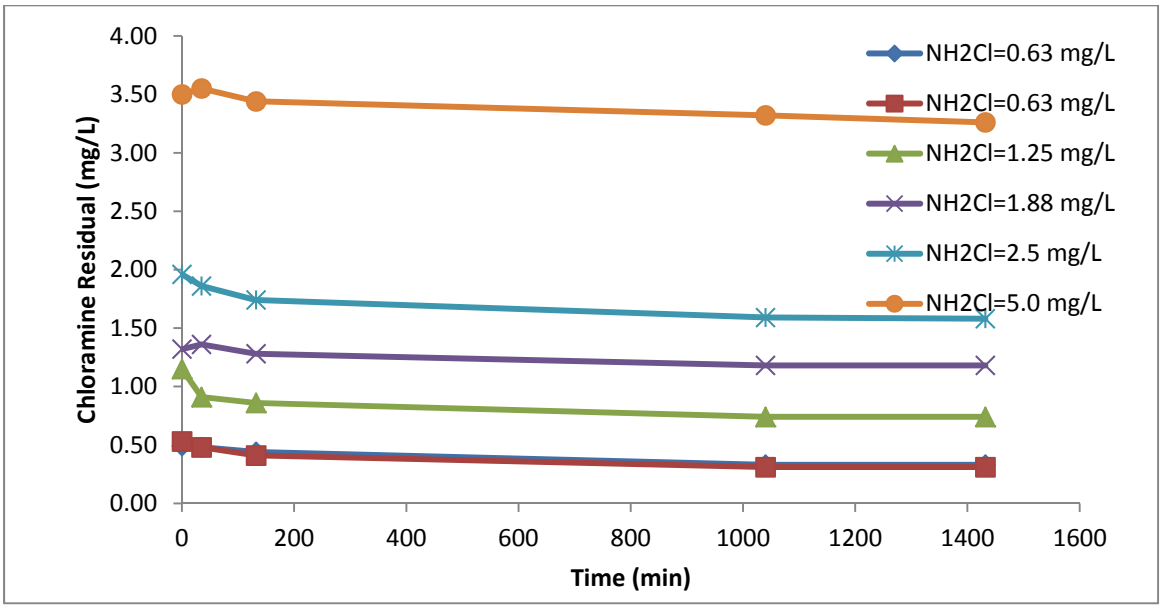

Figure S1.25. – Chloramine residual decay in CRW using 200,000 cells/mL of MA.

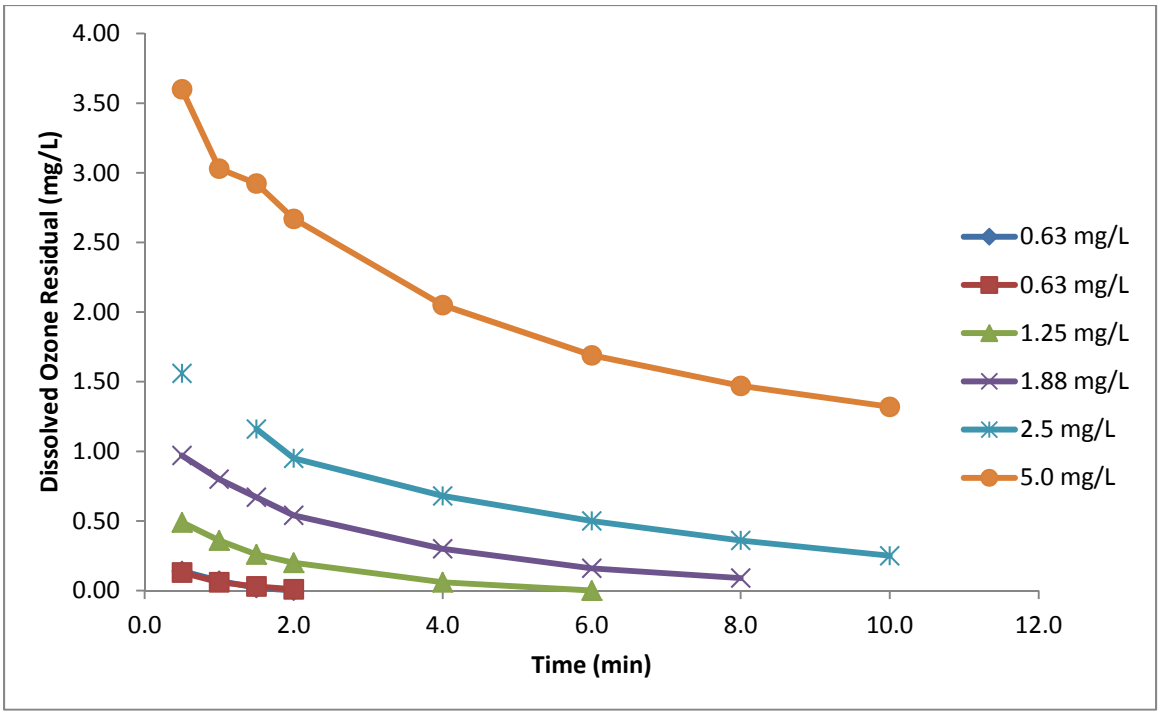

Figure S1.26. – Ozone residual decay in CRW using 2,800 cells/mL of OSC.

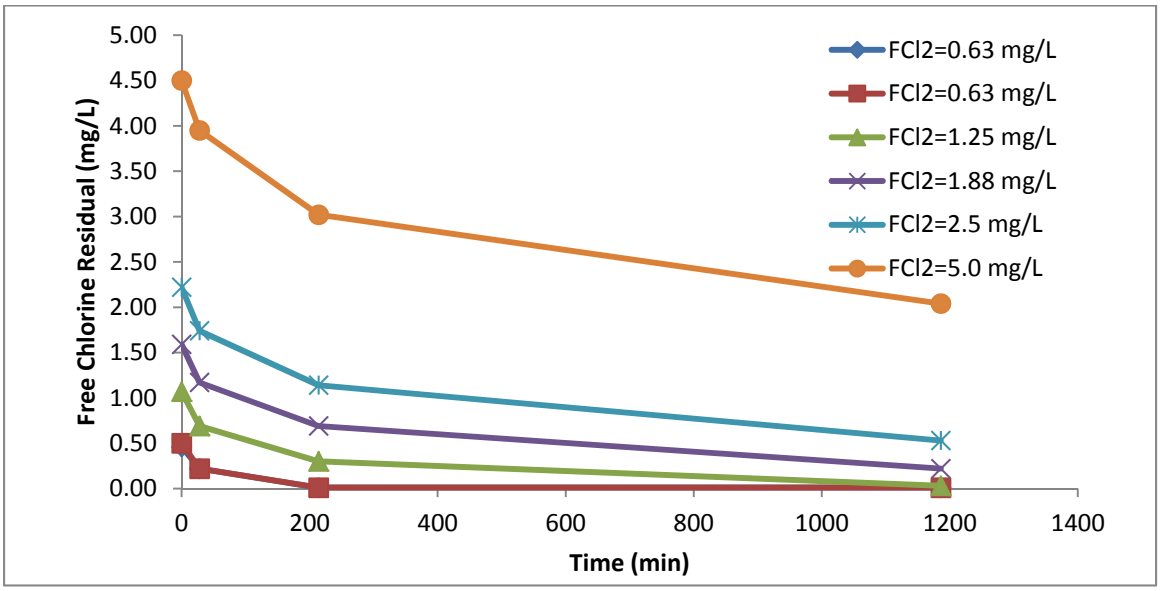

Figure S1.27. – Free chlorine residual decay in CRW using 2,800 cells/mL of OSC.

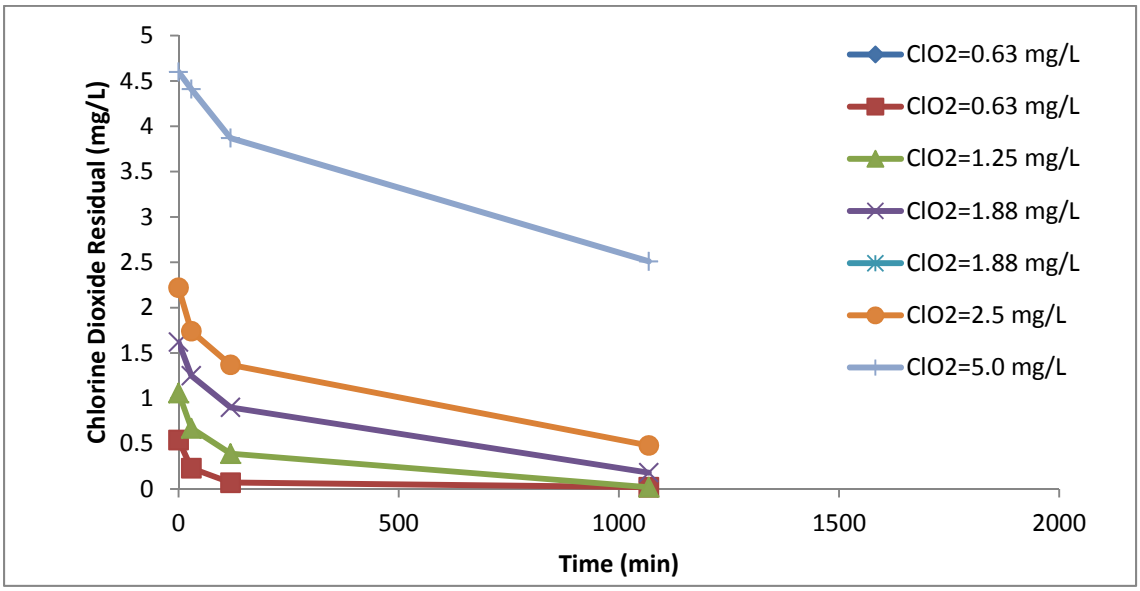

Figure S1.28. – Chlorine dioxide residual decay in CRW using 2,800 cells/mL of OSC.

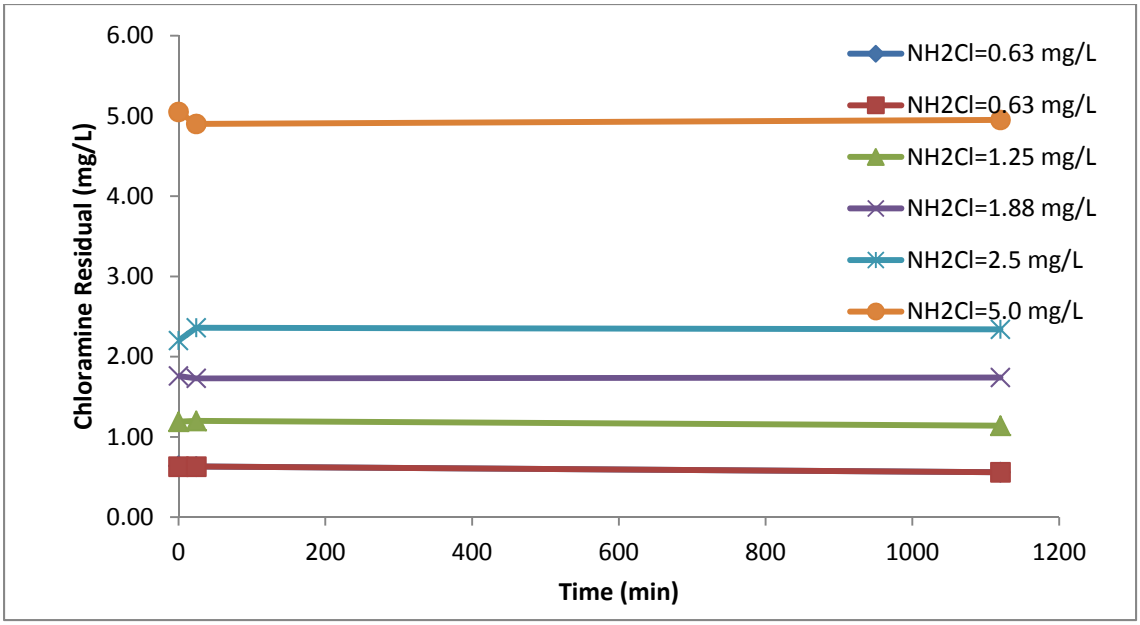

Figure S1.29. – Chloramine residual decay in CRW using 2,800 cells/mL of OSC.

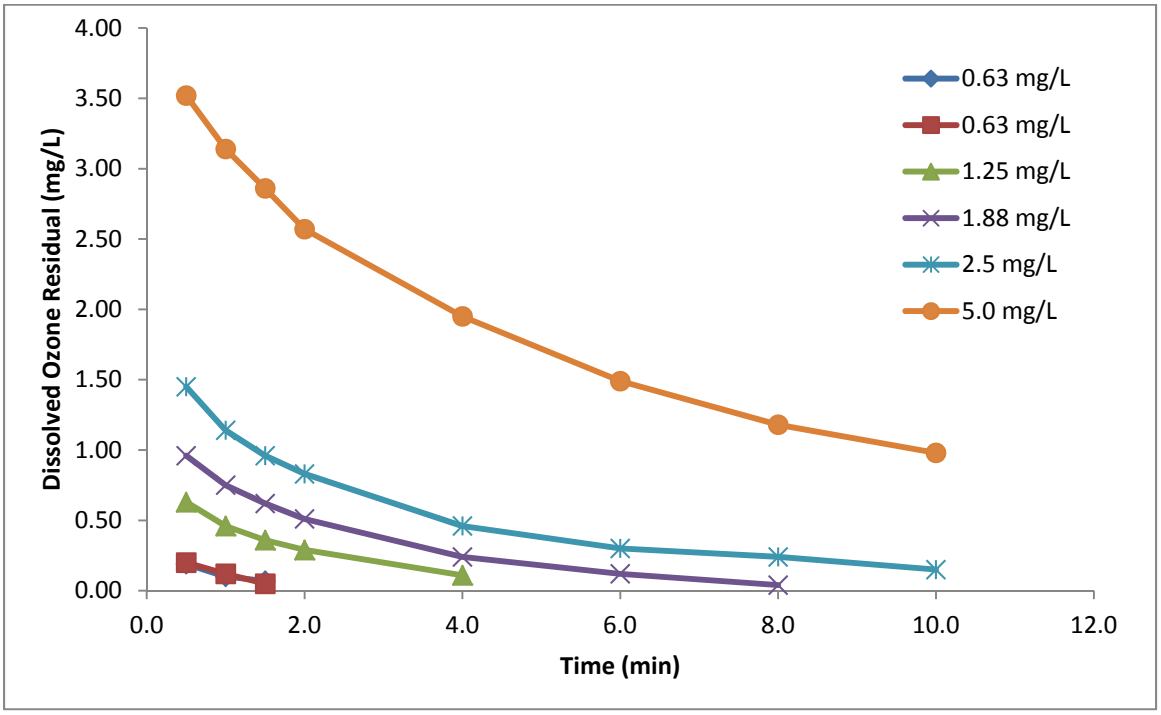

Figure S1.30. – Ozone residual decay in CRW using 1,600 cells/mL of LYN.

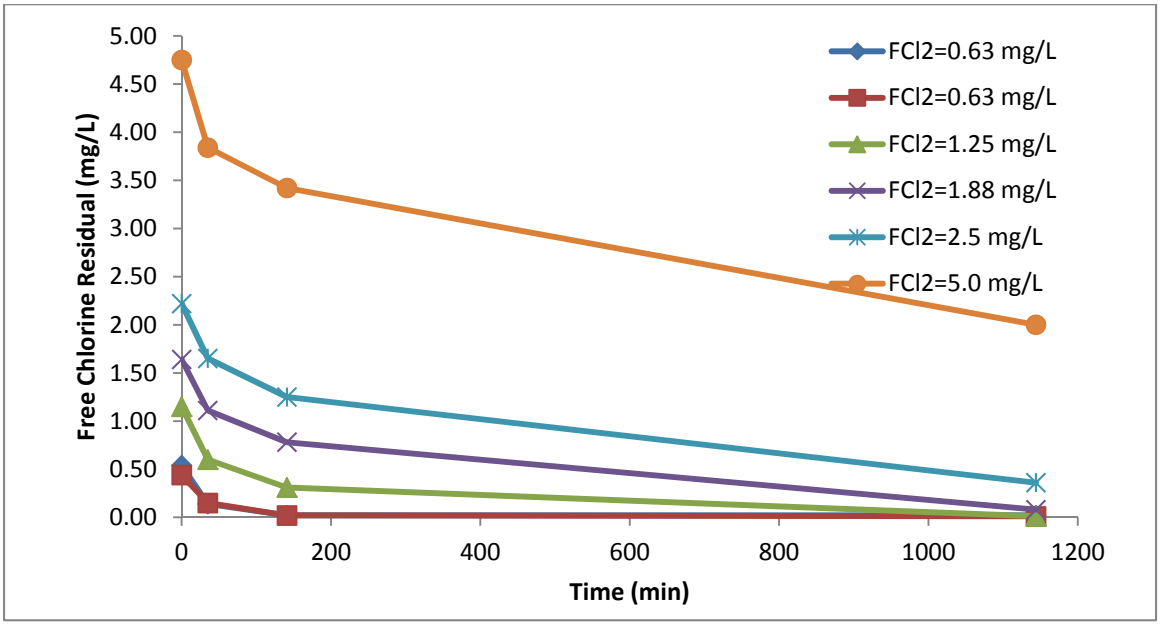

Figure S1.31. – Free chlorine residual decay in CRW using 1,600 cells/mL of LYN.

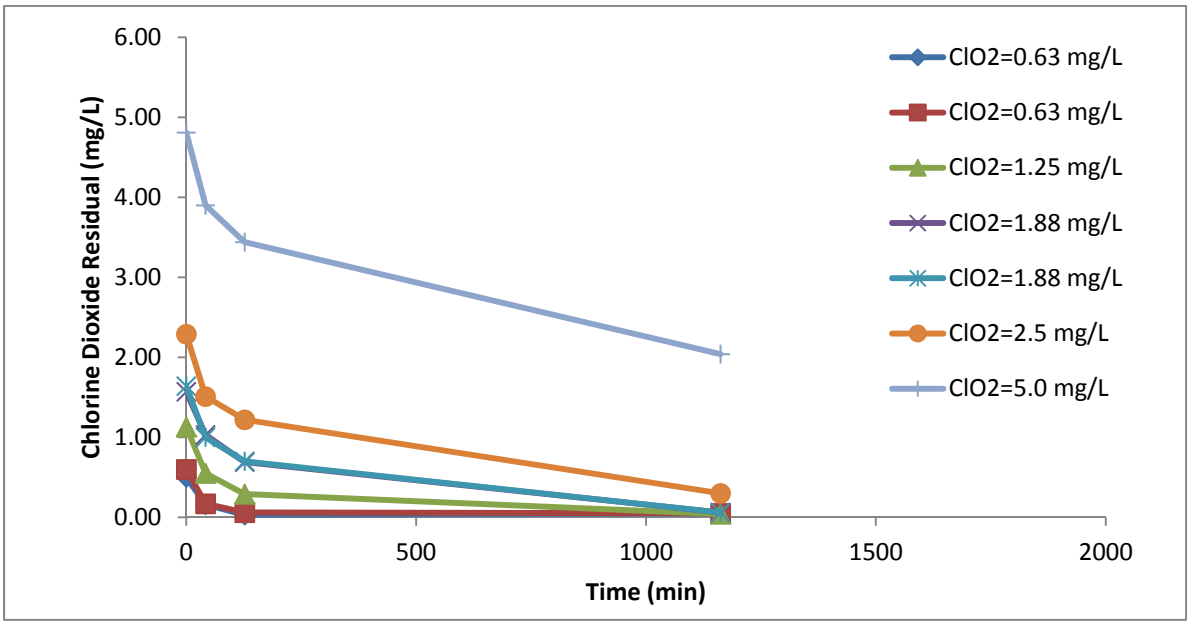

Figure S1.32. – Chlorine dioxide residual decay in CRW using 1,600 cells/mL of LYN.

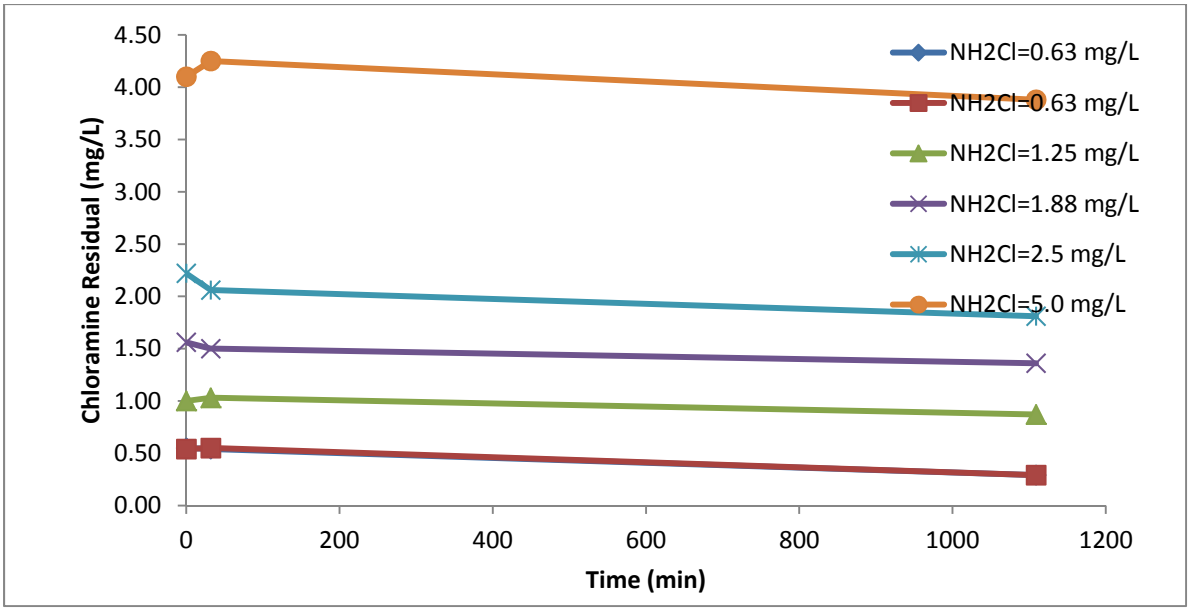

Figure S1.33. – Chloramine residual decay in CRW using 1,600 cells/mL of LYN.

S.2.1 – Intracellular Organic Matter from Cyanobacteria as a Precursor for Carbonaceous and Nitrogenous Disinfection Byproducts.

Table S2.1. Summary of FP Testing Conditions with Free Chlorine and Measured FCl_2 Residuals after 7 days.

Water Source	IOM Addition (mg/L)	O_3 Dose (mg/L)	FCl_2 Dose (mg/L)	Bromide Addition (µg/L)	FCl_2 Residual @ 7 days (mg/L)		
					MA	OSC	LYN
Buffered Milli-Q	0	-	5	-	5.0	4.8	4.1
	1.0	-	15	-	11.1	8.5	7.9
	2.0	-	25	-	7.2	12.0	10.8
	3.0	-	35	-	7.6	-	13.4
	0	-	5	100	5.1	4.7	4.2
	1.0	-	15	100	11.1	8.5	7.7
	2.0	-	25	100	6.6	11.8	11.0
	3.0	-	35	100	7.0	-	-
	1.0	0.6	21	100	10.8	-	13.4
CRW (~2.5 mg/L DOC)	0	-	6	Ambient	3.2	2.1	2.0
	0	1.5	6	Ambient	3.0	2.1	2.1
	1.0	-	21	Ambient	8.0	9.0	9.4
	1.0	2.1	21	Ambient	8.2	9.8	9.9
	1.0	2.1	21	Ambient	8.4	10.0	9.9

Table S2.2. Summary of nitrosamine formation MQ water and CRW.

IOM Source	Nitrosamine	Nitrosamine Yield (ng/mg C) MQ Water			Nitrosamine Formation (ng/L) CRW w/ IOM (1 mg/L)	
		NH_2Cl, No Br	NH_2Cl, w/Br	O_3/NH_2Cl	NH_2Cl	O_3/NH_2Cl
MA	NDMA	52	51	163	< 2.5	2.75
	NPYR	17	12	ND	< 10	< 10
	NPIP	6.6	6.2	ND	< 5.0	6.8
OSC	NDMA	16	15	-	< 2.5	3.45
	NMEA	2.1	2.1	-	< 2.5	< 2.5
LYN	NDMA	10	11	13	< 2.5	< 2.5
	NMEA	4.2	5.0	7.1	< 2.5	< 2.5
	NPIP	3.8	3.3	ND	< 5.0	< 5.0

Table S2.3. Summary of FP Testing Conditions with Chloramines and Measured NH_2Cl Residuals after 7 days.

Water Source	IOM Addition (mg/L)	O_3 Dose (mg/L)	NH_2Cl Dose (mg/L)	Bromide Spike (µg/L)	NH_2Cl Residual @ 7 days (mg/L)		
					MA	OSC	LYN
Buffered Milli-Q	0	-	5	-	3.90	3.55	3.95
	1	-	12	-	7.75	7.90	8.20
	2	-	19	-	13.10	11.40	11.80
	3	-	26	-	17.10	-	15.40
	0	-	5	100	3.95	3.60	3.80
	1	-	12	100	7.80	7.80	8.10
	2	-	19	100	13.00	13.40	11.70
	3	-	26	100	17.00	-	
	1.0	0.6	16	100	11.10	-	10.80
CRW (~2.5 mg/L DOC)	0	-	4	Ambient	3.24	3.25	3.35
	0	1.5	4	Ambient	3.02	2.90	3.05
	1.0	-	16	Ambient	13.00	11.90	12.90
	1.0	2.1	16	Ambient	13.00	11.30	12.30
	1.0	2.1	16	Ambient	13.00	11.50	12.50

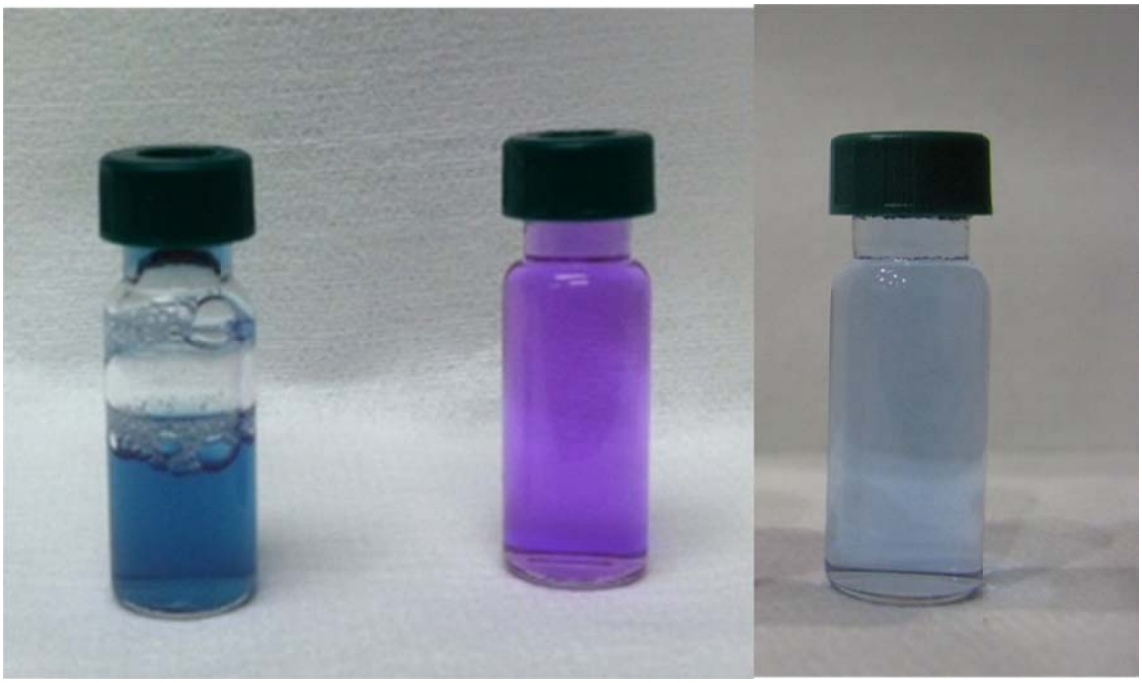

Figure S2.1. Photo of IOM standards: *Microcystis aeruginosa* (left, 320 mg/L), *Oscillatoria sp*. (center, 200 mg/L), and *Lyngbya sp*. (right, 115 mg/L).

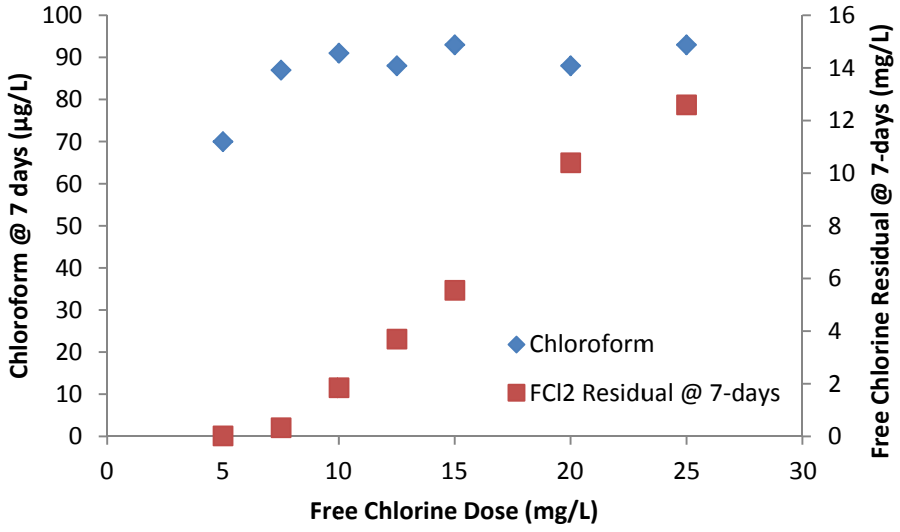

Figure S2.2. Effect of terminal free chlorine residual on overall chloroform yield after 7-days of exposure.

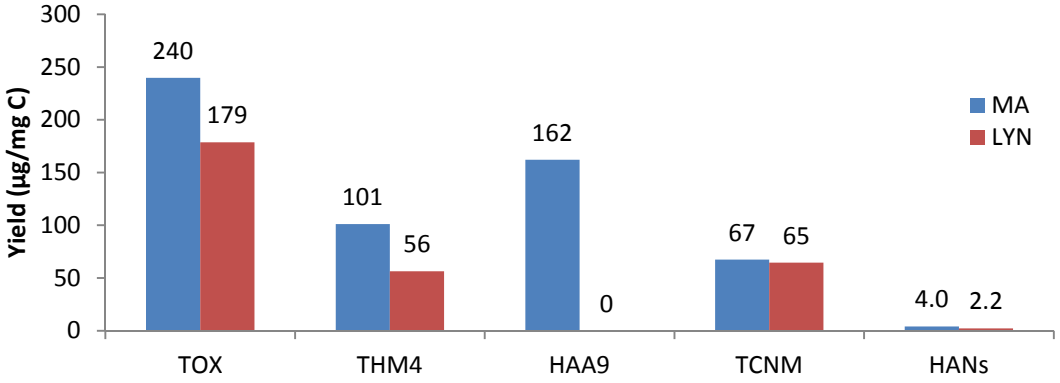

Figure S2.3. DBP yields after O_3/FCl_2 treatment in MQ water (pH=7.5, T=22-24°C, bromide=100 µg/L) with the addition of IOM from MA and LYN.

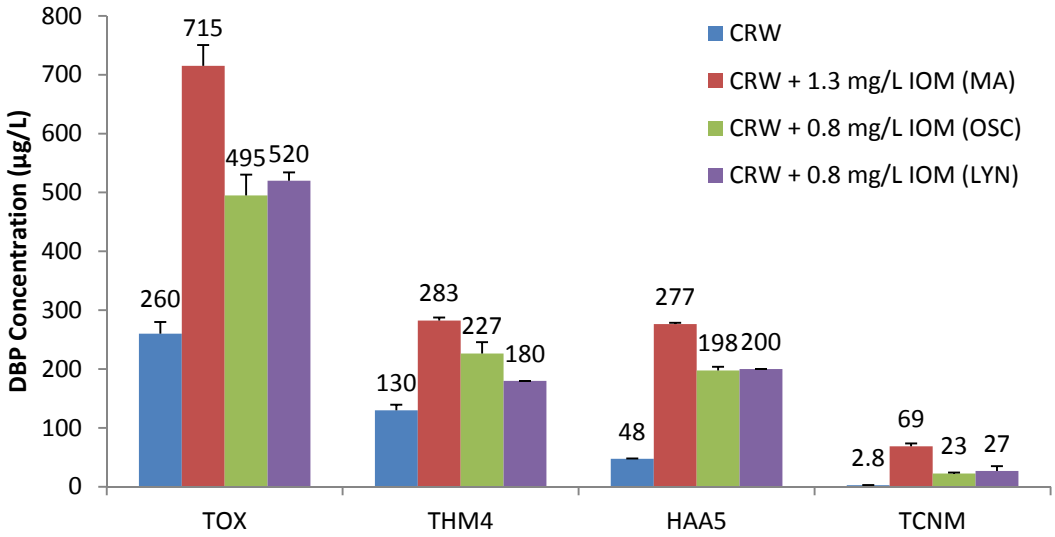

Figure S2.4. DBP formation after O_3/FCl_2 treatment in CRW (pH=8.25, T=23°C) with the addition of IOM from MA (1.3 mg/L), OSC (0.8 mg/L), and LYN (0.8 mg/L).

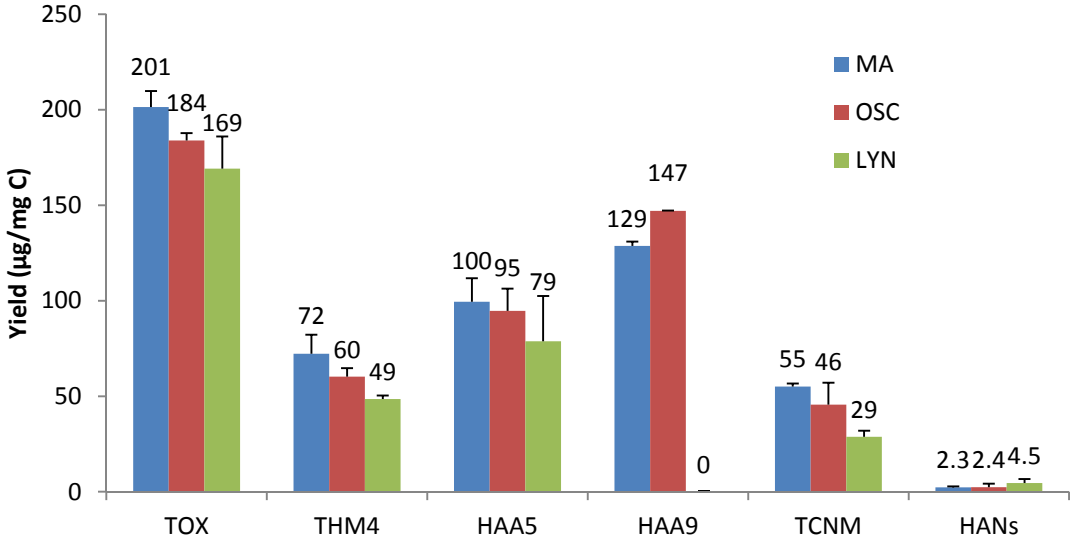

Figure S2.5. DBP yields from IOM extracts (MA, OSC, and LYN) after FP testing with free chlorine in buffered MQ water (pH=7.5, T=22-24°C, 100 µg/L bromide). (Notes: Error bars indicate +1 RSD, *TOX yield in terms of µg Cl/mg C)

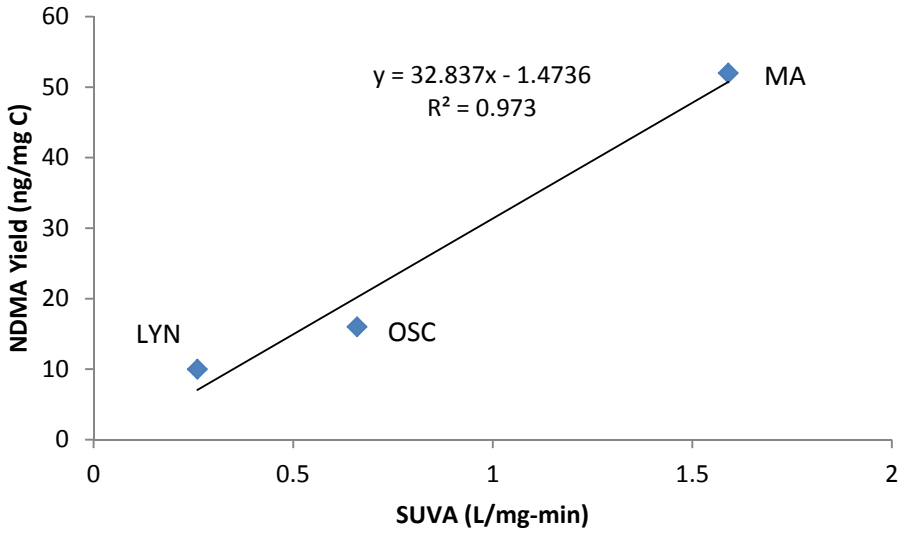

Figure S2.6. – Relationship between NDMA yield and SUVA for the IOM extracted from MA, OSC, and LYN.